IN VITRO MODEL SYSTEMS FOR INVESTIGATION
OF MOTONEURON DEVELOPMENT AND DISEASE

by

Jeremy S. Toma

Submitted in partial fulfilment of the requirements
for the degree of Doctor of Philosophy

at

Dalhousie University
Halifax, Nova Scotia
June 2015

To my family

In case you were wondering:

Research is what I am doing when I don't know what I am doing.
- *Wernher von Braun*

TABLE OF CONTENTS

LIST OF TABLES

LIST OF FIGURES

ABSTRACT

Spinal motoneurons innervate muscle fibres and represent the final component in the motor pathway responsible for producing movement by eliciting muscle contraction. Although the anatomy and physiology of motoneurons have been well studied, many questions remain about how these cells develop or why (and how) they die in motoneuron diseases such as amyotrophic lateral sclerosis (ALS). In this thesis, I present data that supports the use of several *in vitro* approaches to investigate these issues. The first approach uses motoneurons derived from mouse induced pluripotent stem (iPS) cells – stem cells that can be generated from differentiated cells. Using a wide range of experimental approaches I show that motoneurons derived from iPS cells develop the same cellular, anatomical, behavioural and electrophysiological properties as their endogenous counterparts. iPS cell-derived motoneurons fire repetitive action potentials with the same firing pattern as endogenous motoneurons, extend axons out of the neural tube when transplanted *in ovo* and make functional connections with muscle fibres *in vitro* and *in vivo*. In a second approach, I show that motoneurons derived directly from fibroblasts without a stem cell intermediary step (termed induced motoneurons) develop several characteristics typical of normal motoneurons. These include the ability to extend axons out of the developing spinal cord when transplanted *in ovo* and make connections with muscle fibres *in vitro*. Finally, I established a differentiation protocol to preferentially generate a very specific subtype of motoneurons that selectively target dorsal limb muscles during development. Like their endogenous counterparts, these embryonic stem cell derived motoneurons (ESCMNs) express Lhx1 and FoxP1, develop large soma sizes and form large neuromuscular junctions. As occurs in patients with ALS, I show results that suggest that large ESCMNs expressing the G93A SOD1 mutation are more susceptible to death than smaller ESCMNs when co-cultured with muscle fibres. In summary, in this thesis I have developed, and critically examined, several *in vitro* models useful for studying motoneuron development and motoneuron diseases. While additional studies are warranted, I believe that these model systems provide novel ways to study ALS and to possibly become a source of motoneurons for cell replacement therapies.

LIST OF ABBREVIATIONS USED

AChR	Acetylcholine receptor
AHP	afterhyperpolarizing potential
ALS	amyotrophic lateral sclerosis
AP	action potential
Ara-C	1-β-D-arabinofuranosylcytosine
BDNF	brain-derived neurotrophic factor
BMP	bone morphogenetic protein
BTX	bungarotoxin
ChAT	choline acetyltransferase
CNS	central nervous system
CNTF	ciliary neurotrophic factor
DIV	days *in vitro*
DRG	dorsal root ganglia
E	embryonic day
eGFP	enhanced green fluorescent protein
EPP	endplate potential
ESC	embryonic stem cell
ESCMN	embryonic stem cell-derived motoneuron
FACS	fluorescence activated cell sorting
FGF	fibroblast growth factor
FGFR1	fibroblast growth factor receptor
FTD	fronto-temporal dementia
GABA	gamma-aminiobutyric acid
GDNF	glial cell-derived neurotrophic factor
GF	growth factor
hESCMN	human embryonic stem-cell derived motoneuron
HH	Hamburger Hamilton
hiMN	human induced motoneuron
ICM	inner cell mass
iMN	induced motoneuron
iN	induced neuron
iPSC	induced pluripotent stem cell
iPSCMN	iPS cell-derived motoneuron
LC-MS/MS	liquid chromatography tandem mass spectrometry
LMC	lateral motor column
LMC_l	lateral aspect of the lateral motor column
LMC_m	medial aspect of the lateral motor column
MEF	mouse embryonic fibroblast
MG	medial gastrocnemius
MMC	medial motor column
MMC_m	medial aspect of the medial motor column
MMP	matrix metalloproteinase
MRM	multiple reaction monitoring
NMJ	neuromuscular junction

PBS	phosphate buffered saline
PMEF	primary mouse-derived embryonic fibroblast
pMN	motoneuron progenitor domain
qPCR	quantitative polymerase chain reaction
RA	retinoic acid
SAG	smoothened agonist
Shh	sonic hedgehog
SMA	spinal muscular atrophy
SMN	survival motoneuron gene
SOD1	superoxide dismutase
TDP	transactive response DNA-binding protein
TMR	tetramethylrhodamine
TTX	tetrodotoxin
UPR	unfolded protein response

ACKNOWLEDGEMENTS

CHAPTER 1: INTRODUCTION

1.1 *In vitro* modelling: a historical perspective

Studying cells *in vitro* allows researchers to gain insight into fundamental biological processes that are either unable or difficult to be isolated for investigation *in vivo* due to the complex nature of organisms. Typically, cell culture systems are used to model biological processes in a reduced environment whereby the cells exist in a growth permissive media either in free floating suspension or on an adherent substrate. Originally, cells that were isolated from organisms were grown on glass, which the Latin term *in vitro* refers to, however now many alternative substrates are used, most of which are plastics (Studzinski 2001). While in the past cells were isolated directly from tissue (primary cells), many cells are cultured today with the use of immortalized cell lines. Many cellular processes are investigated *in vitro*, including differentiation, cell death, cell division and process extension or outgrowth. Neurons were the first cells to be successfully isolated and cultured *in vitro*, and in fact the first experiments beautifully illustrate the power of *in vitro* modelling for uncovering fundamental biological processes. Early work by Ross Harrison (Harrison 1907, 1910, commented on in Keshishian, 2004) demonstrated evidence in strong support of the neuron doctrine, which holds that neurons are the basic cellular unit of the nervous system and that the nervous system is a network composed of many neurons which grow towards their targets (i.e. each other in the case of the central nervous system (CNS)) during development. At the time, the neuroscience community was divided over whether the nervous system consisted of a continuous syncytium of nervous tissue or if it was composed of contiguous, interconnected neurons. Harrison isolated nervous tissue from frog spinal cord, placed the explant on a glass coverslip inverted onto a glass slide coated with a matrix of lymph and monitored the growth cones of axons as they grew out of the explant. The experiments performed by Harrison proved that neurons do indeed grow to their targets, leading to the first, and arguably some of the most important, *in vitro* modelling experiments in neuroscience history. In the century following these seminal experiments, *in vitro* modelling has become standard practice for studies of the nervous system.

1.2 Development of *in vitro* models for studying motoneurons

One specific type of neuron, the alpha spinal motoneuron, extends an axon from the spinal cord, through the ventral spinal root and finally to its peripheral target, a skeletal muscle. A specialized area of contact where motoneurons connect and communicate with muscle fibres is termed the neuromuscular junction (NMJ). At the NMJ, acetylcholine is released from the motoneuron when it is activated (i.e firing an action potential) and binds to the acetylcholine receptors (AChRs) of the muscle, which depolarizes the muscle fibre and results in muscle contraction. This connection between the CNS and the skeletomuscular system allows for control of movement. For the purposes of this thesis, motoneurons and the efforts to study them *in vitro* will be the focus of further discussion.

Modelling connections between the spinal cord and peripheral muscle

Initial *in vitro* models of motoneurons focussed on the formation of NMJs made between muscle explants and motoneurons from spinal cord explants. Work by Stanley Crain and colleagues in the 1960s and 1970s demonstrated that functional NMJs were capable of forming *in vitro*. Crain and colleagues developed nerve-muscle co-culture systems whereby fetal rodent spinal cord explants containing motoneurons were grown with muscle explants harvested from rodents or humans (Crain, 1964; 1966; 1968; 1970; Peterson and Crain, 1970; Crain et al., 1970). In one study, Crain et al. (1970) managed to maintain fetal rodent (rat and mouse) spinal cord-muscle co-cultures for up to 7 weeks, and demonstrated functional coupling between motoneurons and adult rodent or human muscle fibres by initiating measurable action potentials and muscle contraction through electrical stimulation of the cord or ventral root. Treatment with curare, a known inhibitor of cholinergic transmission at the NMJ, was shown to inhibit neuromuscular coupling in these co-cultures (Crain et al., 1970). One of the most striking results of these experiments was the conserved, compatible nature of NMJs formed from tissues deriving from different species, as motoneurons from either mouse or rats were able to form functional NMJs with mouse, rat, or human muscle (Crain et al., 1970).

Around the same time, work by other groups further characterized NMJs formed *in vitro*. James and Tresman (1968) cultured gluteal muscle explants from the embryonic day (e) 11 chick and, 3 days later, plated down an explant of the e7 spinal cord

approximately 1 mm away from the muscle. Using scanning electron microscopy after only 4 days in co-culture, this group demonstrated that the morphology of newly-formed *in vitro* NMJs in these co-cultures resembled that of developing endogenous NMJs, with thickenings of the plasma membrane of the muscle and localized vesicles at the presumptive nerve terminal. Shimada and colleagues made similar ultrastructural observations when they developed a co-culture system whereby e6 ventral spinal cord cells were dissociated and plated on dissociated myoblasts taken from the thigh muscles of the e12 chick for up to 12 days (Shimada et al., 1969). Further co-culture experiments utilizing dissociated chick muscle and spinal cord similar to the protocol used by Shimada et al. (1969) were conducted by Fischbach, who recorded synaptic potentials in muscle fibres (Fischbach, 1970). He later went on to electrophysiologically characterize these synapses and determined that they are cholinergic and that neurotransmitter is released in a quantal fashion, which is a characteristic of endogenous NMJs (Fischbach, 1972). This is a similar finding to other work by Robbins and Yonezawa (1971a; 1971b) who co-cultured rat embryonic spinal explants and limb muscle (e11-19) and measured synaptic characteristics such as quantal release mechanisms and determined that quantal content, i,e. the amount of transmitter released at the NMJs, increased with the age of the co-cultures. These two studies demonstrated electrophysiological analysis of the developing vertebrate NMJ in its most immature state, i.e. at the earliest stage of synaptogenesis, when the axons were initially contacting muscle fibres, a time when *in vivo* investigations would be technically difficult.

Refining isolation methods of motoneurons

While many *in vitro* studies of the NMJ utilized spinal cord explant or dissociated spinal cord cells in co-culture with muscle, these systems were of little use if high yields of isolated motoneurons were desired for experimental analysis. Progressive advancements in purification techniques allowed for the isolation of more homogeneous populations of embryonic spinal motoneurons from the late 1970s to the 1990s. As described in more detail below, many of these techniques were established to identify trophic factors necessary for maintaining the survival of embryonic motoneurons.

One example of such a technique was developed by Masuko et al. (1979) that involved isolating motoneurons from the embryonic chick spinal cord following treatment with 1-β-D-arabinofuranosylcytosine (Ara-C), which inhibits DNA synthesis and therefore prevents mitosis. The rationale behind treating with Ara-C was that it would enhance the purity of motoneurons by removing mitotic glial and interneuron precursors present in the spinal cord at Hamburger Hamilton (HH) st. 17-18, a time when differentiated, postmitotic motoneurons would be able to be purified (Hollyday and Hamburger, 1977; Hamburger, 1948). Choline acetyltransferase (ChAT) activity, which is necessary for the synthesis of acetylcholine and is high in cholinergic cells such as motoneurons, was higher in Ara-C treated versus untreated spinal cord cells suggesting that motoneurons had been isolated (Masuko et al., 1979). Another technique developed by Berg and Fischbach (1978) separated large, cholinergic cells from other cells of the embryonic chick spinal cord by velocity sedimentation of dissociated spinal cord cells through a gradient composed of Ficoll, a hydrophilic polysaccharide commonly used in density gradients. The fraction containing the largest cells was determined to be enriched with motoneurons, as they contained cells with higher levels of ChAT activity compared to unfractionated spinal cord cells. As well, these cells were capable of innervating myotubes and forming neuromuscular junctions. While this technique had allowed for enrichment of motoneurons in spinal cord culture preparations, it did not result in a homogeneous population of motoneurons and many cholinergic cells were lost in the process (Schnaar and Schaffner, 1981). Schnaar and Schaffner (1981) took the concept of separating motoneurons from other cells of the embryonic chick spinal cord (HH st. 30-32) by density gradient centrifugation and modified it such that metrizamide, a derivative of glucose that had been recently established as a gradient solute (Rickwood and Bernie, 1974), was used rather than Ficoll, which led to a greater yield of cholinergic cells than that reported by Berg and Fischbach (1980). Metrizamide gradients proved easier and faster to separate than Ficoll gradients and they also required less specialized equipment than that prescribed by Berg and Fischbach (1980). Although homogeneous populations of motoneurons were still not able to be isolated by metrizamide density gradient centrifugation, this technique was used by other researchers to isolate motoneurons from the embryonic spinal cord (for e.g., Marchetti and McManaman, 1990; Juurlink et al.,

1990). Nycodenz, a compound chemically related to metrizamide (Rickwood and Graham, 1982), was also used as a gradient solute (Martinou et al., 1989; 1992). Beginning in the 1980s, the use of tract tracers such as horseradish peroxidase and wheat germ agglutinin were employed to retrogradely label motoneurons to aid in their identification in spinal cord preparations *in vitro* (e.g. Bennett et al., 1980; Smith et al., 1986). Further advances in motoneuron purification developed in the late 1980s and early 1990s involved the combined application of fluorescence activated cell sorting and retrograde labelling (Schaffner et al., 1987; Martinou et al., 1989; 1992). In the studies by Martinou and colleagues, motoneurons of the e14 rat were labelled with the fluorescent tracer dye DiI, which was injected into the hindlimbs, and subsequently either sorted based on their fluorescence or isolated using density-gradient centrifugation, or sorted following centrifugation. With these techniques, Martinou and colleagues were able to demonstrate that leukemia inhibitory factor, which they had previously isolated from conditioned media of skeletal muscle (Martinou et al., 1989), promoted both the survival of motoneurons *in vitro* and high levels of ChAT activity (Martinou et al., 1992). A more refined technique for isolating motoneurons involves immunopanning for the p75 neurotrophin receptor, which is selectively expressed by motoneurons in the rat spinal cord during day 15 of embryonic development, following density gradient centrifugation of dissociated spinal cord cells (Camu and Henderson, 1992). This enhanced purification of motoneurons over using centrifugation alone and did not require retrograde labelling and cell sorting. Using this immunopanning technique, Henderson and colleagues were able to investigate mechanisms involved in providing trophic support to specific subpopulations of developing motoneurons. Hepatocyte growth factor secreted from muscle was found to selectively maintain populations of limb-innervating motoneurons present in the brachial and lumbar spinal cord *in vitro* (Yamamoto et al., 1997). While these techniques offer researchers the ability to isolate populations of motoneurons from the spinal cord, there are limitations which make them undesirable as generating large yields of isolated motoneurons from many different animals can be costly and laborious. The advent of embryonic stem cell technology at the turn of the century had offered a promising alternative.

1.3 The advent of embryonic stem cell-derived motoneurons

In 2002, a major breakthrough developed in the laboratory of Tom Jessell allowed for the ability to generate high yield of purified motoneurons through the use of embryonic stem (ES) cells (Wichterle et al., 2002). In order to successfully engineer a protocol to program a fully undifferentiated stem cell into a postmitotic motoneuron, sufficient understanding of the developmental processes regulating motoneurogenesis was required. Here I will summarize key developmental events essential for the formation of spinal motoneurons and how the understanding of these events laid the necessary groundwork for the design of a protocol capable of generating embryonic stem cell-derived motoneurons (ESCMNs). Factors influencing motoneuron subtype development and how these relate to subtypes generated by standard ESCMN protocols will also be discussed.

Motoneuron development: the early stages

Early in neurogenesis, the neural tube is formed from neurogenic ectoderm, and dorso-ventral polarity is established. Inhibition of bone morphogenetic protein (BMP) and fibroblast growth factor (FGF)/Wnt signalling is critical for the initial specification of neurogenic ectoderm (reviewed by Davis-Dusenbery et al., 2014). At about e9.5 in the mouse, defined progenitor domains exist along the dorso-ventral axis of the developing spinal cord, and each domain (12 in total) is responsible for the generation of particular postmitotic cells that will make up the neural and glial components of the spinal cord (reviewed by Alaynick et al., 2011). These domains are defined by signature transcription factor expression profiles (reviewed by: Alaynick et al., 2011; Jessell 2000; Briscoe and Ericson, 2001; Lee and Pfaff, 2001). The most ventral progenitor domain, p3, is defined by expression of the transcription factors Nkx2.2 and Neurogenin 3, and gives rise to populations of V3 spinal interneurons. Dorsal to this is the domain which gives rise to motoneurons (pMN) which is defined by expression of the basic helix-loop-helix protein Olig2 (Novitch et al., 2001). Progenitors of this domain also generate oligodendrocytes, but not until motoneurogenesis is complete (Zhou et al., 2001). Located dorsal to the pMN domain are three other domains (p0-p2) which generate both inhibitory and excitatory interneurons of the spinal cord. The ventral-most domain, p2, which gives rise to both V2a and V2b interneurons (excitatory and inhibitory interneurons, respectively),

is demarcated at its ventral border by its expression of Irx3. There exists cross-repressive interactions between these signature transcription factors that allows for their exclusive expression in different domains. For example, cells of the p2 domain expressing Irx3 are unlikely to express Olig2 because Olig2 actively represses Irx3 expression, and cells of the pMN are unlikely to express Irx3 due to its repression of Olig2. This cross-repressive activity defines the boundaries of the domains as early spinal cord development proceeds (Briscoe et al., 2000; reviewed by: Briscoe and Ericson, 2001; Jessell 2000; Alaynick et al., 2011; Davis-Dusenbery et al., 2014). Other factors in addition to the cross-repressive nature of these transcription factors also contribute to the development of progenitor domains. Early in progenitor domain development, Olig2 is expressed by a wide region that spans from p2 and through the pMN domain to p3; however, Olig2 expression gradually becomes localized to the pMN domain only. Recent evidence suggests that the mechanisms involved in mediating the gradual repression involve small inhibitory RNA molecules known as microRNA. One of these molecules, mir-17-3p, was demonstrated to be necessary for repressing Olig2 expression by binding to Olig2 mRNA. Mice deficient in this microRNA exhibit a dorsal expansion of the pMN domain, which results in reduced V2 interneuron production (Chen et al., 2011). This group also went on to use ES cell-derived ventral spinal progenitor cells to further investigate this phenomena, as described later in this chapter.

Establishing subtype identity in motoneurons

Once postmitotic motoneurons have been generated, different motoneuron subtypes that innervate different muscle groups are defined by characteristic transcription factor profiles. Seminal work from the laboratory of Sam Pfaff identified LIM homeodomain proteins, through cloning experiments in the chick, that are expressed in different combinations in different motoneuron subtypes (Tsuchida et al., 1994). Motoneuron subtypes are grouped within the spinal cord in topographical arrangements; one type of arrangement that runs along the rostral-caudal axis through multiple segments of the spinal cord is the motor column. Motoneurons of the medial aspect of the medial motor column (MMC_m) that innervate epaxial musculature were found to express the LIM homeodomain factors Lhx3, islet-1 and islet-2. Motoneurons located in the lateral motor

column (LMC), which is present at segments of the spinal cord that provide innervation to the limbs, have differential expression of LIM homeodomain factors based on division. Motoneurons of the medial division of the lateral motor column (LMC_m), which project axons to the ventral limb muscle mass (largely flexor muscles), express islet-1 and islet-2 while motoneurons of the lateral division (LMC_l), which project axons to the dorsal limb muscle mass (largely extensor muscles), express Lhx1 and islet-2 (Tsuchida et al., 1994; Landmesser, 1978). These LIM homeodomain proteins were then determined to have functional roles in motor axon guidance. For example, Sharma et al. (2000) demonstrated that ectopic expression of Lhx3 in all motoneurons conferred an MMC_m phenotype, as motoneurons from all columns projected axons toward the developing epaxial musculature, thus defining an essential role for Lhx3 in MMC_m motor axon guidance. Further work by Kania et al. (2000) established a role for Lhx1 in the selective guidance of LMC_l axons to the dorsal limb muscle mass, as removal of the Lhx1 gene in mice resulted in LMC_l axonal projections to either the dorsal or ventral limb muscle mass. Later work by Kania and Jessell (2003) demonstrated that Lhx1 controls expression of the EphA4 receptor in developing LMC_l axons, which is necessary to mediate guidance towards the dorsal limb muscle mass through repulsive signalling induced by the ephrin-A5 ligand expressed by the ventral limb muscle mass.

Factors involved in patterning the spinal cord and defining motoneuron identity: identifying factors necessary to generate motoneurons

Prior to the establishment of motoneuron subtypes, the presence of morphogen gradients are essential for organizing the patterning of the developing spinal cord. Once neural tube formation has occurred, the dorsal and ventral poles become important nodes of morphogen expression required for dictating the patterns of progenitor domain formation. At the dorsal end of the developing spinal cord, morphogens belonging to the transforming growth factor β family, including BMP 4 (secreted from dorsally-located, non-neural ectoderm) and growth differentiation factor 7 (secreted from the roof plate of the neural tube), are responsible for inducing the dorsal-most progenitor domains of the developing spinal cord (reviewed by Alaynick et al., 2011). At the opposite pole, another morphogen, the protein sonic hedgehog (Shh), is expressed by cells of the floorplate and

notochord at the ventral region of the developing spinal cord. Identifying the role of Shh in promoting motoneuron fate identity involved a series of studies begun in the laboratories of Dodd and Jessell in 1991, who first demonstrated that the floorplate and the underlying notochord secrete a morphogen responsible for inducing motoneurogenesis (Yamada et al., 1991; Placzek et al., 1991; reviewed by Chipman et al., 2012). This was done by ectopic placement of the floorplate near dorsal regions of the developing chick spinal cord, which resulted in ectopic motoneuron generation. Further studies elucidated the identity of the secreted factor. Echelard et al. (1993) determined that the polarity protein sonic hedgehog (Shh), which was expressed in the notochord and floorplate, was sufficient to induce floorplate identity in ectopic regions of the CNS, suggesting that Shh was important for initiating gene expression programs essential for development of the ventral spinal cord. The establishment of Shh signalling as being characteristic of a diffusible morphogen which affects cell differentiation based on a concentration gradient was determined by Ericson et al., (1996) (reviewed by Briscoe and Ericson, 2001 and discussed by Chipman et al., 2012). High levels of Shh present at the ventral pole of the developing spinal cord are responsible for inducing ventral progenitor domains such as p3 and pMN, which have a high threshold for Shh activity. Concentrations of Shh are lower further dorsally where more progenitor domains have a low threshold for Shh activity (reviewed by Briscoe and Ericson, 2001). The receptiveness to Shh signalling is evident in the transcription factors necessary for defining the progenitor domain boundaries of the ventral spinal cord, as these factors are either induced (Class II) or repressed (Class I) by Shh signalling. Class II factors such as Olig2, Nkx6.1, and Nkx2.2 promote ventral domain formation and engage in cross-repressive interactions as described above with Class I factors such as Irx3. Based on these discoveries, Shh signalling was determined to be an essential factor for the differentiation of ESCMNs (Wichterle et al., 2002).

Another morphogen critical for the patterning and formation of the developing spinal cord is the vitamin A derivative *all-trans* retinoic acid (RA), which is involved in a number of processes throughout neural tube/spinal cord development necessary for establishing motoneuron identity. During the initial phases of neurogenesis, cells express genes characteristic of forebrain progenitors. One of the factors critical in establishing

caudal (spinal cord) identity in the developing CNS is RA signalling (Durston et al., 1998; Muhr et al., 1999). The role of RA signalling in early spinal cord development was initially determined by experiments in *Xenopus* embryos, where RA treatment was shown to confer a caudal neural identity to rostral neural tissue, as these animals developed enlarged spinal cords and hindbrains with reduced forebrain tissue (Durston et al., 1989). During neural tube development, RA is secreted by the surrounding somites and acts on cells of the developing spinal cord. RA is essential for inducing the expression of the transcription factor Pax6, which is required for patterning ventral progenitor domains. Disruption of Pax6 expression results in dissolution of the ventral border of the pMN domain with p3, indicating that motoneurogenesis relies on RA signalling at various times throughout CNS development. With respect to *in vitro* development, a neurogenic fate in ES cells was found to be promoted by RA treatment (Bain et al., 1995). Taken together, these results suggest that RA signalling is important for motoneuron development *in vitro*, and was used by Wichterle et al. (2002) in their establishment of an ESCMN protocol.

Generation of ESCMNs

In 2002, Wichterle and colleagues in the laboratory of Tom Jessell published a seminal study outlining a protocol for the generation of mouse ESCMNs (see Figure 1.1, left column). Remarkably, the application of only two key factors, a Shh signalling agonist and RA, was sufficient to differentiate motoneurons from embryonic stem cells after only one week in culture. It is almost certain that FGF and Wnt signalling, along with other instructive cues necessary for developing motoneurons, were derived from the differentiating stem cells (Wichterle et al., 2002). Embryonic stem cells were aggregated into what were termed embryoid bodies for 2 days prior to the addition of RA and Shh for 5 days. Midway through the differentiation protocol, developing ESCMNs expressed ventral progenitor domain transcription factors such as Olig2 and Nkx6.1, indicating that the pathway to differentiation for ESCMNs recapitulates that of endogenous motoneurons. To identify differentiated motoneurons, Wichterle and colleagues used ES cells derived from transgenic mice with an enhanced green fluorescent protein (eGFP) reporter element linked to the promoter of the homeodomain gene Hb9, which is a gene

essential for motoneurogenesis and is expressed by postmitotic motoneurons (Arber et al., 1999, Thaler et al., 1999). Following the differentiation protocol, it was determined that approximately 20-30% of total cells differentiated into eGFP$^+$ motoneurons. Later work established that many of the other cells present in the embryoid bodies are likely interneurons (based on patterns of neural activity present within the embryoid bodies) and glia, as indicated by variable levels of S100β and glial fibrillary acidic protein, which are known markers for astrocytes (Miles et al., 2004; unpublished observations, Rafuse laboratory).

Following differentiation, Wichterle and colleagues then attempted to determine the specific subtype identities of the ESCMNs, which will be described in more detail below. Briefly, they found that the majority of ESCMNs (>70%) co-expressed the LIM homeodomain proteins islet 1 and Lhx3, characteristic of motoneurons that innervate epaxial, postural muscles (Tsuchida et al., 1994; Sharma et al., 1998) while only a small percentage (<5%) expressed the LIM homeodomain protein Lhx1, which is present in a subset of motoneurons and is critical for appropriate innervation of the dorsal limb muscle mass (Tsuchida et al., 1994; Kania et al., 2000). Wichterle and colleagues then went on to show, through implantation of ESCMNs into the developing chick spinal cord at a time when motoneurons are being generated (HH st. 15-17, Hollyday and Hamburger, 1977), that these cells are capable of integrating into the developing spinal cord and innervating peripheral muscle targets. ESCMNs were demonstrated to project axons out of the ventral roots and through developing peripheral nerves before terminating on fibres of intercostal muscles. Nerve terminals from ESCMNs interacted with motor endplates on muscle fibres between HH st. 30 and 35, suggesting these cells are capable of forming NMJs *in vivo* (Wichterle et al., 2002). Taken together, these results demonstrated, for the first time, that it is technically possible to generate a high yield of purified motoneurons using ES cells.

Analyses of ESCMN functional capabilities and utilization of ESCMNs as a motoneuron model system

Further studies characterized the functional properties of ESCMNs (reviewed by Chipman et al., 2012). Miles and colleagues performed a number of electrophysiological

experiments and determined that ESCMNs exhibit many of the properties of endogenous motoneurons (Miles et al., 2004). For example, ESCMNs are capable of firing repetitive action potentials that exhibit spike frequency adaptation in response to injections of depolarizing current in a manner similar to that observed in endogenous motoneurons. This is likely because ESCMNs were found to express appropriate ion channels necessary for functional activity such as voltage-gated K^+, Na^+, and Ca^{2+} channels. ESCMNs were also plated on myotubes derived from the C2C12 muscle cell line. It was found that they made functional NMJs that elicited post-synaptic endplate potentials which were blocked by treatment with curare, indicating that ESCMNs were capable of forming functional, physiologically-relevant NMJs *in vitro* (Miles et al., 2004).

Further work by Soundararajan and colleagues from the laboratory of Victor Rafuse followed up on the observation that the majority of the ESCMNs generated with the protocol designed by Wichterle et al. (2002) express the LIM homeodomain protein Lhx3. As described above, Lhx3$^+$ motoneurons reside in the MMC_m of the spinal cord and innervate epaxial (postural) muscles that support the vertebral column (Tsuchida et al., 1994). It was found that ESCMNs possess many characteristics of MMC_m motoneurons. For example, Soundararajan et al (2006) determined that ESCMNs had passive membrane properties similar to endogenous MMC_m motoneurons. In addition, ESCMNs transplanted into the developing chick spinal cord at a time when motoneurons were being generated (HH st. 17, similar to the age of chicks used by Wichterle et al., 2002) migrated and engrafted into the MMC_m and projected axons preferentially towards the epaxial muscles. Further to these observations, ESCMNs preferentially projected axons to epaxial muscles in experiments whereby ESCMNs were flanked by explants of epaxial and limb muscles *in vitro*. This led Soundararajan and colleagues to conclude that a chemotropic factor emanating from the developing epaxial muscles promotes guidance of ESCMN axons towards these muscles (Soundararajan et al., 2006). Around the same time that this work was published, an important *in vivo* discovery was made concerning the guidance of MMC_m axons projecting to developing epaxial musculature (termed the dermomyotome) (Shirasaki et al., 2006). During development, when MMC_m motoneurons are extending axons towards the dermomyotome, the fibroblast growth factor receptor (FGFR1) expressed on the axonal surface responds to FGFs expressed in

the dermomyotome, such as FGF8 (Shirasaki et al., 2006). FGF8 was shown to act as a long-range chemoattractant to MMC_m axons *in vitro*. Furthermore, targeting of MMC_m axons to the epaxial muscles was disrupted in mice lacking FGFR1 in MMC_m motoneurons, demonstrating the importance of FGF signalling in MMC_m axon guidance (Shirasaki et al., 2006). Soundararajan and colleagues followed up on these findings in experiments utilizing ESCMNs in an attempt to discover the cellular signalling mechanisms responsible for mediating chemoattractant FGF signalling in guiding MMC_m axons to their targets (Soundararajan et al., 2010). They demonstrated that ESCMNs grow towards heparin beads coated with FGF8 *in vitro* and that ESCMNs derived from mice lacking the FGFR1 gene had disrupted axonal projections to their peripheral targets (epaxial muscles), as many axons misprojected to the limb (Soundararajan et al., 2010). This result was comparable to the aberrant motor axon outgrowth in mice lacking the FGFR1 receptor (Shirasaki et al., 2006). By using ESCMNs, Soundararajan and colleagues determined that the chemotropic effects of FGFR1 signalling in MMC_m axons that is induced by FGF8 is mediated through the mitogen-activated protein kinase/extracellular signal-regulated kinase pathway (Soundararajan et al., 2010). For the first time, ESCMNs had been used to investigate a cellular signalling pathway. Taken together, these studies demonstrate how ESCMNs can be used to model *in vivo* developmental phenomena and to further our understanding of basic signalling mechanisms involved in fundamental cellular processes such as axon guidance.

ESCMNs have been used to model other aspects of motoneuron development and physiology. For example, other work from the Rafuse laboratory (Chipman et al., 2014) has established a co-culture system to investigate synaptogenesis at the NMJ. It is now possible to use ES cells derived from transgenic animals to investigate genes involved in synaptogenesis at the NMJ *in vitro*. Chipman and colleagues generated ESCMNs from neural cell adhesion molecule knockout mice ($NCAM^{-/-}$) to investigate the role of NCAM in synaptogenesis *in vitro*. They found that $NCAM^{-/-}$ ESCMNs, when co-cultured on chick myotubes, recapitulated impairments in neurotransmission observed in $NCAM^{-/-}$ mice. For example, altered vesicle dynamics leading to compromised neurotransmission were found at the NMJs of $NCAM^{-/-}$ ESCMNs on myotubes. Neurotransmission was somewhat rescued by the treatment of the L-type Ca^{2+} channel antagonist nifedipine

(Chipman et al., 2014). These results highlight the utility of the ESCMN-myotube co-culture system for investigation of synaptogenesis and as a possible tool for screening drugs designed to treat synaptic pathologies in motoneuron diseases.

Studies from the laboratory of Hynek Wichterle have used ES cells to model events involved in spinal cord development. For example, a recent study by Chen et al. (2011) used the developmental program established by the Shh agonist-RA motoneuron differentiation protocol to generate neural progenitors that expressed the pMN and p2 ventral spinal progenitor domain factors Olig2 and Irx3 respectively. This group found that microRNA play a role in establishing boundaries between these domains as described above. By treating ES cells with a 50-100x lower concentration of Shh agonist than that used to differentiate motoneurons, Chen and colleagues were able to generate progenitors with a more dorsal phenotype (Irx3-expressing p2 progenitors) than those used to generate motoneurons. They then went on to show that by disrupting microRNA expression, the levels of Olig2 expression increased in these progenitors at the expense of Irx3 expression in ES cell-derived neural progenitors (Chen et al., 2011). Taken together with the *in vivo* results described above, these experiments nicely demonstrate how using ES cell-derived neural progenitors can complement *in vivo* studies of spinal cord development.

Another study from Wichterle's lab investigated the mechanisms involved in determining rostro-caudal motoneuron fate using alternative methods to differentiate ESCMNs. ESCMNs differentiated using Shh agonist and RA typically generate MMC_m motoneurons that do not innervate limbs (Wichterle et al., 2002). As well, these motoneurons have a Hox gene profile of motoneurons derived in the cervical region *in vivo*, an area that is devoid of limb-innervating motoneurons. Hox genes, which are necessary for orchestrating gene expression patterns in developing tissues are critical for determining rostro-caudal identity in motoneurons of the developing spinal cord (reviewed by Dasen and Jessell, 2009). For example, the Hox gene HoxA5 is essential for establishing rostral spinal cord (cervical) identity in motoneurons, while HoxC6 and HoxC8 are required for the development of motoneurons at the brachial level. The vast majority of ESCMNs (~80%, Peljto et al., 2010) differentiated using the standard Shh agonist-RA protocol express HoxA5. RA has been shown, as described above, to be

important for inducing neurogenic differentiation of ES cells (Bain et al., 1995), however it promotes a rostral spinal identity in ESCMNs which may limit the ability of researchers to develop a variety of ESCMNs including brachial limb-innervating motoneurons (Wichterle et al., 2002; Peljto et al., 2010). To determine the possibility of differentiating ESCMNs that possess an LMC, limb-innervating phenotype, Peljto and colleagues developed a different method for differentiating ESCMNs. They found that ESCMNs that were differentiated at low density (to prevent BMP signalling to promote neurogenic differentiation) in a retinoid and Shh free medium containing Advanced D-MEM/F12/Neurobasal medium with 10% knockout serum promoted a more caudal Hox gene expression characteristic of limb-innervating motoneurons. The majority of the ESCMNs expressed brachial level Hox genes associated with LMC motoneurons at this spinal level (HoxC6 or HoxC8). Furthermore, the majority of the ESCMNs that were either HoxC6$^+$ or HoxC8$^+$ expressed FoxP1, a Hox gene accessory factor that is essential for LMC formation (Dasen et al., 2008; Rousso et al., 2008) although many Lhx3$^+$ motoneurons were generated with these Hox profiles as well. Peljto and colleagues determined that endogenous FGF, Wnt and Shh signalling was essential to the formation of these ESCMNs differentiated using this protocol, as inhibitors of each factor resulted in decreases in brachial ESCMNs as based on Hox gene expression. One caveat using this approach, however, is that the ESCMNs were generated at a 4-5 fold lower percentage compared to those generated with the previously established RA-Shh agonist protocol, possibly because this differentiation method relies solely on endogenous signalling. Finally, through transplantation of these ESCMNs into the developing chick spinal cord, it was determined that FoxP1$^+$ ESCMNs tended to settle more laterally in the ventral horn than Lhx3$^+$ ESCMNs, which settled more medially, indicating that these ESCMNs integrate into the spinal cord according to their molecular identities. As well, axon projection patterns to peripheral muscle targets were also investigated using retrograde tracing, whereby it was determined that ESCMNs expressing FoxP1 preferentially targeted the limbs whereas those expressing Lhx3 preferentially targeted the epaxial musculature, further demonstrating that the functional characteristics of these ESCMNs resembled that of their endogenous counterparts (Peljto et al., 2010).

Using the knowledge gained from experiments applying different methods to differentiate ESCMNs, further investigations into epigenetic factors that regulate the control of cervical versus brachial and thoracic motoneuron identity at the gene expression level were made by Wichterle's group. Mazzoni et al. (2013) found that RA treatment promotes expression of cervical Hox genes by releasing repressive histone modifications that prevent transcription of these genes. In contrast, treatment with Wnt and FGF promotes a more caudal (brachial and thoracic) identity by promoting activation of the transcription factor Cdx2, which in turn removes repressive histone modifications on more caudal Hox genes (Mazzoni et al., 2013). Taken together, these studies illustrate how ESCMNs have become an important tool for modelling critical aspects of motoneuron development.

Preclinical applications of ESCMNs and the development of human ESCMNs
The interest in developing ESCMNs stems not only from the utility of this approach in investigating processes involved in motoneuron development, but also from interest in developing *in vitro* models of motoneuron diseases such as amyotrophic lateral sclerosis (ALS), which will be described in more detail below. Aside from *in vitro* modelling, there is potential for use of ESCMNs in developing therapies for paralysis resulting from muscle denervation (reviewed by Chipman et al., 2012). A few studies have demonstrated the capacity of ESCMNs to functionally innervate muscle following denervation. For example, Deshpande et al. (2006) demonstrated that ESCMNs derived from mice that were transplanted into the adult rat spinal cord could reinnervate hindlimb muscles that had been denervated as a result of application of the neuroadapted Sindbis virus, which specifically targets and kills motoneurons. The transplanted ESCMNs managed to grow axons out of the spinal cord, with trophic support, and formed NMJs with denervated hindlimb muscle fibres, which resulted in partial recovery from viral-induced paralysis (Deshpande et al., 2006). Further investigation into the ability of mouse ESCMNs to recover loss of muscle function due to denervation was conducted by Yohn et al. (2008). In this study, Yohn and colleagues determined that ESCMNs can reinnervate the medial gastrocnemius muscle following tibial nerve transection when the ESCMNs were implanted into the injured nerve. ESCMNs made functional connections

capable of restoring muscle force and partially prevented denervation atrophy of the medial gastrocnemius muscle. Approximately 40% of pre-injured muscle force was recovered in muscles receiving input from ESCMNs when nerves were electrically stimulated. Importantly, the only innervation to the muscle was provided by the implanted ESCMNs as the tibial nerve was ligated proximally, indicating that force recovery was contributed solely by connections with ESCMNs. Interestingly, ESCMNs were found to survive in the nerve up to 18 months post transplantation, suggesting that functional integration into the host muscle promoted their survival (Yohn et al., 2008). While these were important discoveries illustrating the potential utility of ESCMNs as therapeutic tools following nerve injury, it remained important to determine whether human ESCMNs (hESCMNs) could be generated for therapeutic purposes.

hESCMNs were first successfully generated by Li and colleagues (2005) utilizing a protocol whereby were human ES cells were plated down for differentiation for approximately a week until neuroectodermal rosettes that expressed the neuroectodermal transcription factor Sox1 were identified. These cells were then isolated and treated with RA and Smoothened agonist (SAG, an agonist of the Shh signalling pathway) in much the same manner as mouse ESCMNs. Following this, treatment with the growth factors brain-derived neurotrophic factor (BDNF), glial cell-derived neurotrophic factor (GDNF) and insulin-like growth factor 1 were required to promote mature motoneuron characteristics, such as expression of ChAT and the ability to form NMJs in co-culture with the C2C12 myoblast cell line (Li et al., 2005). In total, the amount of time required to generate hESCMNs from human ES cells was about 1 month, much longer than the time needed to generate mouse ESCMNs. Further assessment of the functionality of hESCMNs was carried out by Lee et al. (2007). This group transplanted hESCMNs into the developing chick spinal cord and found that these cells successfully engrafted and extended axons into the periphery. As well, hESCMNs successfully engrafted into (and extended neurites within) the adult rat spinal cord. Taken together, the results of these studies demonstrate that hESCMNs exhibit characteristics of spinal motoneurons, much like ESCMNs derived from mice.

Multiple techniques have now been established for developing hESCMNs from pluripotent stem cells to increase efficiency and reduce time required for motoneuron generation. Inhibition of the SMAD signalling pathway with two inhibitors (an inhibitor of activin/nodal signaling and noggin) promotes neuralization of hES cells in a more efficient manner than isolation of neuroectodermal rosettes, which may be contaminated with cells of other lineages (Chambers et al., 2009; Boulting et al., 2011). Another technique developed to shorten differentiation time involves utilizing programming genes that, when delivered by adenoviral vectors to human neural progenitor cells derived from hES cells, promotes motoneuron identity. Delivery of Neurogenin 2, Islet-1 and Lhx3 resulted in hESCMNs that possessed mature electrophysiological characteristics only 11 days after gene delivery, allowing for a total of 30 fewer days needed to generate hESCMNs as compared with previous techniques (Hester et al., 2011). Another recently developed technique for differentiation of hESCMNs was developed by Amoroso et al. (2013). This group demonstrated that by treating hES cells with RA and a combination of SAG and another Shh signalling agonist, purmorphamine, hESCMNs largely differentiated into motoneurons that expressed FoxP1 rather than Lhx3, suggesting that they may possess physiological properties of limb-innervating motoneurons (Amoroso et al., 2013). The interest in developing human motoneurons that possess a limb-innervating phenotype goes beyond *in vitro* developmental studies, as high yields of these motoneurons are sought for therapeutic purposes because some limb-innervating motoneurons are the earliest to degenerate and die in ALS. The study I present in Chapter 4 of this thesis describes attempts I have made to generate ESCMNs that possess a limb-innervating phenotype.

1.4 Modelling motoneuron disease: amyotrophic lateral sclerosis

Before I describe methods used to model ALS, I will describe both key genes involved in, and elements of, the pathophysiology of the disease. ALS results in the degeneration and death of both spinal and cortical motoneurons, resulting in paralysis and death, usually as a result of loss of ability to swallow and breathe due to denervation of the diaphragm. It is a late onset disease, with the majority of patients being diagnosed in middle age. The vast majority (~90%) of ALS cases are sporadic, meaning that there is

no known inheritable cause. The first gene found to be involved in ALS was the Cu/Zn-binding superoxide dismutase (SOD)1 enzyme, which is involved in approximately 20% of familial ALS cases (Rosen et al., 1993). There are currently over 100 known mutations of SOD1 that result in ALS symptoms (reviewed by Boillée et al., 2006). The first animal model of ALS was developed in the early 1990's, which showed that mutated SOD1 was a causative agent in ALS. Using genetic studies identifying SOD1 mutations in families, Gurney and colleagues generated a mutated human SOD1 gene with an amino acid substitution at position 93 (alanine replaced glycine, SOD1G93A) that did not affect the function of the enzyme (Rosen et al., 1993; Gurney et al., 1994). Expression of SOD1G93A in mice resulted in ALS-like symptoms such as motoneuron degeneration, progressive paralysis and shortened lifespan (5-6 months). Following this discovery, other variants of mutated SOD1 have been discovered and studied, including G85R and G37R (Bruijn et al., 1997; Wong et al., 1995). The mechanisms of disease action induced by SOD1 mutations include misfolding of SOD1 protein, which results in aggregation and is associated with eventual mitochondrial dysfunction leading to degeneration and death of motoneurons. Other pathogenic events include neurofilament disorganization and impaired transport in the motor axon, which ultimately degenerates and withdraws from the NMJ prior to cell death, resulting in paralysis (reviewed by Boillée et al., 2006). In addition, other neighbouring cells, such as microglia and astrocytes, express toxins which further exacerbate disease progression (reviewed by Boillée et al., 2006).

More recent work has uncovered further molecular targets involved in RNA processing that underlie ALS pathophysiology. For example, in 2006, it was discovered that there was a factor linking fronto-temporal dementia (FTD) with ALS, diseases which often present in the same individuals (Lomen-Hoerth et al., 2002). The transactive response DNA-binding protein (TDP-43), a nuclear protein which also binds RNA, was found to be associated with both diseases, as it was isolated in ubiquitinated cytoplasmic aggregates (or inclusions) isolated from the cortex of individuals suffering from either ALS or FTD (Neumann et al., 2006; reviewed by Ajroud-Driss and Siddique, 2014). Mutations in TDP-43 that cause toxic gain of function have been associated with ALS, resulting in cytoplasmic aggregates containing bound RNA molecules. However, wildtype TDP-43 is also associated with cytoplasmic aggregates in ALS, and unlike the

case with wildtype SOD1 protein, high levels of wildtype TDP-43 are toxic to cells, proving that developing models to study the role of TDP-43 in ALS can be difficult (reviewed by Wegorzewska and Baloh, 2011; Ajroud-Driss and Siddique, 2014). The exact role of TDP-43 in ALS pathophysiology is unclear, but it appears to stem from either the loss of normal TDP-43 function (due to cytoplasmic sequestration) or as a result of toxic gain of function due to cytoplasmic aggregation (Ajroud-Driss and Siddique, 2014). Modelling the role of mutant TDP-43 in ALS has proved challenging as well. For example, mice that express the human TDP-43 A315T mutation develop neurodegeneration in the colon and die before showing any apparent symptoms of ALS, indicating the need for more appropriate models to study TDP-43 pathology as it relates to ALS (Esmaeili et al., 2013; Hatzipetros et al., 2013). To that end, a very recent study by Alami and colleagues has shown that mutations in TDP-43 introduced into *Drosophila* motoneurons and primary cultures of mouse cortical neurons along with mutations present in human pluripotent stem cell-derived motoneurons (TDP-43 A315T, M337V and G298S mutations) taken from patients result in mRNA trafficking defects to distal regions of axons, indicating that TDP-43 likely plays an important role in the transport of mRNA to the axons. Mutations that disrupt this process are therefore involved in the pathophysiology of ALS (Alami et al., 2014). Another RNA binding protein, fused in sarcoma/translocated in liposarcoma (FUS/TLS), was discovered to be associated with ALS at around the same time as TDP-43 and has been found to account for approximately 4 % of familial ALS cases, as well as being associated with sporadic ALS (Kwiatkowski et al., 2009; Vance et al., 2009). Inclusions containing both TDP-43 and FUS/TLS protein have been isolated in brain and spinal cord tissue of ALS patients, indicating a similar involvement of the two RNA binding proteins in ALS pathophysiology (Deng et al., 2010).

Further discoveries elucidating the roles of dysregulated RNA processing and protein aggregation in ALS were published in 2011. Mutations in the first intron sequence of the C9ORF72 gene resulting in a hexanucleotide repeat sequence (GGGGCC) were found to be associated with FTD and ALS (DeJesus-Hernandez et al., 2011; Renton et al., 2011; reviewed by Ajroud-Driss and Siddique, 2014). These mutations cause RNA foci to form, resulting in aggregations involving the sequestration

of key mRNA binding proteins and other RNA transcripts. To date, C9ORF72 has been shown to be involved with up to 30% of familial and 5% of sporadic ALS cases (DeJesus-Hernandez et al., 2011; Renton et al., 2011; reviewed by Ajroud-Driss and Siddique, 2014). While the function of the protein encoded by this gene remains unknown, investigations of the mouse ortholog of C9ORF72 have shown that this gene is highly expressed in populations of neurons that are affected in both FTD and ALS, including spinal motoneurons (Suzuki et al., 2013).

The final factor involved in ALS that I will discuss is the ubiquitin-proteasome protein degradation pathway. Mutations that result in dysregulation of this pathway have been recently implicated in the pathophysiology of ALS and FTD (Deng et al., 2011; reviewed by Ajroud-Driss and Siddique, 2014). One of these mutations involves the ubiquilin family protein UBQLN2, which is involved in shuttling proteins tagged with ubiquitin to the proteasome for degradation (Ko et al., 2004). Mutations in this gene result in disruption of the proteasomal degradation pathway and the presentation of ALS pathology (Deng et al., 2011). Although mutations in this gene account for only a small percentage of ALS cases, it does link ALS and FTD with other neurodegenerative diseases such as Alzheimer's and Parkinson's disease, where proteins of the ubiquitin-proteosomal pathway are found in cytoplasmic inclusions (Kuusisto et al., 2001; reviewed by Ajroud-Driss and Siddique, 2014). These results demonstrate that faulty protein clearance is of central importance in neurodegenerative diseases including ALS.

Susceptibility of different motoneuron populations to disease

One important clinical aspect of ALS is the susceptibility of different motoneuron populations to the disease (reviewed in Kanning et al., 2010). Larger motoneurons that innervate fast-fatigable muscle fibres, such as those present in the LMC that innervate limb muscles, are most susceptible to axonal withdrawal from muscle (axonal dieback), degeneration and death as demonstrated in SOD1G93A mice (Frey et al., 2000). In contrast, smaller motoneurons that innervate slow muscles are preserved late into disease progression but ultimately degenerate and die. The relative resistance of slow motoneurons to death may be due to increased sprouting capacity compared to fast motoneurons (Pun et al., 2006; Frey et al., 2000). As well, an increased unfolded protein

response (UPR) in fast motoneurons may accelerate axonal dieback and degeneration in the presence of misfolded proteins such as mutant SOD1 (reviewed by Kanning et al., 2010). Not all motoneurons, however, are vulnerable to degeneration in ALS. Motoneurons that innervate either extraocular muscles or anal sphincter and urethral muscles remain healthy into late stages of ALS (reviewed by Kanning et al., 2010). Investigations into the gene expression differences between vulnerable and resistant populations of motoneurons have yielded interesting results. Using a genetic screening approach, Kaplan and colleagues found that the extracellular matrix molecule matrix metalloproteinase-9 (MMP-9) was selectively expressed by fast motoneurons (Kaplan et al., 2014). By inhibiting MMP-9 expression in SOD1G93A mice through a variety of approaches including the use of viral gene therapy and genetic knockout of MMP-9, fast muscles denervated at a protracted rate. Additionally, expression of MMP-9 was found to promote early activation of the UPR in fast motoneurons (Kaplan et al., 2014). Together these results indicate that MMP-9 could be a potential therapeutic target for slowing the progression of ALS.

It is interesting to note, however, that susceptibility of fast motoneurons to death does not seem to be a feature of all motoneuron diseases, including spinal muscular atrophy (SMA). SMA is an early-onset motoneuron disease that is caused by insufficient levels of the survival motoneuron gene (SMN), resulting in degeneration and death of spinal motoneurons. The precise role of SMN in SMA is unclear, but it is known that the while the ubiquitously expressed SMN protein is involved in intron splicing in many cell types, it does have a specific function only associated with motoneurons, i.e. interacting with a ribonuclear protein involved in pre-mRNA processing associated with axonogenesis (reviewed by Hamilton and Gillingwater, 2013). Dysregulation of this process may contribute to SMA pathology (reviewed by Fallini et al., 2012). Interestingly, populations of motoneurons are differentially susceptible to degeneration in mouse models of SMA (Murray et al., 2008), however the reasons for this susceptibility remain unclear. A recent study by Thomson et al. (2012) could find no correlation between morphological parameters (including motor unit size, which is larger in fast motoneurons) and susceptibility to degeneration in a mouse model of SMA. These results suggest that susceptibility of motoneurons to degeneration in SMA may be influenced by

dysfunction in other cell types including muscle, where underdeveloped myotubes form as a result of dysregulated myogenic gene expression (Hamilton and Gillingwater, 2013; Boyer et al., 2014).

The use of ESCMNs for in vitro models of motoneuron disease

Although *in vivo* models have undoubtedly been useful in understanding motoneuron diseases, ESCMNs have been used to model motoneuron disease *in vitro* in order to further investigate cell autonomous and non-cell autonomous mechanisms involved in motoneuron disease pathology. Mouse and human ES cell lines containing mutant human SOD1 constructs have been generated for use in studies modelling ALS *in vitro*. For example, Di Giorgio and colleagues in the laboratory of Kevin Eggan found that ESCMNs generated from mice harbouring the human SOD1G93A mutation are susceptible to early death compared to healthy control ESCMNs over weeks in culture, suggesting a possible cell autonomous effect of the mutant SOD1 transgene (Di Giorgio et al., 2007). Both Di Giorgio et al. (2007) and Nagai et al. (2007) demonstrated that a non-cell autonomous toxic effect was conferred to ESCMNs that were plated on a monolayer of either SOD1G93A^{+} glial cells (Di Giorgio et al., 2007) or SOD1 mutant astrocytes alone (Nagai et al., 2007), resulting in degeneration and death of ESCMNs. Nagai and colleagues went on to show that interneurons were not affected by this glial toxicity, suggesting a motoneuron-specific susceptibility (Nagai et al., 2007). This group then investigated cell death pathways in ESCMNs and found that glial toxicity resulted in increased activation of the apoptotic proteins Bax and Caspase-3 (Nagai et al., 2007). A follow-up study by Di Giorgio and colleagues found that hESCMNs were susceptible to glial toxicity as well (Di Giorgio et al., 2008). Other groups have reported similar non-cell autonomous, toxic glial effects with hESCMNs cultured with hSOD1G37R[+] astrocytes (Marchetto et al., 2008) or astrocytes isolated from patients with spontaneous ALS (Re et al., 2014) and mouse ESCMNs cultured with astrocytes generated from neural progenitor cells of sporadic ALS patients (Haidet-Phillips et al., 2011). In the study conducted by Di Giorgio et al. (2008), the authors used a genetic screen to identify possible sources of glial toxicity, and one candidate, the prostaglandin D2 receptor, was more highly expressed in SOD1G93A[+] glia than healthy control glia. Treatment of

healthy glia-hESCMN co-cultures with prostaglandin D2 promoted death of the hESCMNs and inhibition of the D2 receptor in SOD1G93A$^+$ glia promoted survival of co-cultured hESCMNs (Di Giorgio et al., 2008). A recent study by Eggan's group has further investigated this finding and demonstrated that the DP1 isoform of the D2 receptor is responsible for mediating glial toxicity. SOD1G93A$^+$ mice that lacked DP1 exhibited longer lifespans (~7%) compared to SOD1G93A$^+$ mice with normal DP1 expression. In addition, these mice displayed reduced microglial activation and had greater motoneuron survival compared to SOD1G93A$^+$ mice with wildtype DP1 expression (de Boer et al., 2014). This series of studies provides an illustrative example of how *in vitro* systems utilizing ESCMNs and other cells (in this case, glia) can be used as tools to investigate mechanisms inherent in ALS pathology and elucidate potential therapeutic targets.

1.5 The Advent of Induced Pluripotent Stem Cells for Motoneuron Disease Modelling

While ESCMNs have proven to be of use in motoneuron disease modelling, the use of human ES cells is not ideal for modelling disease. It is fraught with ethical considerations and the ability to model sporadic disease is lacking. In the case of late-onset diseases such as Alzheimer's disease or ALS, it is essential to be able to generate neurons from patients in order to study disease pathophysiology to discover potential therapeutic targets for drug treatment. The advent of induced pluripotent stem (iPS) cell technology has allowed researchers to circumvent the problems of working with human ES cells. This technology was first introduced by Shinye Yamanaka's group in 2006, whereby they managed to de-differentiate postmitotic, somatic cells (for e.g. fibroblasts) into pluripotent stem cells using viral transduction of a combination of only four genes: Klf4, c-Myc, Sox2 and Oct4 (known as the Yamanaka factors) (Takahashi and Yamanaka, 2006). Since then, many different approaches have been used to generate iPS cells, including a variety of methods used to deliver pluripotency factors to differentiated cells (such as use of lentiviruses and episomes) involving different combinations of pluripotency-promoting genes, including the Yamanaka factors, Lin28 and Nanog (Yu et al., 2007; 2009). A very recent study by Buganim and colleagues has demonstrated that generation of iPS cells with the genes

Sall4, Nanog, Esrrb, and Lin28 resulted in the most efficient generation of high quality iPS cells as defined by pluripotency potential (Buganim et al., 2014). A recent iPS cell generation protocol has been developed utilizing small molecule inhibition of the Notch signalling pathway and avoiding the use of the potent oncogenes c-Myc and Klf4, which is an important development limiting the danger of iPS cells used in transplantation studies (Ichida et al., 2014; Nakagawa et al., 2008).

After only 2 years following the first report of iPS cell technology, iPS cell-derived motoneurons (iPSCMNs) were generated from ALS patients by Kevin Eggan's group. Fibroblasts were isolated from the skin of patients and then subsequently de-differentiated into iPS cells using viral vectors containing the 4 Yamanaka factors. The iPS cells were then differentiated into motoneurons using standard ESCMN factors including RA and a Shh signalling agonist (Dimos et al., 2008) (see Figure 1.1, middle column). In the same year, iPS cells generated from fibroblasts of an SMA patient were differentiated into motoneurons capable of exhibiting features of SMA, including decreased SMN expression (Ebert et al., 2008). These findings demonstrate the capacity of iPSCMNs to faithfully recapitulate a disease phenotype and support the use iPS cells to model disease *in vitro*. While these studies were important in demonstrating that differentiation of cells which express proteins expressed by motoneurons (such as ChAT, Hb9 and Tuj1, a neurofilament protein), many questions remained regarding the functional properties of the motoneurons generated from iPS cells. Since these initial studies, iPSCMNs have been found to fire repetitive action potentials in response to injected current (Karumbayaram et al., 2009; Hu et al., 2010) and form putative NMJs when co-cultured with a muscle cell line, as evidenced by association of motoneurons with AChRs (Mitne-Neto et al., 2011). While these findings are indeed indicative of iPSCMNs possessing motoneuron-like characteristics, many questions remain about the functional capabilities of iPSCMNs. For example, do iPSCMNs exhibit the passive membrane properties and active firing properties of developing and mature spinal motoneurons? Can iPSCMNs form physiologically-relevant NMJs with co-cultured muscle, and do these NMJs develop in a manner similar to their endogenous counterparts? Determining whether iPSCMNs develop in a similar manner as endogenous

motoneurons and whether they truly possess the mature, functional characteristics of motoneurons is the focus of the study I present in Chapter 2.

Despite many questions remaining about the functional properties of iPSCMNs, several studies have since used iPSCMNs for research into motoneuron disease mechanisms and potential therapeutic targets. For example, Bilican and colleagues generated iPSCMNs from fibroblasts of a patient harbouring the TDP-43 M337V mutation and found that these cells exhibited enhanced expression of detergent-resistant, insoluble TDP-43 and reduced survival compared to healthy control iPSCMNs, which demonstrates that iPSCMNs can recapitulate key aspects of TDP-43-associated ALS pathology (Bilican et al., 2012). Burkhardt and colleagues managed to recapitulate TDP-43 accumulation in iPSCMNs from spontaneous ALS patient fibroblasts that correlated with TDP-43 aggregation in the same patient's motoneurons as revealed by post-mortem analysis, further verifying the ability of iPSCMNs to recapitulate ALS pathology (Burkhardt et al., 2013). Egawa and colleagues found similar increases in insoluble TDP-43 levels in ALS patient-derived iPSCMNs and identified a drug, the histone acetyltransferase inhibitor anacardic acid, which lowered insoluble TDP-43 protein levels (Egawa et al., 2012). It remains to be determined if anacardic acid can be used to treat TDP-43-mediated ALS pathology.

In addition to TDP-43 pathology, iPSCMNs have been used to investigate other target genes involved in ALS. For example, recently Sareen and colleagues investigated iPSCMNs derived from patients who presented with C9ORF72 hexanucleotide repeats (Sareen et al., 2013). They found that these motoneurons developed hexanucleotide repeat-containing RNA foci, which is similar to that seen in patient motoneurons. As well, patient iPSCMNs exhibited reduced capacity to fire repetitive action potentials due to a decrease in membrane excitability. This effect was found to be caused by altered expression of genes associated with regulating membrane excitability, including DPP6, a membrane protein that interacts with voltage-gated K^+ channels, which has previously been associated with ALS (van Es et al., 2008). Treating iPSCMNs with antisense nucleotides to knockdown expression of C9ORF72 reduced RNA foci and corrected expression of DPP6, suggesting that this approach may prove useful as a therapeutic strategy (Sareen et al., 2013). These results, along with the finding that the knockdown of

C9ORF72 had no apparent effect on healthy iPSCMNs, support the hypothesis that the deleterious effects of the hexanucleotide repeat are due to a toxic gain of function. Altered fired properties were also observed in a more recent study of iPSCMNs generated from ALS patients with SOD1, FUS and C9ORF72 mutations (Wainger et al., 2014), however this group found that these iPSCMNs were hyperexcitable in comparison to healthy controls. The authors postulate that the discrepancy between their findings and those of Sareen et al. (2013) may be due to differences in the ages of the iPSCMNs, as the cells are weeks older in the study by Sareen and colleagues at the time of recording. Wainger and colleagues suggest that as iPSCMNs containing ALS-causing mutations age, their resting membrane properties could change and they lose their hyperexcitability as a result of changes in Na^+ channel activation. A more depolarized resting membrane potential might result in progressive inactivation of Na^+ channels, thus resulting in a decline in excitability. Indeed, embryonic motoneurons from $SOD1G93A^+$ mice exhibit hyperexcitability while adult motoneurons do not, suggesting a possible developmentally-regulated change in membrane excitability in these motoneurons (Kuo et al., 2004; Pieri et al., 2003; van Zundert et al., 2008; Delestree et al., 2014). Wainger and colleagues suggest that the hyperexcitability observed in their study was possibly due to a dampening of delayed rectifier K^+ currents that was present in ALS patient-derived iPSCMNs compared to healthy controls. Treatment with retigabine, a K^+ channel activator, reduced hyperexcitability and increased survival of iPSCMNs carrying mutated SOD1 as measured up to 30d. in culture (Wainger et al., 2014). Taken together, these results suggest that iPSCMNs are a useful tool that can be employed to study the progressive pathophysiology of ALS. As well, work continuing along these lines should allow researchers to identify specific therapeutic targets and test drugs directed towards those targets.

In addition to ALS, iPSCMNs have been used to investigate other motoneuron diseases such as SMA. Corti and colleagues generated iPSCMNs from an SMA patient and found that these motoneurons formed fewer NMJs on mouse myotubes, had reduced axon length and had smaller cell body diameters than control iPSCMNs at 8 weeks in culture (Corti et al., 2012). When patient iPSCMNs were genetically corrected with a functional SMN gene, these deficits were partially overcome and when healthy or

corrected iPSCMNs were transplanted into the spinal cord of neonatal mice with a severe form of SMA, the motoneurons were found to successfully engraft into the spinal cord, resulting in increased body size and survival of the mice (Corti et al., 2012). These results suggest that iPSCMNs have a neuroprotective effect in a mouse model of SMA and further emphasize the ability of iPSCMNs to be utilized in therapeutics designed to treat SMA.

The utilization of iPSCMNs for modelling motoneuron diseases and developing therapeutics remains a high priority for researchers of these diseases (for recent reviews, see Arbab et al., 2014; Veyrat-Durebex et al., 2014; Richard and Maragakis, 2014). However, while these developments remain exciting, questions remain about the effectiveness of iPS cells with regards to disease modelling. As mentioned above, the ability of iPSCMNs to exhibit mature functional properties of motoneurons, and whether the developmental characteristics of iPSCMNs resembles that of maturing endogenous motoneurons (or ESCMNs) still remains largely untested (see Chapter 2). Other issues with iPS cells concern their pluripotency capabilities. Reports of the inability to remove epigenetic memory of the cells retained from their cell type of origin may prove a limiting factor on the use of iPS cells and the cell types derived from them, including iPSCMNs (Kim et al., 2010; Ma et al., 2014). As well, the variety of techniques used to generate iPS cell may have an effect on their capacity for pluripotency, as described above (Buganim et al., 2014). Despite these concerns, the evidence presented in this thesis and elsewhere suggests that iPSCMN technology can provide a powerful tool for the development of therapeutics for the treatment of motoneuron diseases.

1.6 Induced motoneurons as a tool for modelling motoneurons *in vitro*

While iPSCMNs allow for the isolation and generation of motoneurons from individuals, a more direct approach that bypasses the need for dedifferentiation has been developed that allows conversion of one postmitotic cell type to another – a process known as transdifferentiation. Son and colleagues from the Eggan lab have employed this approach to generate motoneurons from fibroblasts. Using retroviral transduction, this group has found that 7 factors – Ascl1, Brn2, Myt1l, Lhx3, Hb9, Isl1 and Ngn2 – were sufficient for transdifferentiating mouse embryonic fibroblasts into motoneurons (Figure 1.1, right

column). Some of these genes were selected based on previous work showing that three of these factors, Ascl1, Brn2 and Myt1l, were required for the transdifferentiation of fibroblasts into neurons of a generic phenotype (Vierbuchen et al., 2010). The other four factors – Lhx3, Hb9, Isl1 and Ngn2 – were chosen based on their importance for motoneuron development (reviewed by Alaynick et al., 2011). One extra factor, Neurod1, which was previously demonstrated to be necessary for the conversion of human fibroblasts into neurons (Pang et al., 2011), was required to reprogram human fibroblasts into human iMNs along with the other seven factors. Interestingly, iMNs were found to be directly reprogrammed from fibroblasts without an intermediary progenitor step, as transdifferentiating iMNs did not express the neural progenitor marker Nestin (Son et al., 2011).

iMNs were found to exhibit a gene expression pattern that more closely resembled that of embryonic motoneurons and ESCMNs than fibroblasts, indicating that successful transdifferentiation had taken place. They expressed voltage-gated Na^+ channel subunits along with voltage-gated and Ca^{2+}-activated K^+ channels found in embryonic motoneurons, which presumably allowed for the similar electrophysiological profile between iMNs and endogenous embryonic motoneurons. iMNs were found to be capable of firing repetitive action potentials when depolarized and treatment with GABA, glycine and the glutamate receptor agonist kainate induced inward currents. Further to these electrophysiological observations, iMNs were found to extend neurites in culture and express genes associated with motoneurons including ChAT and the cytoskeletal protein MAP-2, suggesting that the morphological and cellular characteristics of iMNs resemble those of endogenous motoneurons (Son et al., 2011).

iMNs also displayed functional and survival characteristics of motoneurons. When these cells were co-cultured on myotubes derived from the C2C12 muscle cell line, treatment with curare, a nicotinic AChR antagonist, abrogated contraction of myotubes by 10 days in co-culture, suggesting that iMNs were making synaptic contact with myotubes. iMNs also displayed similar survival rates as ESCMNs when exposed to toxic glia as they were susceptible to death in response to co-culture with SOD1G93A expressing glia (Di Giorgio et al., 2007; Nagai et al., 2007). These results, along with other functional characteristics of iMNs that I went on demonstrate as discussed in

Chapter 3, indicate that these cells could be as useful for *in vitro* motoneuron disease modelling as ESCMNs and iPSCMNs.

1.7 Thesis Objectives

The studies I present in this thesis are centred on the main theme of *in vitro* motoneuron modelling. As mentioned above, many uncertainties remain concerning the utility of stem cell-derived motoneurons for appropriately modelling motoneuron development and disease. The work presented in this thesis addresses some of these concerns. The specific objectives of each chapter are as follows:

Chapter 2: To determine whether iPSCMNs exhibit the necessary functional capabilities and phenotypes of endogenous motoneurons to validate their use in motoneuron disease modelling.

Chapter 3: To determine if iMNs possess functional characteristics of endogenous motoneurons in order to validate their use in motoneuron disease modelling.

Chapter 4: To establish a protocol for developing ESCMNs with a predominantly limb-innervating phenotype for use in modelling both motoneuron development and disease.

Figure 1.1 Illustration showing the derivation of motoneurons using three distinct techniques

(1) ES cells isolated from the inner cell mass of a blastocyst differentiate into motoneurons when treated with RA and a Smoothened agonist. (2) Skin cells are converted into iPS cells by forced expression of specific genes (typically Oct4, Klf4, Sox2, and c-Myc). iPS cells later differentiate into motoneurons when exposed to RA and a Smoothened agonist. (3) Skin cells are directly converted into motoneurons by forced expression of seven genes. Figure legend (altered) and figure reprinted with permission (Chipman et al., 2012).

Motoneurogenesis

1. Embryonic stem (ES) cells

Fertilized egg

Blastocyst

Inner Cell Mass (ICM) (ES cells)

RA Smo-Agonist

2. Induced pluripotent stem (iPS) cells

Skin Biopsy

Oct4
Klf4
Sox2
c-Myc

Fibroblasts

Pluripotent Stem (iPS) Cells

RA Smo-Agonist

3. Induced motor neurons (iMNs)

Skin Biopsy

Ascl1   Myt1l
Isl1   Ngn2
Lhx3   Brn2
Hb9

Fibroblasts

Motor Neuron

Drug screening

Motor neuron transplantation

©www.maritimemedicaldesign.com

CHAPTER 2: MOTONEURONS DERIVED FROM INDUCED PLURIPOTENT STEM CELLS DEVELOP MATURE PHENOTYPES TYPICAL OF ENDOGENOUS SPINAL MOTONEURONS

Contribution statement

Abstract

Induced pluripotent cell-derived motoneurons (iPSCMNs) are sought for use in cell replacement therapies and treatment strategies for motoneuron diseases such as amyotrophic lateral sclerosis (ALS). However, much remains unknown about the physiological properties of iPSCMNs and how they compare to endogenous spinal motoneurons or embryonic stem cell-derived motoneurons (ESCMNs). In the present study, we first used a proteomic approach and compared protein expression profiles between iPSCMNs and ESCMNs to show that <4% of the proteins identified were differentially regulated. Like ES cells, we found that mouse iPS cells, treated with retinoic acid and a smoothened agonist, differentiated into motoneurons expressing the LIM homeodomain protein Lhx3. When transplanted into the neural tube of developing chick embryos iPSCMNs selectively targeted muscles normally innervated by Lhx3^{+} motoneurons. In vitro studies showed that iPSCMNs form anatomically mature and functional neuromuscular junctions (NMJs) when co-cultured with chick myofibres for several weeks. Electrophysiologically, iPSCMNs developed passive membrane and firing characteristic typical of postnatal motoneurons after several weeks in culture. Finally, iPSCMNs grafted into transected mouse tibial nerves projected axons to denervated gastrocnemius muscle fibres where they formed functional NMJs, restoring contractile force and attenuated denervation atrophy. Taken together, iPSCMNs possess many of the same cellular and physiological characteristics as ESCMNs and endogenous spinal motoneurons. These results further justify using iPSCMNs as a source of motoneurons for cell replacement therapies and to study motoneuron diseases such as ALS.

Introduction

Induced pluripotent stem (iPS) cell-derived motoneurons (iPSCMNs) are being explored as a means to study motoneuron diseases and to develop therapeutics to treat amyotrophic lateral sclerosis (ALS) (Dimos et al., 2008; Bilican et al., 2012; Burkhardt et al., 2013; Yao et al., 2013) and spinal muscular atrophy (SMA) (Corti et al., 2012). Preclinical studies are proceeding using iPSCMNs, harboring genetic mutations causing ALS, to screen for small molecules promoting motoneuron survival and function (Egawa et al., 2012; Yang et al., 2013). While it is hopeful that this approach will yield novel findings, its success is highly dependent on the supposition that iPSCMNs possess the same cellular and physiological traits as their endogenous counterparts. This assumption, however, has not been rigorously examined.

Embryonic stem cell-derived motoneurons (ESCMNs), on the other hand, have been shown to be remarkably similar to their endogenous counterparts (reviewed by Lopez-Gonzalez and Velasco, 2012; Chipman et al., 2012). ESCMNs develop mature electrophysiological firing properties and acquire the same passive membrane properties as spinal motoneurons (Miles et al., 2004). ESCMNs project axons to muscles lining the vertebral column when transplanted into the neural tube of chick embryos because they express the LIM homeodomain factor conferring medial motor column identity (Wichterle et al., 2002; Soundararajan et al., 2006; Soundararajan et al., 2007; Soundararajan et al., 2010). ESCMNs form functional, and remarkably mature, neuromuscular junctions (NMJs) when co-cultured with muscle fibres for several weeks (Chipman et al., 2014). Finally, ESCMNs restore contractile force to denervated muscles by forming functional NMJs with denervated myofibres when transplanted into the distal stump of a transected peripheral nerve (Yohn et al., 2008) in a manner analogous to embryonic motoneurons (Thomas et al., 2000). Thus, ESCMNs develop the same cellular, behavioural and physiological characteristics as their endogenous counterparts, and they are the same traits desired for iPSCMNs.

In this study, we compared mouse iPSCMNs with mouse ESCMNs to determine whether they possess the same developmental and physiological characteristics. We

began by comparing global protein expression profiles between iPSCMNs and ESCMNs and found that less than 3% of the proteins were differentially regulated. These results indicate that iPSCMNs and ESCMNs are similar at the level of protein expression. We then went on to systematically compare iPSCMNs with known traits of ESCMNs and found that they were also very similar with respect to axon targeting, the development of passive and active firing properties and their ability to form anatomically mature and functional NMJs with co-cultured muscle fibres. Finally, iPSCMNs restored contractile force to denervated muscles to the same extent as ESCMNs when transplanted into transected peripheral nerves of mice. These findings support the hypothesis that iPSCMNs form functional motoneurons that are remarkably similar to both ESCMNs and endogenous motoneurons. These traits further validate their use for studying motoneuron diseases and for developing therapeutics aimed to treat them.

Methods

Culturing of induced pluripotent stem cells

Isolated mouse iPS cell colonies (and ES cell colonies for experiments using ESCMNs) containing enhanced green fluorescent protein (GFP) under the Hb9 promoter were differentiated into motoneurons (iPSCMNs) as described previously for ES cell colonies (Wichterle et al., 2002; Miles et al., 2004; Soundararajan et al., 2006; Chipman et al., 2014). In brief, iPS cells were grown as aggregated cultures in DFK10 or ADFNK media to form free floating embryoid bodies. DFK10 medium consisted of DMEM (Gibco 11995-073) and Ham's F-12 media (Specialty Media) in a 1:1 ratio supplemented with knock-out serum replacement (10% by volume; Invitrogen), penicillin/streptomycin (1% by volume; Sigma), N2 supplement (2.4% by volume; Invitrogen), glucose (4500 mg/l), L-glutamine (200 mM), heparin (1 u/l; Sigma), and β-mercaptoethanol (0.1 mM; Sigma). After 2 days, the embryoid bodies were treated with a smoothened agonist (500 nM; Enzo Life Sciences) and retinoic acid (1 μM; Sigma, St. Louis, MO) and cultured as free-floating cells for an additional 5 days. GFP expression was monitored as an assessment of differentiation and only embryoid bodies with robust and homogeneous GFP expression were used for further assessment.

Culturing iPSCMNs and immunocytochemistry

iPSCMNs were dissociated using TrypLE (Invitrogen) and plated on Matrigel (BD Biosciences) coated coverslips (~ 350 000 cells/coverslip) and grown for 24-48 hrs. in DFK10 and fixed for approximately 20 min. in 3.7% formaldehyde. Cells were then immunostained for both Lhx1 (mouse monoclonal, 1:2, supernatant, developmental studies hybridoma bank, (DSHB)) and Lhx3 (mouse monoclonal, 1:5, supernatant, DSHB) expression. Cells were incubated in primary antibody with 0.3% Triton X/PBS solution and goat serum for 1 hour. Cells then underwent a 1 hour incubation with the following secondary antibodies in 0.3% Triton X/PBS solution: goat anti-mouse Cy3 (Jackson Immunoresearch Laboratories, 1:500) and goat anti-rabbit Alexa Fluor 488 (Molecular Probes, 1:500) for 1 hour at room temperature. Cells were then washed in PBS for 3x10 min. before mounting on superfrost slides (Fischer Scientific) coated in a mounting media consisting of a 50% glycerol/PBS mixture containing 0.03 mg/mL ρ-

phenylenediamine to prevent loss of fluorescent signal for visualization. For cell counts, all Lhx3$^+$/GFP$^+$ or Lhx1$^+$/GFP$^+$ cells in 4 fields of view per coverslip (at 20x) were counted. Total cell numbers were as follows for 3 experiments: Lhx3$^+$/GFP$^+$ cells = 844, Lhx1$^+$/GFP$^+$ cells = 1008 with mean cell counts of 281.3 ± 131.9 (Lhx3$^+$/GFP$^+$, mean ± one standard deviation) and 336 ± 63.6 (Lhx1$^+$/GFP$^+$). Images were acquired on a laser scanning-confocal microscope (Zeiss LSM 510) and contrast and brightness adjustments were made on Adobe Photoshop CS5 software.

Proteomic analysis of iPSCMNs and ESCMNs

Following fluorescent-activated cell sorting to purify the GFP$^+$ iPSCMNs and ESCMNs, cells were stored at -80 ^{0}C until processed. Samples were thawed and diluted in 500 μl of 50 mM TEAB pH 8 (Sigma T7408) with protease inhibitor (Set III Calbiochem 539134). Cells were lysed cells by probe sonication, 3x5 second cycles at power setting 1 (Fisher Sonic dismembrator model 100). An aliquot containing 50 μg of protein from each sample was diluted to a final volume of 600 μl in 50 mM TEAB containing 0.1% Rapigest surfactant (Waters 186001861) samples sonicated a further 3x5 second cycles to ensure dissolution. Samples were reduced with 5mM DTT (Sigma D9163) at 60°C for 30 min, alkylated with 15 mM iodoacetamide (Sigma I6125) for 30 min at room temp, and then digest with trypsin (Promega V5113) at a 50:1 protein to trypsin ratio overnight at 37°C. Resulting peptides acidified to pH<3 with TFA (Sigma 299537), filtered through 0.45 μm filter to remove hydrolyzed Rapigest detergent and desalted using SPE cartridges (Waters HLB 186000383). Samples resuspended in 50 μl water with 3% acetonitrile 0.1% formic acid. Each sample was injected 6 times in random order using 1 μl injection volume. Chromatographic separations were conducted using a Dionex Ultimate 3000RSLCnano system equipped with a 15 cm x 100 μm Onyx monolithic C18 column (Phenomenex CHO-7646). The separation was carried out using the following gradient (A: 0.1% formic acid in water, B: 0.1% formic acid in acetonitrile) at 300 nl/min (see Table 2.1).

Mass spectra were acquired on a Thermo Orbitrap Velos Pro using Xcalibur software. Data was acquired using data directed analysis where the m/z values of tryptic

peptides were measured using a MS scan in FT-MS mode followed by MS/MS scans of the 10 most intense peaks using IT-MS mode.

Data analysis was conducted using Proteome Discoverer for protein identification and Sieve for chromatographic alignment, normalization and peak integration. Data was then extracted from the Sieve sdb database files using a series of custom scritpts written in R. Protein ontologies were assigned using gene list analysis tools in PANTHER (pantherdb.org).

In ovo transplantation of iPSCMNs and immunohistochemistry

Transplants were grafted into male and female chick embryos as previously described (Soundararajan et al., 2006) in accordance with the guidelines of the Canadian Council on Animal Care and the Dalhousie University Committee on Laboratory Animals. Eggs (*Gallus Domesticus* from Truro, NS, Canada) were kept at 37^0C in a humidified incubator. A 1-2cm^2 section of the eggshell was removed with a dental drill to access the embryos of chicks at Hamburger Hamilton (HH) st.17. The vitelline membranes were visualized with 0.1% neutral red (Sigma) dissolved in distilled water and opened with forceps at the level of the hind limb bud. An incision of 1-1.5 somites in length was made along the midline of the neural tube at the rostral extent of the developing hind limb bud (T7-L1) using a flame-sterilized tungsten needle (0.077mm wire, World Precision Instruments). The neural tube was then splayed open and a portion of the medial aspect of the ventral neural tube (corresponding to the ependymal layer lining the lumen adjacent to the ventral horn) was removed with suction pipetting. For this procedure, a borosilicate pipette (World Precision Instruments) was pulled to produce a sharp tip at one end (for tissue removal) while the blunt end was inserted into polyethylene tubing (BD Intramedic, PE 190). The tubing was placed in mouth to generate suction. An embryoid body of iPSCMNs containing approximately 200 cells was then guided into the resultant hole in the neural tube using a tungsten needle. The eggs were resealed with scotch tape and returned to the incubator. 5 or 7 days later, the chick embryos (HH st.31 or st.35-36, respectively) were harvested and processed as follows: embryos were decapitated and fixed in 4% paraformaldehyde for 1 hr. at 4^0C, washed once in PBS followed by an overnight wash in PBS at 4^0C. Embryos were then cryoprotected in a

30% sucrose/PBS solution for 2 hrs. at 4^0C, mounted in OCT (Tissue Tek) and frozen at -80^0C. 30 μm transverse sections were cut on a cryostat and mounted on superfrost slides (Fischer Scientific). Slides were dried and washed in PBS prior to immunohistochemistry.

For immunohistochemical analyses, the following primary antibodies were used: rabbit anti-GFP (Chemicon, 1:1000), mouse anti-Tuj1 (Covance, 1:1000) and mouse anti-SV2 (1:50, DSHB). Slides were incubated with primary antibodies in a solution of 0.3% Triton X/PBS with goat serum overnight. Following multiple washes in PBS for 30 min., slides were incubated with the following secondary antibodies in 0.3% Triton X/PBS solution: goat anti-mouse Cy3 (Jackson Immunoresearch Laboratories, 1:500), goat anti-mouse Alexa Fluor 647 (Molecular Probes, 1:500) and goat anti-rabbit Alexa Fluor 488 (Molecular Probes, 1:500) for 1 hour at room temperature. As well, slides were incubated with Alexa Fluor 647 conjugated α-btx (Molecular Probes, 1:500) for 1 hour at room temperature where required. Following washes in PBS, slides were then mounted as described above. Images were captured with a digital camera (C4742; Hamamatsu Photonics, Hamamatsu, Japan) in conjunction with digital imaging acquisition software (IPLab; Version 4.0; BD Biosciences, Rockville, MD, USA).

Analyses of axonal projections from the chick spinal cord were performed as follows: using Neurolucida projections from 3 separate embryos, the width of a line drawn across the GFP$^+$ fascicle projecting dorsally towards the epaxial muscles was compared to the width drawn across GFP$^+$ fascicles projecting ventrally towards the limb. The cross-sectional areas of the fascicles were then calculated (assuming a circular area, πr^2) and relative sizes compared.

iPSCMN/myofibre co-cultures and immunocytochemistry
For generating myofibres, the medial head of the adductor superficialis muscles of Hamburger Hamilton St. 36 chicks were isolated and plated on 13mm sterile thermanox plastic coverslips (Nunc) in 24-well plates as previously described before addition of iPSCMNs (Chipman et al., 2014, reprinted here with permission). Prior to plating, the

cells were triturated in Hanks Balanced Salt Solution (HBSS, Gibco) or F10 media (Gibco) and counted (100 000 cells plated per well). Cultures were maintained in a 37^0C incubator in F10 media (Gibco) supplemented with 0.44 mg/mL calcium chloride, 10% horse serum, 5% chicken serum and 2% penicillin:streptavidin for 2-3 days. 1 hour prior to addition of motoneurons, the F10 media was replaced with Neurobasal media (Gibco) supplemented with 1x B27 (Gibco), 1% L-glutamine and 1% penicillin:streptomycin. Approximately half of the media in each well was replaced every 2-3 days until fixation with 3.7% formaldehyde. Co-cultures were supplemented with 5 ng/mL ciliary neurotrophic factor (CNTF) and 10 ng/mL glial cell-derived neurotrophic factor (GDNF) every two days for the first week following plating of motoneurons. For immunohistochemical analysis of the co-cultures, cells were incubated in a solution containing rabbit anti-GFP IgG (Chemicon, 1:2000), mouse anti-SV2 (1:50, DSHB) primary antibodies and goat serum for approximately 1 hr. Cells were then washed in PBS multiple times for 30 min. before incubating in goat anti-rabbit Alexa Fluor 488 (Molecular Probes, 1:500), goat anti-mouse Alex Fluor 647 (Molecular Probes, 1:500) and tetramethylrhodamine-conjugated (TMR) α-bungarotoxin (btx) (Invitrogen, 1:500). All antibodies were in a 0.3%Triton X/PBS solution. Coverslips were washed in PBS and mounted as described above. Images were acquired on a laser scanning-confocal microscope (Zeiss LSM 510 or 710) or with a digital camera (C4742; Hamamatsu Photonics, Hamamatsu, Japan). Acetylcholine receptor area (based on TMR α-btx labelling) was quantified using IPLab software (Version 4.0; BD Biosciences, Rockville, MD, USA). Orthogonal images were rendered and edited with LSM imaging software (Zeiss) and further contrast and brightness adjustments were performed on Adobe Photoshop version CS5.

FM4-64FX dye loading and imaging

To assess vesicular cycling at neuromuscular junctions, co-cultures were incubated with 5 μM FM4-64FX (hereafter referred to as FM4-64) and motor terminals of iPSCMNs were loaded by electrical stimulation. Experiments were then conducted as previously described and reprinted here with permission (Chipman et al., 2014). Co-cultures were preincubated for 30 minutes prior to 5 minutes of high frequency, repetitive stimulation.

1 second trains of 50 Hz stimuli (20V pulses with 0.5ms pulse widths), delivered at a 0.5Hz train rate for 5 minutes were used to stimulate the co-cultures. A maximum of 4 wells (in a 24 well dish) containing co-cultures were stimulated at a time and connected in parallel with silver electrodes immersed into the culture media. Myofibre contraction was used as an indicator of effective stimulation. Wells filled with 3M KCl flanked those containing the co-cultures and were connected in parallel via silver wires as well as attached to a Grass technologies S88 stimulator. Following stimulation, co-cultures were left to rest for 10 minutes to allow for compensatory endocytosis (Gaffield and Betz, 2007). They were then washed in 1:3 Neurobasal/HBSS solution to reduce extracellular calcium concentration (0.66 mM) which, along with 2.5 µM tetrodotoxin, was used to inhibit further vesicular cycling. TMR α-btx was added during the washes to label postsynaptic endplates. Co-cultures were then fixed with 3.7% formaldehyde. Z stacks of identified neuromuscular junctions were captured with an LSM510 laser scanning confocal microscope (Zeiss Microimaging, Thornwood, NY, USA) and managed using Zen 2009 or 2011 software (Zeiss Microimaging). A 488nm laser was used to excite FM4-64 and emission was captured with a 685 nm longpass filter.

Intracellular recordings of iPSCMN-chick myofibre co-cultures
Sharp electrode recording techniques were used to assess synaptic function at 12-27 day old co-cultured neuromuscular junctions as described previously (Miles et al., 2004; Soundararajan et al., 2007; portion reprinted from Chipman et al., 2014 with permission). Experiments were performed in a recording chamber containing 1 ml of 50% Neurobasal/Hibernate low fluorescence solution (Brain Bits, Springfield, IL, used to buffer pH). The application of a non-function blocking AChR antibody, mAb35, conjugated to an Alexa Fluor546 fluorochrome using a Monoclonal Antibody Labeling Kit (Invitrogen, 1:1000) was used to visually identify postsynaptic endplates. Cells were incubated with mAb35 for approximately 1 hour prior to the recording session to ensure sufficient labelling. A CCD camera mounted on an Olympus upright fluorescence microscope (Centre Valley, PA) was used to visually monitor neuromuscular junctions which were identified by the expression of GFP in the axons of iPSCMNs in apposition to mAb35-labelled endplates. Images of neuromuscular junctions were captured using a

Nikon digital camera. Micropipettes used for recordings were filled with 3M KCl and had tip resistances of approximately 30 MΩ. A Sutter amplifier in oscilloscope mode and Clampex 10.2 (Molecular Devices) were used to acquire and process postsynaptic responses. All data were analyzed and representative traces were generated using MiniAnalysis (Synaptosoft, Decatur, GA) and AxoScope 10.2 software (Molecular Devices). Frequency histograms were constructed using SigmaPlot 11.0 (Systat Software). All cells recorded from had resting membrane potentials that varied from ~ -25mV to -65mV, values which were similar to those previously reported for post-synaptic membrane potentials of in vitro rat spinal cord-myotube co-culture (Robbins and Yonezawa, 1971).

Whole Cell Patch Clamp Recordings of iPSCMNs

iPSCMNs on matrigel-coated coverslips were continuously perfused in a recording chamber with oxygenated (95% O_2 + 5% CO_2) Ringer's solution (111 mM NaCl, 3.08 mM KCl, 11mM glucose, 25 mM $NaHCO_3$, 1.25 mM $MgSO_4$, 2.52 mM $CaCl_2$, 1.18 mM KH_2PO_4, pH 7.4) at room temperature for approximately 20 min. prior to recording to allow the cells to adjust to recording conditions. Perfusion continued throughout the recordings, where a DAGE-MTI IR-1000 CCD camera connected to an Olympus BX51WI microscope was used to visualize GFP^+ iPSCMNs. Recordings were made in current-clamp mode using a MultiClamp 700B amplifier (Molecular Devices). A Digidata 1400A board (Molecular Devices), controlled by pCLAMP10.3 (Molecular Devices), was used to filter analog signals at 10 kHz. Recording solution containing 128 mM K-gluconate, 4 mM NaCl, 0.0001 mM $CaCl_2$, 10 mM HEPES, 1 mM glucose, 5 mM Mg-ATP, 0.3 mM GTP-Li, (pH 7.2) was loaded into patch-clamp recording pipettes with a resistance of 4-7 MΩ. 0.4 mg/ml lucifer yellow dilithium salt (LY, Sigma-Aldrich) was added to the pipette solution prior to recording to allow visualization of recorded iPSCMNs. To assure similar measuring conditions, all cells were held at -60mV with a tonic DC current. Data were obtained by Clampex 10.3 (Molecular Devices) and analyzed by AxoScope 10.2 (Molecular Devices) software. Input resistance and capacitance of iPSCMNs were calculated by measuring response to repetitive, small negative steps of -10 mV for 100 ms. For investigating firing properties of iPSCMNs, 1

sec. pulses of depolarizing current were delivered in increments of 5, 10 or 20 pA. Data were analyzed and statistics were generated with SigmaPlot 11 software (Systat Software).

iPSCMN implantation and force recording

All procedures performed were approved by the Dalhousie Animal Care Committee and complied with the Canadian Council of Animal Care. All surgeries were performed on male mice. The surgical technique used in this study has been previously described (Yohn et al., 2008). C57BL/6 male mice at 6-7 weeks of age (Charles River Laboratories) were anesthetized with the inhalant anesthetic isoflurane. Using sterile technique, the sciatic nerve was transected and its proximal stump was embedded under the gluteus maximus muscle in order to prevent endogenous reinnervation through the graft site. Approximately 10,000 dissociated iPSCMNs contained within 0.1µl of medium were injected into the tibial nerve ~ 15 mm from the point where the MG nerve entered the MG muscle. Injections were performed using a fine borosilicate glass capillary tube (World Precision Instruments) pulled to an inner diameter of ~ 60 µm using PP830 pipette puller (Narishige). The injectate was confined within the tibial nerve by ligating it proximally. In order to channel all axonal outgrowths to the MG muscle, all branches of the tibial nerve except for the MG nerve were transected. Animals receiving implants are compared with control animals (uninjured, not implanted) and denervated surgical control animals.

After 6-7 weeks of implantation, the animals were sacrificed following which the tibial nerve containing the graft, along with the MG nerve and MG muscle were removed and immediately transferred to a recording chamber perfused with oxygenated mouse Tyrode solution (125mM NaCl, 24mM $NaHCO_3$, 5.4mM KCl, 1.8mM $CaCl_2$, 1mM $MgCl_2$ and 5% dextrose) at room temperature flowing at a rate of 4-5 ml/min. The tendo calcaneous was secured to a force displacement transducer (Grass Instruments FT03) using a silk suture. The tibial nerve was stimulated with a suction electrode connected to an S88 square pulse stimulator (Grass Instruments). Force signals were amplified with an AC DC strain gage amplifier (Grass P122) and captured using Axoscope software (Molecular Devices).

Maximal force was determined by adjusting the tension on the muscle and increasing the intensity of the stimulus (20 µs pulse) until stable force was reached. Tetanic forces were recorded with a stimulation frequency of 50Hz (1s).

Immunohistochemistry of nerve and muscle was performed in animals that were transcardially perfused with 4% paraformaldehyde. After overnight post fix, the tissue was cryoprotected and then frozen in Tissue Tek OCT (Sakura). The frozen tissue was cut on a cryostat (nerve-12µm, muscle 30µm). Feret's diameter of MG muscles and muscle fibres was measured using ImageJ software (National Institutes of Health).

iPS cell lines

Two mouse iPS cell lines were used in this study: one derived from a pure C57BL/6 background and one derived from a BL6/129 mixed background. Lines were generated using standard methods; mouse embryonic fibroblasts were transduced with Klf4, Sox2, and Oct4. The chick transplant studies and iPSCMN-myofibre co-culture experiments were conducted with both lines. The iPSCMN implantation studies were performed solely with the line derived from C57BL/6 background to prevent immune rejection.

Statistical Analyses

All statistics were performed using SigmaPlot 11 Software (Systat). Values are cited as mean ± one standard deviation. All tests used are described in the text.

Results

Protein expression is comparable between iPSCMNs and ESCMNs

Throughout this study, we used a mouse iPS cell line derived from transgenic mice (B6.Cg-Tg(Hlxb9-EGFP)1Tmj/J) expressing enhanced green fluorescent protein (GFP) under the direction of the motor neuron-specific promoter Hb9 (Arber et al., 1999; Wichterle et al., 2002). Approximately 20% (mean: 21.3% ±3.09) of the cells from this iPS cell line differentiated into GFP$^+$ motoneurons when treated with RA and SAG, as determined by FACS analysis. This is not significantly (p=0.162, n=3) different from the percentage of motoneurons derived from mouse HBG3 ES cells using the same differentiation protocol (mean: 17.5% ±2.29). Thus, the propensity for mouse iPS cells and ES cells to differentiate into motoneurons when treated with RA and SAG is the same.

To determine if there are differences between ES cell-derived motoneurons (ESCMNs) and iPS cell-derived motoneurons (iPSCMNs) we first undertook an unbiased proteomic approach and compared protein expression profiles between iPSCMNs and ESCMNs. Here, ESCMNs and iPSCMNs were sorted by fluorescence-activated cell sorting following differentiation prior to proteomic analysis. After trypsin digestion of the proteins, we performed a label-free, LC-MS/MS analysis of the resulting peptides in order to compare expression profiles, as described in the methods section. Quantification was perfomed using peptide peak areas and peptides with good precision (relative standard deviation less than 30%) were retained. These peptides were then filtered to eliminate peptides that match to multiple proteins. The unique peptides were then averaged to give overall expression levels for 3025 proteins. We next imported the data set into Panther (www.pantherdb.org) to annotate known gene ontology (GO) terms to determine if there were overall differences in the types of proteins identified in our screen. Over half (1531) of the proteins in the data set matched a GO term. The half that did not match were likely unstudied proteins with no known function. When the 1531 proteins were grouped into each GO term we found that the number (shown as a percentage) of proteins within each group was identical (Figure 2.1A). This indicates that the types of proteins identified by the screen, in the two cell types, were very similar.

Further analysis showed that ESCMNs and iPSCMNs express the same proteins of each GO term except for the general binding category (Figure 2.1B). Here, while over 500 general binding proteins were the same in ESCMNs and iPSCMNs, 93 were unique to ESCMNs and 50 to iPSCMNs (Figure 2.1B).

To determine whether the same proteins in ESCMNs and iPSCMNs are expressed at similar levels we integrated the intensity of each peptide and then averaged the peptides for any given protein to provide a fold change, defined here as the protein expression from the iPSCMNs divided by the intensity in the ESCMNs. Based on the variability measured, a p-value was also calculated, as shown in Figure 2.1(C). We detected 28 proteins up-regulated in iPSCMNs, and 87 down-regulated proteins (Tables 2.2 and 2.3, respectively). Therefore, of the original number of proteins identified, less than 4% met our criteria for differentially regulated (i.e. a ln expression ratio >0.7 or <-0.7 in Figure 2.1 C). Interestingly, the degree of differential regulation was also modest with the average fold change for the upregulated and downregulated proteins being 2.4 and -2.5, respectively.

Finally, we focused on several transcription factors known to be involved in neuron and/or motor neuron differentiation (Alaynick et al., 2011; Son et al., 2011). Although we focused on a number of transcription factors including Olig2, Nkx6.1, Nkx6.2, Ngn1, Ngn2, Lhx3, Hb9, Isl1, Isl2, Lmo4, Lhx1, FoxP1, Ascl1, Myt1l, and Brn2, we only detected Myt1l in our data set. Nine unique peptides were identified for Myt1l, so it was conclusively identified. Of note, Myt1l was not differentially regulated between the two samples (ratio of 1.1, p-value=0.5). Taken together, these results indicate that ESCMNs and iPSCMNs contain similar proteins at comparable levels of expression. The few proteins that were differentially expressed are not directly involved in motoneuron differentiation.

iPS cells preferentially differentiate into Lhx3$^+$ motor neurons when treated with RA and SAG

Previous studies showed that mouse ES cells treated with SAG and RA preferentially differentiate into a specific subpopulation of motoneurons expressing the LIM

homeodomain protein Lhx3 (Soundararajan et al., 2006; Soundararajan et al., 2007; Soundararajan et al., 2010). Lhx3$^+$ motoneurons reside in the medial aspect of the medial motor column and innervate epaxial muscles lining the vertebral column (Tsuchida et al., 1994). To determine whether iPS cells differentiate into the same motor neuron subset we plated embryoid bodies containing GFP$^+$ iPSCMNs onto a matrigel substrate and cultured them for an additional 2 days. The cells were then fixed and immunostained for LIM homeodomain proteins Lhx3 or Lhx1, the latter being a marker of motoneurons innervating the dorsal muscle mass in limbs (Tsuchida et al., 1994) (Figure 2.2 A). As observed with ESCMNs (Soundararajan et al., 2006; Soundararajan et al., 2007; Soundararajan et al., 2010), we found that the vast majority of the GFP$^+$ iPSCMNs were Lhx3$^+$ (82 ± 3.7%, n=3) while only 13 ± 1.4% (n=3) expressed Lhx1 (Figure 2.2 B). These results suggest that the process of motoneurogenesis using SAG and RA is similar between iPS and ES cells.

iPSCMNs project axons to peripheral targets appropriate for Lhx3$^+$ motor neurons when transplanted into the developing chick spinal cord

In the spinal cord, Lhx3$^+$ motor neurons reside in the medial aspect of the medial motor column (MMC$_m$; Sharma et al., 1998). In the periphery, their axons selectively project to epaxial muscles lining the vertebral column (Tosney and Landmesser, 1985). This selective guidance of axons is orchestrated, at least in part, by intracellular signalling pathways that are activated downstream of Lhx3 expression (Sharma et al., 2000; Soundararajan et al., 2010). As a result, mouse Lhx3$^+$ ESCMNs selectively, and correctly, extend axons to epaxial muscles when transplanted into the neural tube of developing chick embryos at the time of motoneurogenesis (i.e. HH St. 17; Soundararajan et al., 2006; Soundararajan et al., 2007; Soundararajan et al., 2010). To determine whether similar guidance mechanisms direct the growth of axons from motoneurons derived from iPS cells we transplanted GFP$^+$ iPSCMNs into the neural tube of HH St. 17 chick embryos (n=7). The embryos were killed 5 days later, fixed, sectioned and processed for Tuj1 and GFP immunohistochemistry to visualize chick and transplanted neurons, respectively. Figure 2.3 shows a representative pattern of axonal growth from one transplanted embryo. GFP$^+$ axons extended out of the chick spinal cord

via the ventral root (Figure 2.3 A, D; short arrow), around the dorsal root ganglia (DRG; Figure 2.3 A, D; arrow) to innervate epaxial muscles; the appropriate target for Lhx3$^+$ motoneurons (Figure 2.3 B, D; white arrowhead). However, consistent with the transplants containing a small proportion of Lhx1$^+$ iPSCMNs (see above), a few GFP$^+$ axons projected into the developing hindlimb bud (Figure 2.3 C, D; yellow arrowhead); an appropriate target for Lhx1$^+$ motoneurons. In order to estimate the relative number of GFP$^+$ axons projecting to the epaxial muscles and limb buds, we created Neurolucida reconstructions of the axonal projection patterns from each coronal section taken from 3 transplanted embryos. We then measured the width of the projections and found that 4.5 ± 2.0 times as many GFP$^+$ axons projected to the epaxial muscles compared to the limb. This number is close to the expected distribution of axonal projections based on the relative number of Lhx3$^+$ to Lhx1$^+$ iPSCMNs in the transplants (i.e. the grafts contain ~6.2 times as many Lhx3$^+$ motoneurons as Lhx1$^+$ neurons; see Figure 2.2 B). Thus, the pattern of axonal growth accurately reflects the phenotypic identity of the transplanted iPSCMNs and that iPSCMNs use the same axonal guidance mechanisms as their endogenous Lhx3$^+$ and Lhx1$^+$ counterparts.

iPSCMNs form functional neuromuscular junctions in vivo and in vitro

Chicks transplanted with iPSCMNs were sacrificed at HH st. 35-36, a time when neuromuscular junctions are known to have formed between motor axons of transplanted ESCMNs and peripheral muscle targets (Wichterle et al., 2002). At nerve branches into epaxial muscle (Fig. 3A), iPSCMNs were found to express SV2, a synaptic vesicular protein present at functional synapses (Figure 2.4 B, C, E). In addition, SV2$^+$ iPSCMNs were associated with α-btx labelled endplates (Figure 2.4 C, x-z and y-z orthogonal planes in E). The ability of iPSCMNs to form neuromuscular junctions in vitro was then tested on primary chick myofibres. Previous studies showed that ESCMNs form functional connections with muscle fibres *in vitro* (Miles et al., 2004; Soundararajan et al., 2007). To determine whether iPSCMNs have the same capacity, we first performed immunocytochemical analysis of pre- and postsynaptic structures associated with neurotransmission at the neuromuscular junction (NMJ) using co-cultures containing GFP$^+$ iPSCMNs and chick myofibres (Miles et al., 2004). In the first week after plating,

numerous GFP⁺ neurites were observed to extend radially from spherical clusters of iPSCMNs along individual chick myofibres (Figure 2.5 A). In addition, discrete, oval plaque-like clusters of α-btx positive AChRs were observed around the neurites (Figure 2.5 B-F). This pattern of clustering closely resembles normal *in vivo* development where AChRs first cluster near, but not always in direct contact, with innervating motor axons (Lupa and Hall, 1989; Dahm and Landmesser, 1991). The oval shape and sizes of the plaques (41 ± 24 μm^2; n = 60, 20 plaques measured in each of 3 separate co-cultures) were similar to AChR clusters found on developing muscles fibres *in ovo* during the first week of motoneuron innervation (i.e. E9; Phillips et al., 1985). iPSCMNs continued to maintain the GFP⁺ neurites after 4 weeks *in vitro* (Figure 2.5 G); however, now the individual clusters of α-btx positive AChRs at the end of GFP⁺ neurites formed structures resembling mature NMJs (Figure 2.5 H, I). Higher magnification showed α-btx positive AChR clusters were more complex, pretzel-shaped structures (Figure 2.5 J-K). These endplates were also significantly larger than AChR clusters (plaques) present during the first week in culture (95 ± 37 μm^2, n = 60, 20 endplates measured in 3 separate co-cultures, $p < 0.001$, Mann-Whitney Rank Sum Test). This change in morphology is similar to what occurs *in vivo* as the NMJ matures postnatally (Slater, 1982; Balice-Gordon et al., 1993). By the fifth week in culture, SV2⁺ positive puncta were enriched at the α-btx positive AChR rich endplates relative to the axonal shaft (Figure 2.5 L, M). Although many motoneurons die after approximately 5-6 weeks in co-culture (data not shown), neuromuscular junctions formed by iPSCMNs were found to be stable for up to 5 months in co-culture (Figure 2.6 A-D). Contractions of myotubes were present in all co-cultures at the time of fixation (at both 5 weeks and 5 months) and were used as an indicator of viability. Taken together these results suggest that GFP⁺ neurites extend from the iPSCMNs and make appropriate synaptic connections with chick myotubes that can remain stable for months in co-culture.

We next tested whether synaptic vesicles actively cycle at the endplate to determine whether the NMJs were functional by incubating 4 week old iPSCMN-myofibre co-cultures with FM4-64 (Betz and Bewick, 1992; Gaffield and Betz, 2006). FM dyes are widely used to image synaptic vesicle cycling at the NMJ because the dye is

readily taken up from the extracellular media into endocytosed vesicles that have fused with the plasma membrane during nerve stimulation. Once the dye is trapped inside a vesicle, it can only escape from the NMJ by subsequent exocytosis of the vesicle (Gaffield and Betz, 2007). Consistent with the formation of functional synapses, we found that FM4-64 was readily taken up into cycling vesicles at presynaptic terminals using 50 Hz field electrical stimulation (1 sec. train of pulses, every 2 sec. for 5 min.) (Figure 2.7 A-D). As expected, the vast majority of the FM4-64 puncta (Figure 2.7 A, D) was adjacent to α–btx positive AChRs (Figure 2.7 C, D). We then performed intracellular sharp electrode recordings from NMJs labelled with a rhodamine conjugated AChR antibody. Endplates chosen for recordings (n=22; in 12-27 day old co-cultures) had mature morphologies (i.e. pretzel-shaped distribution of AChRs) and were contacted by a single GFP$^+$ axon (Figure 2.8 A, B). The amplitude of the endplate potentials (EPPs) recorded varied between ~0.5 mV – 6 mV, which is comparable to those recorded from myofibres co-cultured with embryonic rate spinal cord explants (Robbins and Yonezawa, 1971), a neuronal cell line (Chen et al., 2001) and ESCMNs (Miles et al., 2004). Figure 2.8 C (top trace) shows 3 EPPs during a typical 5 sec recording in normal solution while the lower trace shows a similar recording in the presence of 100 μM glutamate. The increased frequency and amplitude of the EPPs in the presence of glutamate indicates that, like ESCMNs (Miles et al., 2004) and endogenous motoneurons (Jiang et al., 1990), iPSCMNs express functional glutamatergic receptors. Bath application of 25 μM TTX completely blocked the large (> 1.5 mV), but not the small EPPs (Figure 2.8 D). These results indicate that the smaller EPPs were miniature EPPs (mEPPs), while the larger EPPs resulted from evoked neurotransmitter release induced by action potentials in the motoneuron. As expected, all EPPs were blocked shortly after bath application of 100-300 μM D-tubocurarine (Figure 2.8 E) (n=3) indicating that the EPPs were due to nicotinic neurotransmission. Taken together, these results indicate that iPSCMNs form functional NMJs similar to endogenous motoneurons and their ESCMN counterparts.

iPSCMNs develop appropriate passive membrane and firing properties
Motoneurons in the spinal cord undergo significant physiological changes during early postnatal development (Fulton and Walton, 1986; Gao and Ziskind-Conhaim, 1998;

Nakanishi and Whelan, 2010). For example, input resistance decreases while whole cell capacitance increases during the first 2 weeks of postnatal life. These changes in passive membrane properties reflect an overall increase in cell size and alteration in channel properties, both of which set the threshold for motor neuron excitability (Pinter et al., 1983; Fulton and Walton, 1986; Gao and Ziskind-Conhaim, 1998). Setting an appropriate threshold for activation is an essential feature of motoneurons as it ensures proper motoneuron recruitment and force gradation during muscle contraction.

To ascertain whether iPSCMNs develop appropriate passive membrane properties over time we performed whole cell patch clamp recordings on iPSCMNs cultured for 1-6 weeks on matrigel-coated coverslips. We found that membrane input resistance (R_m) decreased between 1-2 and 3-4 weeks (666 ±574 MΩ to 189 ±105 MΩ; Table 4). This decrease in resistance correlated well with the simultaneous increase in membrane capacitance (C_m) (45 ±27 pF to 121 ±45; Table 4). These changes suggest that the average size and/or membrane area of the iPSCMNs increased over the first few weeks in culture, although significant size variations remained. The resting membrane potential of iPSCMNs, however, remained similar at all time points investigated (Table 4). These results are similar to those observed in cats and rats, where input resistance decreases overtime (Fulton and Walton, 1986; Gao and Ziskind-Conhaim, 1998; Xie and Ziskind-Conhaim, 1995) while the resting membrane potential does not change between late embryonic and early postnatal time periods (Xie and Ziskind-Conhaim, 1995).

The probability of generating repetitive action potentials in spinal motoneurons injected with a sustained depolarizing current increases between late embryogenesis and early postnatal life (Fulton and Walton, 1986; Gao and Ziskind-Conhaim, 1998). This change reflects maturation in channel properties over time. To determine whether channel properties in iPSCMNs mature over time we applied stepwise injections of depolarizing current to iPSCMNs grown in culture for 1, 2 and 5 weeks. Figure 2.9 shows that iPSCMNs were able to generate repetitive action potentials at all 3 time points (Figure 2.9 A). However, the amount of current required to evoke repetitive action potentials decreased between 1 and 5 weeks (Figure 2.9 A). In addition, the maximum firing rate increased over time in culture (Figure 2.9 A,C) such that by 5 weeks the average

frequency during the late phase of activity (>250 ms) was 41 ± 10 Hz (n=3). This firing

rate is comparable to the firing patterns of individual motor units in freely walking rats

(Hennig and Lomo, 1985). Finally, the discharge rate of the evoked action potentials

decreased overtime during the sustained injection of depolarizing current at all three time

points (Figure 2.9 A, B). This phenomenon, known as spike-frequency adaptation, is a

typical firing pattern of spinal motoneurons (Granit et al., 1963; Kernell and Monster,

1982).

Action potential duration decreases in motoneurons between late embryonic to

early postnatal life (Gao and Ziskind-Conhaim, 1998). The same was true for cultured

iPSCMNs (Figure 2.10 A, B) where action potential duration (measured at half-maximal

peak amplitude in sweeps where a single spike was generated) was found to decrease

from 5.9 ± 1.6 ms (n=11) at 1-2 weeks to 2.29 ± 0.43 ms (n=10) by 5-6 weeks.

Furthermore, like embryonic rat motoneurons (Gao and Ziskind-Conhaim, 1998), only a

minority (38%, n=13) of the recorded iPSCMNs elicited an afterhyperpolarizing potential

(AHP) after 1 week *in vitro*. This percentage increased to 67% after 5-6 weeks in culture

(n=15). Taken together, these findings suggest that cultured iPSCMNs mature over time

and develop passive membrane and firing properties similar to their endogenous

counterparts.

Implanted iPSCMNs innervate denervated muscle fibres and restore force following
peripheral nerve injury

Embryonic rat ventral spinal cord cells (Thomas et al., 2000; Liu et al., 2013) and mouse

ESCMNs (Yohn et al., 2008) restore skeletal muscle function when transplanted into the

distal stump of transected tibial nerves. To determine whether iPSCMNs have the same

capacity we cut the sciatic nerve and implanted ~10,000 iPSCMNs into the tibial nerve in

mice ~15 mm proximal to the medial gastrocnemius (MG) muscle. Reinnervation of

muscles other than the MG was prevented by ligating all of the tibial nerve branches

distal to the graft site (Yohn et al., 2008). To determine whether the contacted endplates

formed functional NMJs, we used an *ex vivo* nerve/muscle preparation to measure

contractile force of the reinnervated MG muscles. Isometric twitch and tetanic

contractions were elicited by applying single and repetitive electrical pulses (50 Hz for 1

sec; 20 μs pulse duration) to the distal nerve stump via a suction electrode (Figure 2.11 A, B). Reinnervated muscle forces were compared to both an age-matched, unoperated control MG muscle group, whose nerve was left intact, and a surgical muscle control group where the sciatic nerve was cut and ligated to prevent regeneration. The transected tibial nerve stumps of the surgical control group were injected with media alone. As expected, electrical stimulation of the tibial nerve stump in the control animals did not elicit muscle contraction (data not shown). In contrast, nerve/muscle preparations from mice implanted with iPSCMNs 6 weeks previously produced an average twitch force of 51.4 ± 6.5 mN (n=3) and tetanic force of 147 ± 18 mN (n=3), respectively. These values are approximately two-thirds that of unoperated age-matched control muscles which produced twitch and tetanic forces of 80 ± 7 mN (n=3) and 203 ± 15 mN (n=3), respectively. Interestingly, the contractile forces of the muscles reinnervated by iPSCMNs, when calculated as a percent of unoperated control values, were greater than those reported for rat and mouse MG muscles reinnervated by embryonic spinal cord cells (Thomas et al., 2000) or ESCMNs (Yohn et al., 2008). Although considerable force recovery was observed following implantation of iPSCMNs, twitch force profiles differed between treated and control groups (Figure 2.11 A). Rise times to peak force were significantly longer in the implanted group (76 ± 12 ms) versus control (47 ± 5 ms; n=3 for each group, p=0.022, t-test) and relaxation times (measured as the time taken for the force to decline to that of half of peak force) were also significantly longer in the implanted group (implanted group = 52 ± 12 ms, control group = 28 ± 8 ms; n=3 for each group, p=0.046, t-test). As expected from the force recordings, denervation-induced muscle atrophy was dramatically attenuated when the muscles were reinnervated by iPSCMNs. MG muscle diameter of implanted animals was significantly greater than those of surgical controls (control group = 2.94 ± 0.08mm, implanted group = 2.19 ± 0.05mm, surgical control group = 0.92 ± 0.05mm; n=3 for each group, p<0.001, one-way ANOVA, Holm Sidak method). Further, the diameters of individual muscle fibres in the implanted group were significantly greater than those of the surgical control group (control=34.5 ± 9.4μm, implanted group=21.6 ± 6.9μm, surgical control group = 14.3 ± 3.9μm; n=90 fibres, N=3 animals for each group, p<0.001, one-way ANOVA, Holm Sidak method). Taken together, these results indicate that iPSCMNs form functional

connections with denervated muscles fibres and that this innervation limits denervation atrophy.

Discussion

The current study provides a thorough assessment of iPSCMNs with respect to their capacity to develop into spinal motoneurons. Proteomic analysis revealed that iPSCMNs and ESCMNs have comparable protein expression profiles. The identified proteins in the ESCMNs and iPSCMNs were not only similarly grouped into known gene ontology terms, but the proteins in each group were the same except for 143 binding proteins that were uniquely expressed in ESCMNs or iPSCMNs. These results indicate that the cellular make up of ESCMNs and iPSCMNs are remarkably similar. In addition, when protein expression levels were compared between the two cell types we found only 28 proteins to be up-regulated and 87 proteins down-regulated in iPSCMNs compared to ESCMNs. None of the up- or down-regulated proteins are known play a significant role in motoneuron differentiation. The remarkable similarities in protein identification and expression between ESCMNs and iPSCMNs suggests that these two cell types are very similar in nature. It will be interesting, nonetheless, to pursue whether proteins identified as being differentially regulated can affect motoneuron phenotypes that are more subtle than those used in this study. For example, BetaIVSigma1 spectrin (Sptbn4 in Table 2.2) is concentrated at the nodes of ranvier in the peripheral nervous system (Berghs et al., 2000), and regulates, at least in part, its size (Lacas-Gervais et al., 2004). Whether the nodes of ranvier would differ between iPSCMNs and ESCMNs remains to be determined.

Interestingly, even though we focused on 15 transcription factors involved in neuron and/or motoneuron differentiation, only Myt1l was identified in our data set. Myt1l has previously been found to play a role in early neuronal precursor differentiation in the developing *Xenopus* embryo, and has been established to be an essential factor for the transdifferentiation of fibroblasts into functional neurons and motoneurons (Bellefroid et al., 1996; Vierbuchen et al., 2010; Son et al., 2011). Myt1l was not differentially expressed in ESCMNs and iPSCMNs. The reasons why we did not detect more transcription factors involved in motor neuron differentiation in unclear, but likely reflects the proteomic approach used in this study. Some peptides are better at being ionized and thus are more amenable to identification in a mass spectrometer. Future studies could use a more targeted approach using multiple reaction monitoring (MRM)

analysis to identify all known transcription factors involved. Despite this limitation, the present study indicates that the protein composition of motoneurons derived from ES cells and iPS cells are remarkably similar.

Axonal trajectories of iPSCMNs are appropriate for their LIM homeodomain expression pattern

Similarities in LIM homeodomain protein expression between ESCMNs and iPSCMNs suggest that they undergo similar developmental programs when cultured in the presence of SAG and RA. The vast majority of ESCMNs (Soundararajan et al., 2006) and iPSCMNs were immunopositive for the Lhx3 (Figure 2.2), a LIM homeodomain protein expressed by motoneurons in the medial aspect of the medial motor column (Sharma et al., 1998). Like ESCMNs (Soundararajan et al., 2006; Soundararajan et al., 2007; Soundararajan et al., 2010), their axonal trajectories reflected the nature of their LIM homeodomain protein expression pattern when transplanted into the neural tube of developing chick embyros at the time of motoneurogenesis. The majority of iPSCMNs projected axons out of the ventral root and then dorsally around the DRG to the epaxial muscles along nerve pathways taken by developing chick Lhx3$^+$ motoneurons (Figure 2.3). Far fewer axons targeted limb musculature. These results suggest that iPSCMNs express guidance factors necessary for this targeting such as EphA4 (expressed by both Lhx1$^+$ motoneurons that innervate the dorsal limb muscle mass as well as Lhx3$^+$ motoneurons that innervate epaxial muscles) and FGFR1 (expressed by Lhx3$^+$ motoneurons). Both molecules are known to be required for proper guidance of developing Lhx3$^+$ motoneurons (Helmbacher et al., 2000; Shirasaki et al., 2006; Soundararajan et al., 2010).

iPSCMNs form functional NMJs in vitro

Previous studies have shown that iPSCMNs contact myotubes, formed from muscle cell lines (i.e. C2C12 cells), and extend neurites in close vicinity to AChR clusters (Hu and Zhang, 2009; Mitne-Neto et al., 2011). The present study extends these findings to show

that iPSCMNs form stable NMJs with anatomical and physiological features typical of mature endplates when co-cultured with chick myotubes for several weeks. Anatomically, iPSCMNs initially formed endplates that were plaque-shaped (Figure 2.5 E), but later became characteristically pretzel-shaped (Figure 2.5 K). This transition in endplate appearance normally occurs during the first postnatal weeks in mice and likely involves bidrectional signaling between motoneurons and muscle fibres (Balice-Gordon et al., 1993; Bolliger et al., 2010). Our SV2 immunolabelling (Figure 2.5 L) and FM dye studies (Figure 2.7) indicated that iPSMNCs correctly localized synaptic vesicles at endplates where they cycled appropriately in response to neural stimulation (Betz and Bewick, 1992; Ribchester et al., 1994). Furthermore, we showed EPPs and TTX-insensitive mEPPs were present at NMJs formed by iPSCMNs *in vitro* (Figure 2.8) indicating that the junctions were functional and capable of inducing depolarization in post-synaptic myofibres. As expected, the largest EPPs were blocked upon bath application of d-tubocararine indicating that they were induced through cholinergic stimulation (Fischbach and Cohen, 1973). Taken together, our results strongly indicate that iPSCMNs develop multiple characteristics of endogenous motoneurons including the acquisition of appropriate synaptic machinery for neurotransmission as well as nerve-derived signals (presumably agrin; McMahan, 1990; Bezakova and Ruegg, 2003) that form, stabilize and mature the NMJ throughout development.

Passive membrane and firing properties of iPSCMNs

The present work extends upon previous electrophysiological studies on iPSCMNs (Karumbayaram et al., 2009; Hu et al., 2010; Egawa et al., 2012; Bilican et al., 2012; Yao et al., 2013) by characterizing passive and active membrane properties for several weeks after differentiation. Trends in maturation of passive membrane properties of iPSCMNs resembled those seen in developing motoneurons *in vivo* (Fulton and Walton, 1986; Gao and Ziskind-Conhaim, 1998; Nakanishi and Whelan, 2010). Membrane resistance progressively decreased over the first few weeks in culture, concomitant with an increase in membrane capacitance. Both changes occur during normal motoneuron devlopment (Ulfhake and Cullheim, 1988) and are indicative of an overall increase in cell size over time. We also showed that iPSCMNs develop firing properties such as fast-firing action

potentials and spike frequency adaptation in response to injections of depolarizing current (Figure 2.9). Both firing properties are signatures of endogenous motoneurons (Granit et al., 1963; Kernell and Monster, 1982) and ESCMNs (Miles et al., 2004). In addition, an increasing proportion of motoneurons developed AHPs (38-67%) typical of endogenous motoneurons (Fulton and Walton, 1986) one week after plating. Taken together, these results suggest that iPSCMNs acquire voltage-gated channel properties characteristics of normal spinal motoneurons. The few differences observed between iPSCMNs and endogenous motoneurons (i.e. AHPs being absent in 33% of iPSCMNs after 5 weeks *in vitro*) may be due to intrinsic differences between the two cell types or it could simply reflect differences in growth environment. Further studies will be required to determine whether addition of spinal interneurons, sensory neurons, glial cells and/or myofibres to the cultures would further the development of iPSCMNs into more mature motoneurons.

Implanted iPSCMNs project axons to target muscle and promote force recovery following injury

Denervated murine muscles recover approximately 10% of their original contractile force values when reinnervated by embryonic ventral spinal cord cells transplanted into the peripheral nerve near the muscle/nerve entry point (Thomas et al., 2000). Recovery of force is improved if trophic factors are added to the graft at the time of transplant (Grumbles et al., 2009) or if the cells were stimulated for 1 hr immediately post-transplantation (Grumbles et al., 2013). ESCMNs also reinnervate denervated muscle fibres, reduce muscle atrophy and restore contractile force to 40% that of control muscles when transplanted near the MG nerve/muscle entry point in mice (Yohn et al., 2008). In the present study, iPSCMNs formed anatomically normal NMJs (data not shown; see also Su et al., 2013) with previously denervated muscle fibres when transplanted near the mouse MG nerve/muscle entry point. Interestingly, the contractile force of the MG muscles reinnervated by iPSCMNs was approximately 70% that of control values (Figure 2.11). Thus, iPSCMNs are at least as efficient as embryonic spinal neurons (Thomas et al., 2000) or ESCMNs (Yohn et al., 2008) in restoring force to denervated muscles when transplanted into the distal nerve.

As observed for grafted ESCMNs (Yohn et al., 2008), transplanted iPSCMNs dramatically reduced muscle atrophy associated with denervation (Figure 2.11 G). These results indicate that iPSCMNs in the graft were actively inducing muscle fibre contractions by firing action potentials. This assumption is based on previous studies where marked muscle atrophy was shown to occur in animal models of chronic disuse even when myofibres were passively stretched (Roy et al., 1998). That is, atrophy is only prevented if the innervated myofibres are actively contracting. Furthermore, the slower rise times of the twitch contractions in muscles reinnervated by iPSCMNs compared to the contralateral control muscles indicates that the transplanted neurons were active for a significant period of time during the day (Kernell et al., 1987). This supposition is based on the wealth of studies showing that slowing of contractile speed occurs with increased neuromuscular activity (reviewed by Gordon and Pattullo, 1993). It is presently not known why iPSCMNs fire action potentials in the transplants, but it is likely due to mechanical stimulation by surrounding tissue and/or by glutamatergic excitation from additional neurons in the graft that differentiated with the motoneurons prior to transplantation (Yohn et al., 2008; Chipman et al., 2014).

iPSCMNs: future considerations

The results in this study further endorse the use of iPSCMNs to study the pathology of motoneuron diseases such as ALS (Bilican et al., 2012; Egawa et al., 2012; Burkhardt et al., 2013; Serio et al., 2013; Yao et al., 2013) and spinal muscular atrophy (Corti et al., 2012). Recent studies using iPSCMNs from ALS patients to screen drugs promoting motoneuron survival have also yielded novel findings that would likely not have been achieved without this technology (Yang et al., 2013). However, most studies to date have examined iPSCMN behavior in isolation over short periods of time or co-cultured with cells within the CNS rather than cells found in the periphery. Because motor axons withdraw from endplates prior to cell death (Fischer et al., 2004) future studies should also include long-term iPSCMN/myofibre co-cultures. This assertion is underscored by the fact that the onset of symptoms associated with ALS occurs later in life and that neuroprotection alone is insufficient to attenuate disease progression (Gould et al., 2006).

Finally, the finding that iPSCMNs remain functional several weeks after transplantation lends support to their use in cell-replacement therapies designed to restore function to permenantly denervated muscles following injury.

Chapter 2 Figures

Figure 2.1. Proteomic analysis of iPSCMNs and ESCMNs

A, Proteins identified in the proteomic screen from the ESCMNs and iPSCMNs were assigned a gene ontology term using Panther classification (http://www.pantherdb.org/). The percent of proteins matching to a GO term from either the ESCMNs or iPSCMNs were then plotted. **B,** The number of proteins identified that mapped to a defined GO term from either the ESCMNs (red) or iPSCMNs (green) or both (yellow) were compared. **C,** Volcano plot of all data, which consists of 3025 unique, low variability peptides. Each data point represents a protein identified by mass spectrometry. The natural log of the ratio of expression in iPSCMNs divided by the expression in ESCMNs is plotted against the p value.

A

GO Ontology
- ■ binding (GO:0005488)
- ■ catalytic activity (GO:0003824)
- ■ structural molecule activity (GO:0005198)
- ■ nucleic acid binding transcription factor (GO:0001071)
- ■ enzyme regulator activity (GO:00030234)
- ■ translation regulator activity (GO:0045182)
- ■ transporter activity (GO:0005215)
- ■ receptor activity (GO:0004872)
- ■ protein binding transcription factor activity (GO:0000988)
- ■ antioxidant activity (GO:0016209)

B

C

Figure 2.2. The vast majority of iPSCMNs express the LIM/homeobox protein Lhx3
Ai-iii, Immunolabeling showed that the majority of the GFP$^+$ iPSCMNs expressed Lhx3
after 2 days *in vitro*. **Bi-iii,** In contrast, very few GFP$^+$ iPSCMNs expressed Lhx1 after
the same time period. ***C,*** Percentage of Lhx3/GFP and Lhx1/GFP positive cells after 2
days *in vitro* (n = 3 for each group). Scale bars = 10 μm.
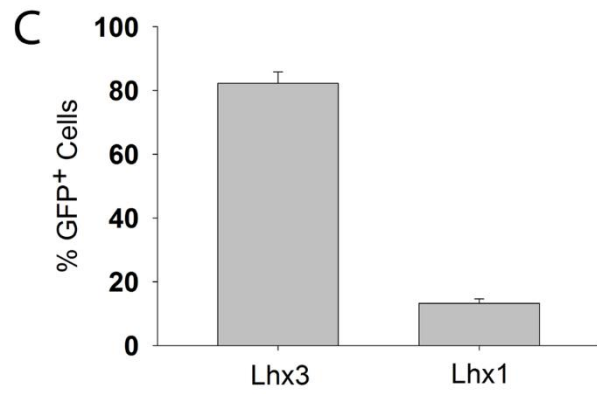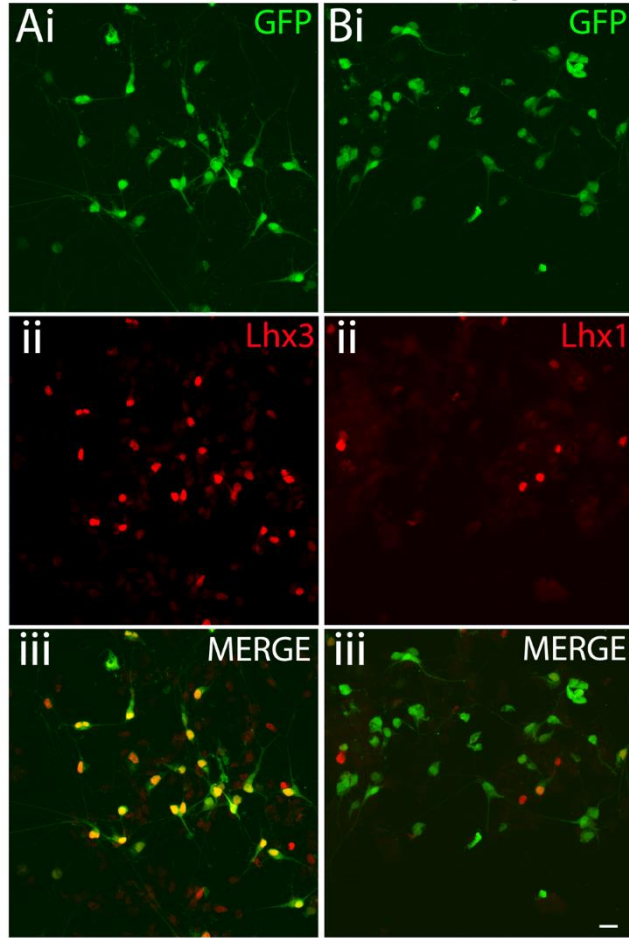
Figure 2.3. iPSCMNs project axons to epaxial muscles when transplanted *in ovo*

A-C, Cross-section through a HH St. 31 chick embryo showed GFP$^+$ motor axons extended out of the spinal cord through the ventral root (**A**, short arrow). The majority of the GFP$^+$ axons extended around the DRG (**A**, arrow) and into epaxial muscles (**B**, white arrowhead). A few GFP$^+$ axons extended ventrally into the limb bud (**C**, yellow arrowhead). All sections were immunolabeled with Tuj1 to visualize the endogenous chick neurons (appear red) and transplanted GFP$^+$ iPSCMNs (appear yellow). **D,** Neurolucida reconstruction of all cross-sections from one chick embryo receiving an iPSCMN transplant. GFP$^+$ iPSCMNs are shown in green. Scale bar = 100 μm.
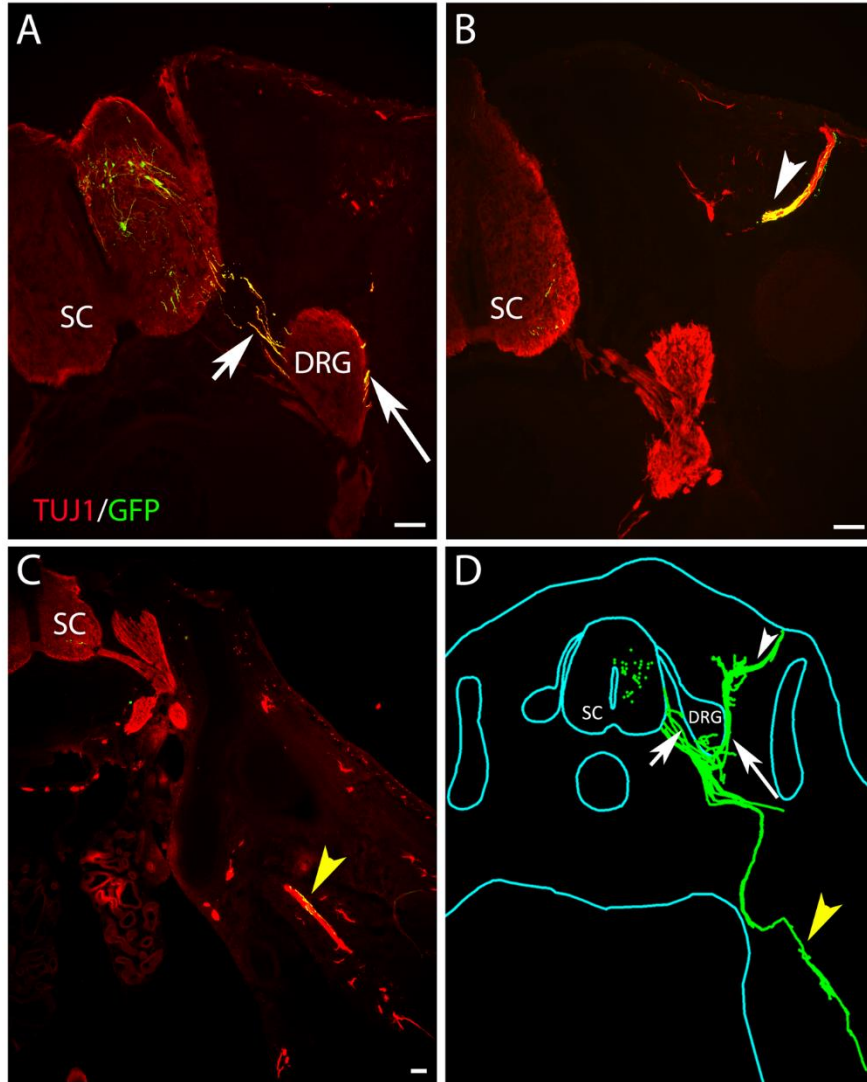
Figure 2.4. iPSCMNs make contact with endogenous synaptic endplates at neuromuscular junctions *in vivo* and express the synaptic vesicle marker SV2

A, An axon of an iPSCMN projecting towards the epaxial muscle in a HH st. 36 chick. Boxed area shown in **B – E**. This axon co-expresses GFP and SV2 (asterisk in **B**, **C**, merge in **E**) and overlies an α-bungarotoxin (btx)-positive endogenous endplate (**D**, arrowheads in x-z and y-z orthogonal planes in **E**). Scale bar = 20 μm. SC = spinal cord.
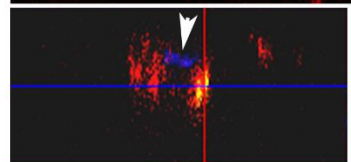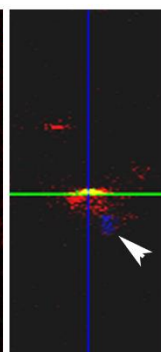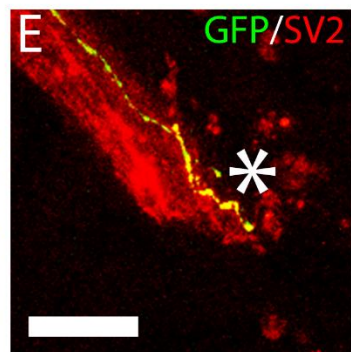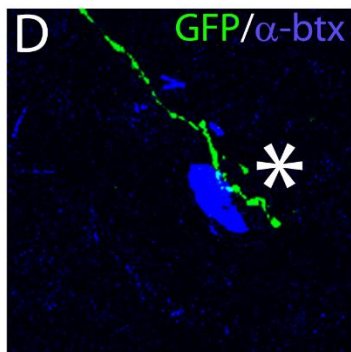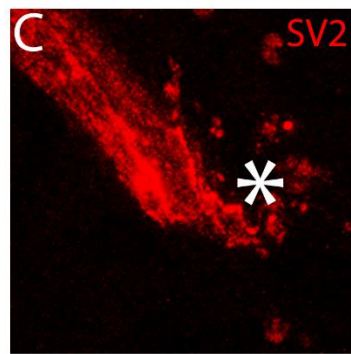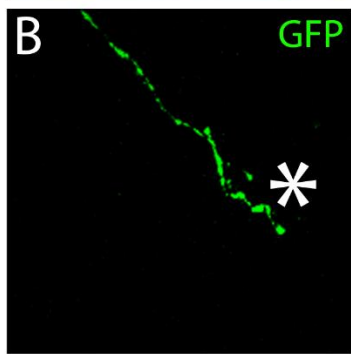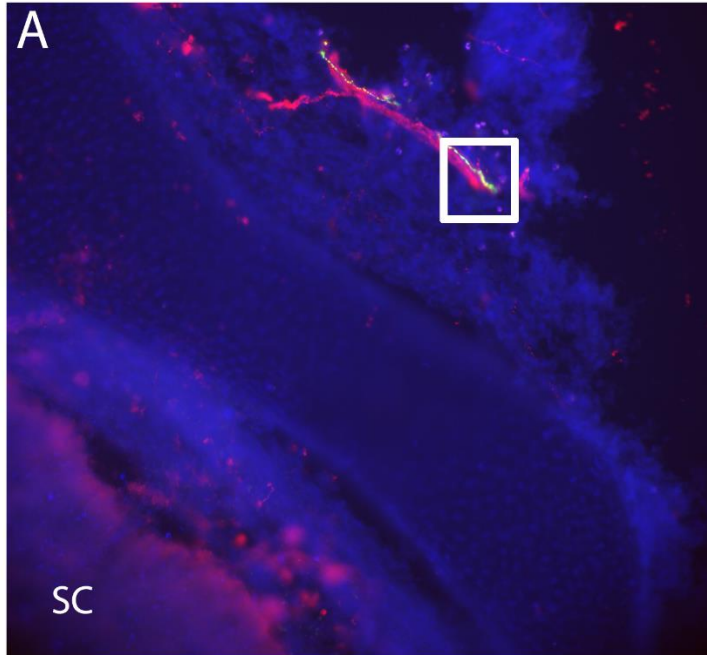
Figure 2.5. iPSCMNs form NMJs with co-cultured chick myofibres

A-C, GFP$^+$ motoneurons extend axons along myofibres (**A**) and associate with plaques of α-btx labelled AChRs during the first week in culture (**B,C**). **D-F**, Boxed area in C. **G-I**, Contact between GFP$^+$ axons and AChRs continues into week 5, when AChR clusters become much larger and maintained at myofibre regions in close proximity to GFP$^+$ axons. **J-L,** Boxed area in J shows GFP$^+$ axons (**J**) contacting α-btx labelled AChRs with pretzel-like morphologies (**K**). SV2$^+$ synaptic vesicles are prominent at the endplate in the presynaptic axon (**L**). **M**, Merged image of J-L and x-z and y-z orthogonal planes of the NMJ indicated by the asterisk. Note the blue signal in the orthogonal planes and merge panel is SV2 labelling. Scale bar = 100 μm in **C** and I; 20 μm in **F** and **M**.

Week 1

A GFP   B α-BTX   C MERGE

D   E   F

Week 5

G   H   I

J GFP   K α-BTX

L SV2   M MERGE

*

72
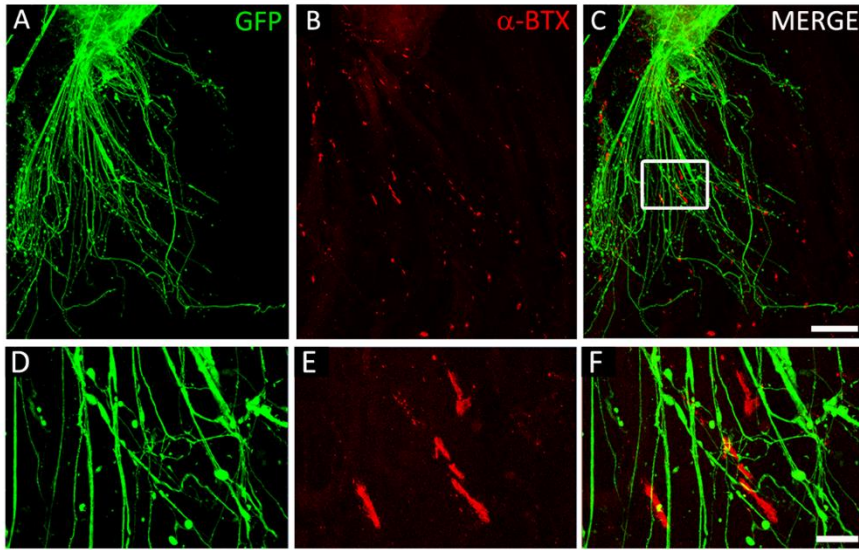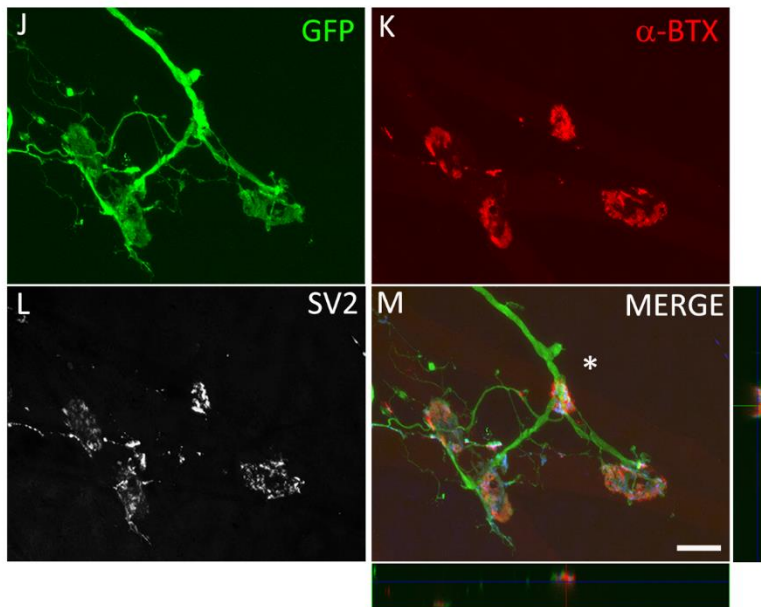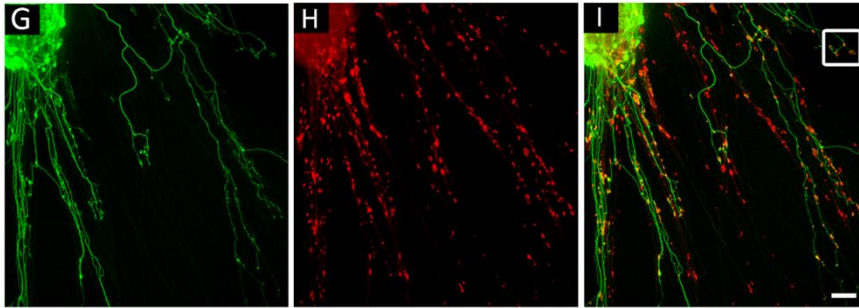
Figure 2.6. iPSCMNs maintain synaptic contact at neuromuscular junctions for up to 5 months on chick myofibres

Neuromuscular junctions at 5 months *in vitro* between a GFP$^+$ iPSCMN (**A**) and α-btx labelled AChRs on chick myofibres (**B**). The presence of SV2 labelling indicates synaptic activity (**C**). The asterisk in **D** indicates the neuromuscular junction displayed in x-z and y-z orthogonal planes. Note that blue signal in orthogonal planes and merge panel = SV2 labelling. Scale bar = 20 μm.
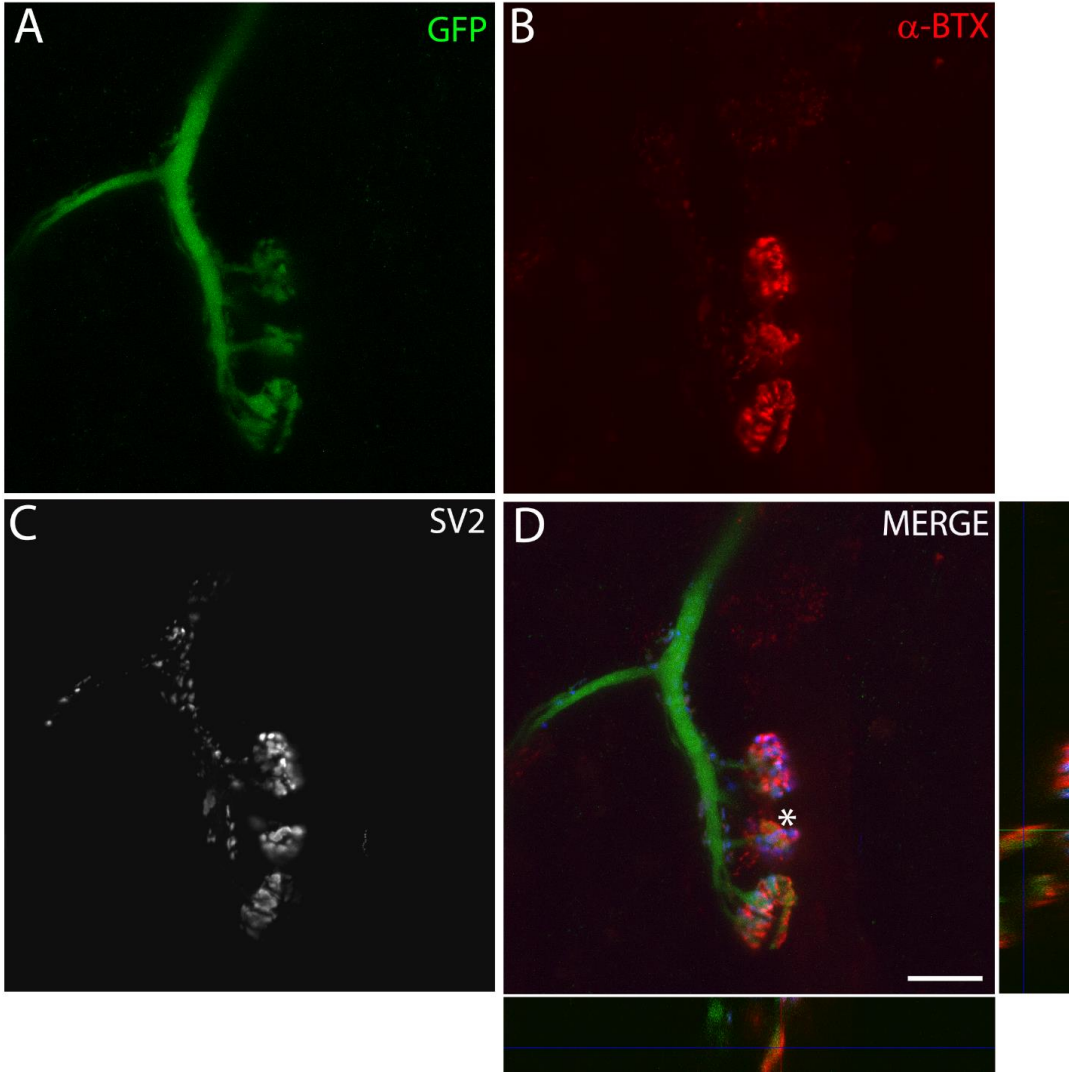
Figure 2.7. Active vesicular cycling occurs at NMJs formed between iPSCMNs and chick myofibres

A-C, FM4-64 puncta (**A**) is present in GFP$^+$ axons (**B**) at endplates labelled with α-btx (**C**) following field electrical stimulation at 50 Hz every 2 sec for 5 min. **D,** Merged image of panels **A-C** where the blue signal is FM4-64. Scale bar = 20 μm.
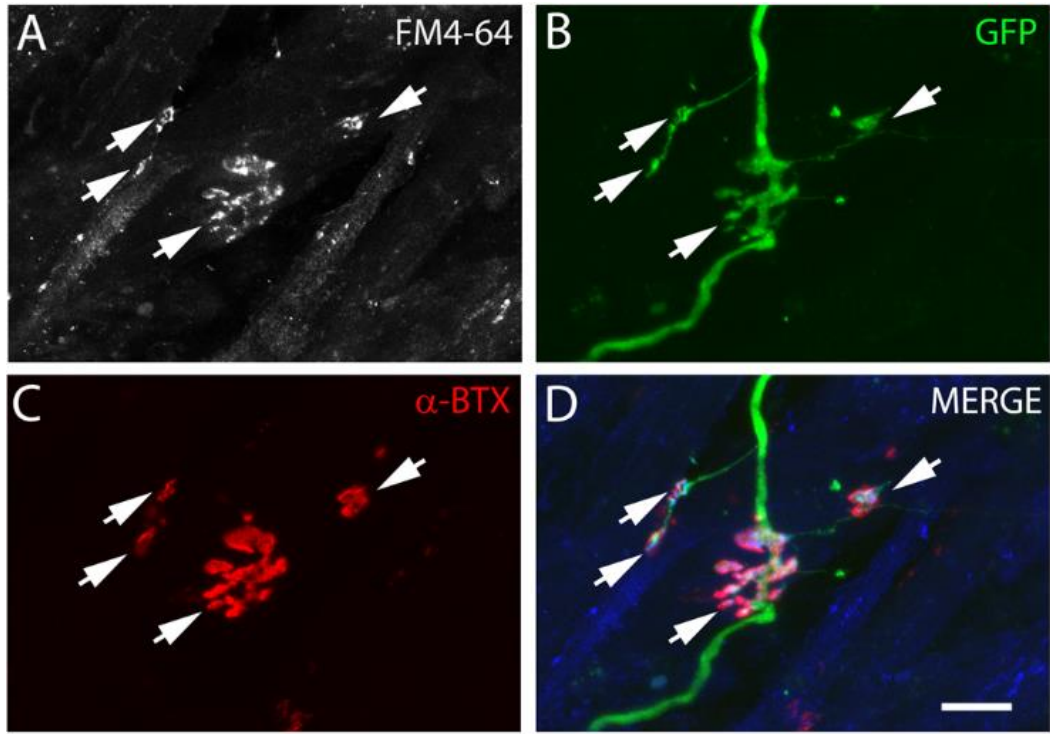
Figure 2.8. iPSCMNs form functional NMJs when co-cultured with chick myofibres

A, Differential interference contrast image of a chick myofibre impaled with a sharp electrode for intracellular recordings (placement of electrode indicated by white lines). **B,** Innervated endplates were identified as a cluster of mAb35-labelled AChRs contacted by a single GFP$^+$ axon. Asterisks in (**A**) and (**B**) denote region impaled by the recording electrode. **C,** Upper trace shows EPPs recorded over a 5 sec period in normal solution while the lower trace shows recording from the same cell after bath application of 100 μM glutamate. Note the increase in number of EPPs. **D,** EPPs with an amplitude greater that 1.5 mV were inhibited after bath application of 25 μM TTX (right panel). Left panel is a recording from the same cell prior to TTX application. Histograms show the amplitudes of all EPPs recorded a 90 sec recording in the absence (left panel) or presence (right panel) of TTX. **E,** Intracellular recordings in the absence (left panel) or presence (right panel) of bath applied D-tubocurarine (300 μM). Note complete absence of EPPs in the right panel.

A

B GFP/AChR

C Control

Glutamate (100μM)

1mV
500 ms

D Control   TTX (25μM)

1mV
200 ms

E Control   D-tubocurarine (300μM)

1mV
1s
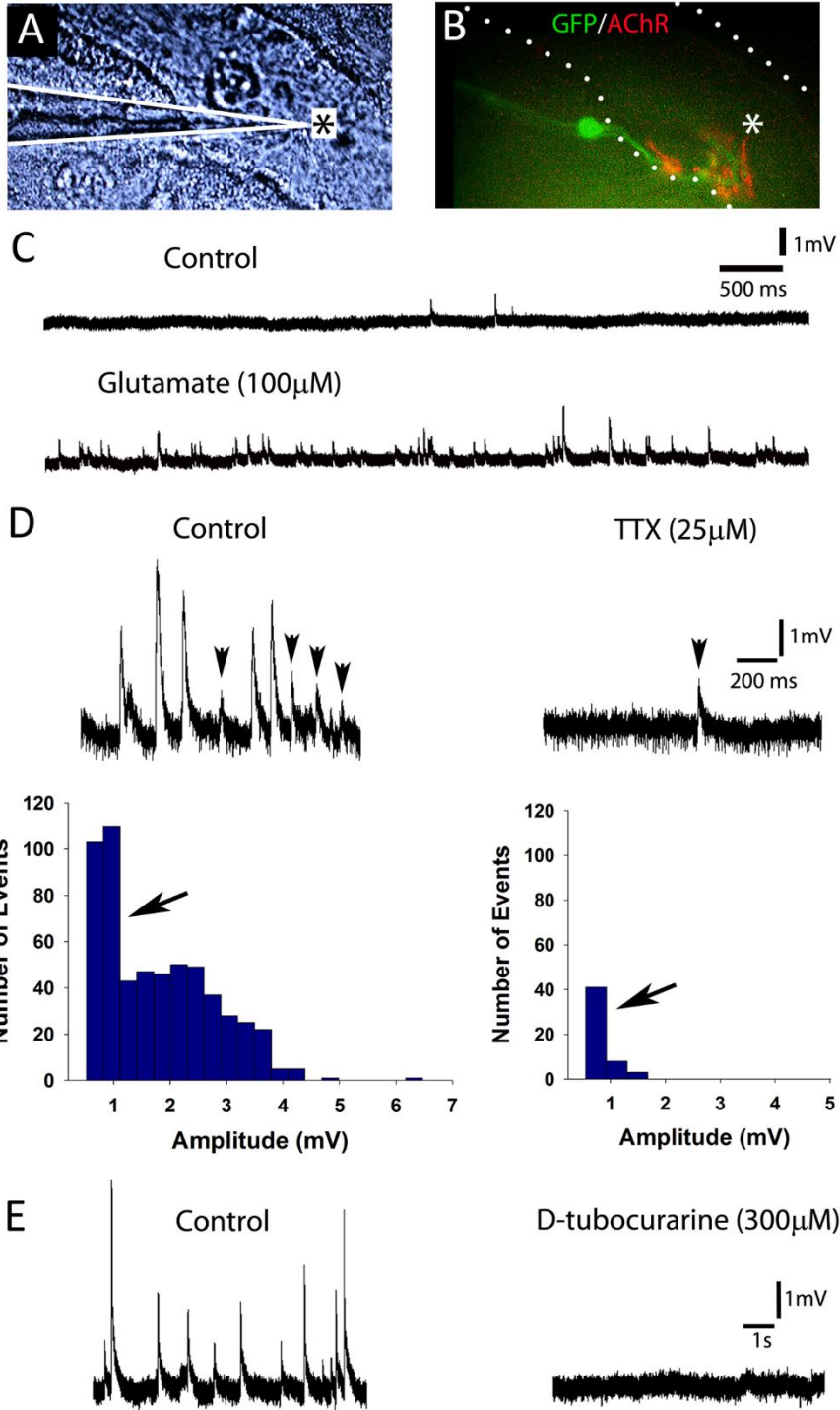
Figure 2.9. iPSCMNs develop appropriate motoneuron firing properties

A, Current-clamp recordings of membrane potentials in response to 500 ms current injections measured from iPSCMNs after 1, 2 and 5 weeks *in vitro*. iPSCMNs were capable of firing repetitive action potentials at all ages, however the amount current required decreased with age. Values of injected current (from top to bottom trace) for 1 week = 25 pA, 70 pA, 110 pA; 2 weeks = 30 pA, 65 pA, 185 pA; 5 weeks = 20 pA, 90 pA, 220 pA. **B**, Plots of instantaneous firing frequency versus time during a single current pulse shows spike frequency adaptation. **C**, Plot showing that maximum firing frequency increases with days in culture (i.e. 1 week, 2 weeks, and 5 weeks).
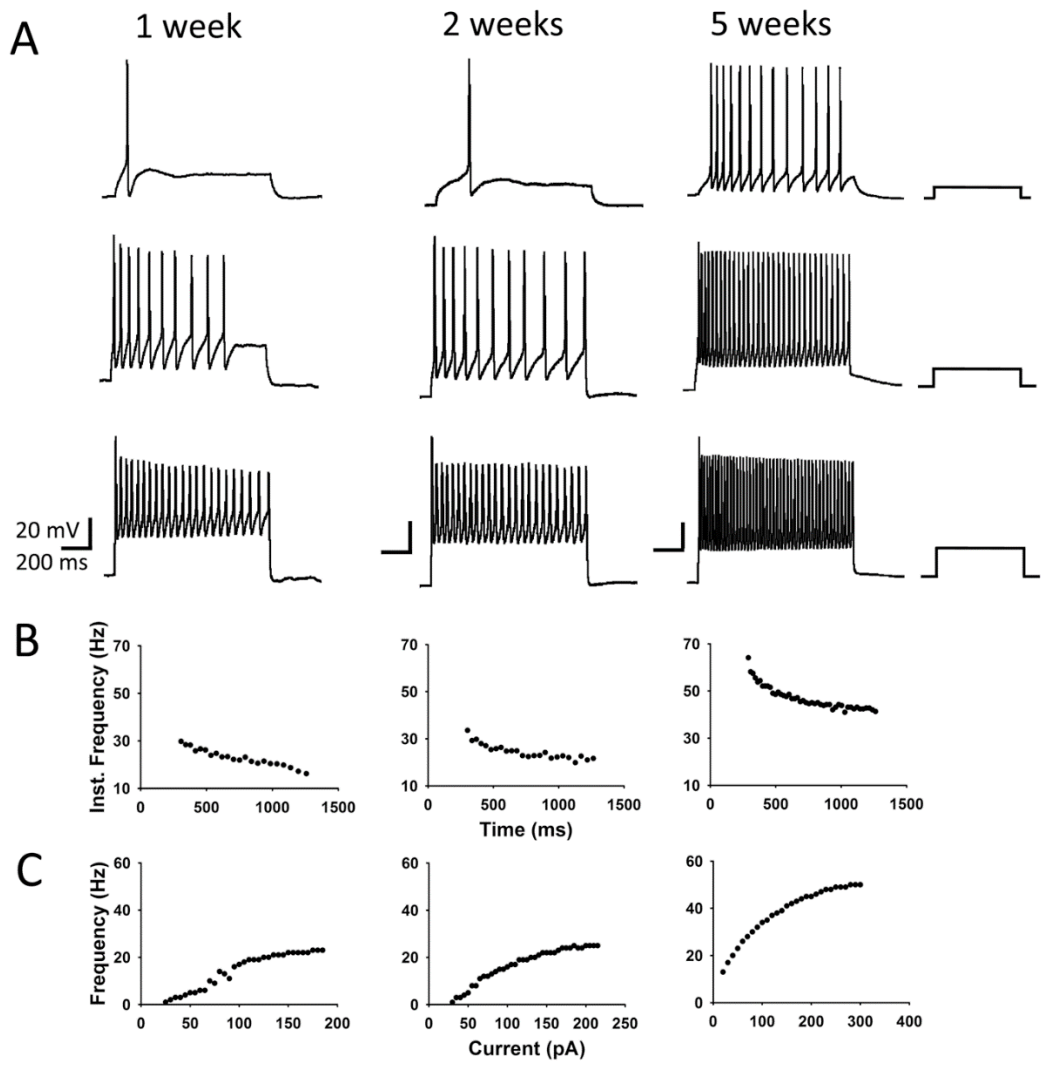
Figure 2.10. iPSCMNs action potential profiles mature with age

A, Representative spikes at Early and Late time points following injection of depolarizing current. Note the presence of the afterhyperpolarization in the action potential (AP) generated at the Late time point. **B,** AP duration (measured at half-maximum peak amplitude) significantly decreases as motoneurons mature (Kruskal-Wallis one-way ANOVA on ranks, $p < 0.05$ for Early vs. Late and Middle vs. Late. n values: Early = 11; Middle = 8; Late = 10). Early = 9-14 days in culture, Middle = 21-29 days in culture and Late = 37-43 days in culture.
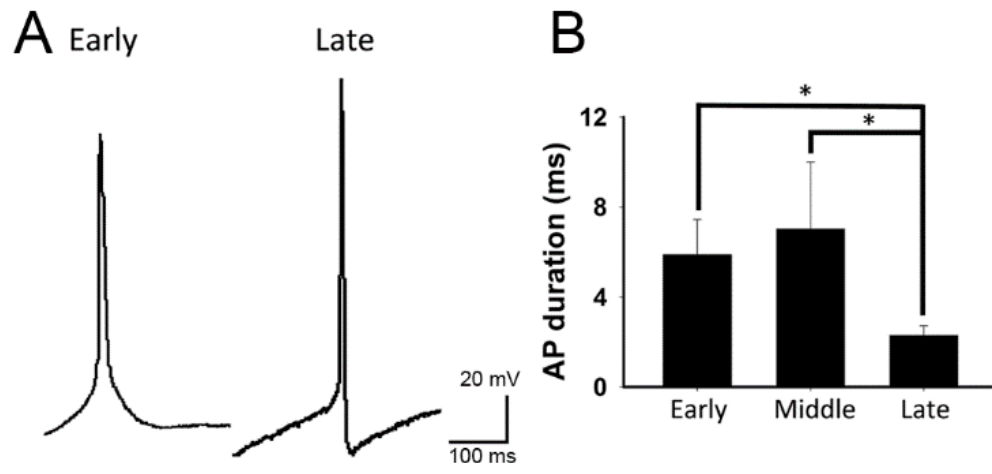
Figure 2.11. Implanted iPSCMNs promote recovery of muscle force following nerve injury.

MG muscle force profiles elicited by a single electrical pulse (**A**), or by a train of pulses (50 Hz for 1 sec) (**B**), to control tibial nerves (Unoperated Control) and nerves implanted with iPSCMNs 5 weeks previously.
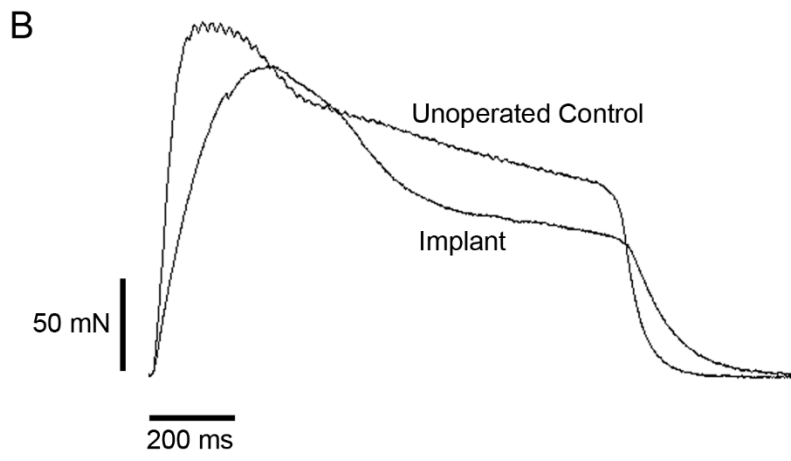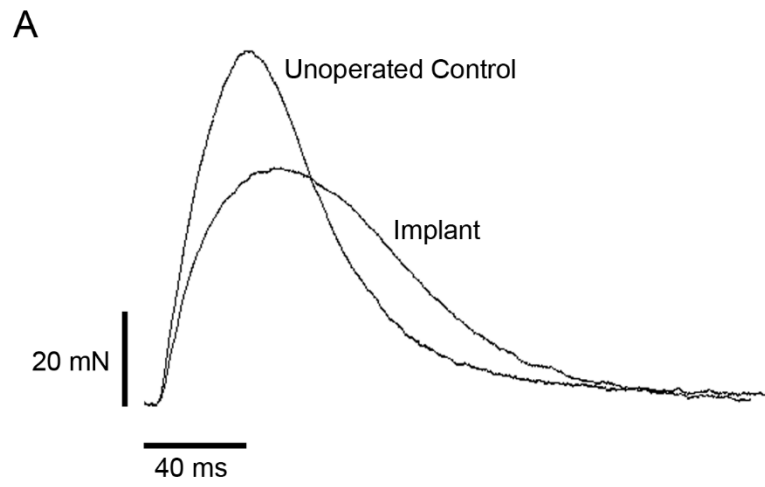
Chapter 2 Tables

Table 2.1 Chromatographic separation gradient protocol

Time	%A	%B
3	97	3
5	95	5
90	70	30
95	3	97
97	3	97
100	97	3
120	97	3

A: 0.1% formic acid in water, B: 0.1% formic acid in acetonitrile

Table 2.2 Proteins up-regulated in iPSCMNs (with a Ln expression ratio > 0.7) compared to ESCMNs

Protein ID	Protein Name	Ln Expression Ratio	GO Term
G5E8H3	DNA binding protein Ikaros	1.68	No hit
P09041	Phosphoglycerate kinase 2	1.21	Catalytic activity
Q6ZPI3	Ligand dependent corepressor	1.02	Binding & Catalytic activity
Q2TPA8	Hydroxysteroid dehydrogenase like protein 2	1.01	Catalytic activity
P52927	High mobility group protein HMGI-C	0.99	Binding activity
Q6PAL8	DENN domain-containing protein 5A	0.92	Transporter activity
Q9QUG2	DNA polymerase kappa	0.92	Binding & Catalytic activity
Q62470	Integrin alpha 3	0.91	No hit
F2Z4B7	Protein Raph1	0.89	No hit
Q60953	Protein PML	0.89	No hit
E9PY58	Caseinolytic peptidase B protein homolog	0.88	No hit
P70278	Stimulated by retinoic acid gene 8 protein	0.87	No hit
E9Q9J4	Inositol hexakisphosphate and diphosphoinositol-pentakisphosphate kinase 2	0.85	No hit
E9QN98	Inactive dipeptidyl peptidase 10	0.83	Catalytic activity
Q9CR58	Kidney mitochondrial carrier protein 1	0.83	Binding & Transporter activity
Q8C0E3	Tripartite motif containing protein 47	0.81	No hit
Q9QUG9	RAS guanyl-releasing protein 2	0.76	Binding & Catalytic activity & Enzyme regulator activity
A2RT91	Ankyrin and armadillo repeat-containing protein	0.75	No hit
F6TMC0	Protein 9930021J03Rik	0.75	No hit
Q8K0F1	TBC1 domain family member 23	0.75	No hit
Q9ET80	Junctophilin 1	0.74	No hit
S4R2F7	RNA binding protein 25	0.72	No hit
E9PYH2	Cytosolic acyl coenzyme A thioester hydrolase	0.72	No hit
Q3V3R4	Integrin alpha-1	0.71	No hit
P00405	Cytochrome c oxidase subunit 2	0.71	Catalytic activity
E9QP35	Protein 2310042D19Rik	0.71	Catalytic activity
F7CHR4	Inositol oxygenase	0.71	No hit
E9PXP1	Protein Brpf1	0.7	No hit

Table 2.3 Proteins down-regulated in iPSCMNs (with a Ln expression ratio < -0.7) compared to ESCMNs

Protein ID	Protein Name	Ln Expression Ratio	GO Term
E9PX29	Sptbn4	-1.83	Binding & Structural molecular activity
Q3UVI3	Tumor protein 63	-1.71	No hit
Q9Z0R6	Intersectin 2	-1.68	No hit
P23780	Beta galactosidase	-1.58	Catalytic activity
O08644	Ephrin type B receptor 6	-1.57	No hit
E9QM22	WD repeat containing protein 64	-1.56	No hit
P47226	Testin	-1.35	No hit
Q9JJ00	Phospholipid scramblase 1	-1.27	No hit
D3YYI5	Glyceraldehyde-3-phosphate dehydrogenase	-1.21	Catalytic activity
B7ZCC9	Probable G-protein coupled receptor 112	-1.19	Receptor activity
Q8CF02	Protein FAM25C	-1.18	No hit
Q9D823	60S ribosomal protein L37	-1.15	Binding & Structural molecular activity
Q6RHR9	Membrane associated guanylate kinase WW and PDZ domain containing protein 1	-1.14	Catalytic activity
P97807-2	Cytoplasmic Isoform of Fumarate hydratase, mitochondrial	-1.11	Catalytic activity
P28658	Ataxin 10	-1.02	No hit
Q920I9	WD repeat containing protein 7	-1.02	Binding & Structural molecular activity & Enzyme regulator activity
P97807	Fumarate hydratase mitochondrial	-0.99	Catalytic activity
P56960	Exosome component 10	-0.95	Binding & Catalytic activity
Q6P1J1	Crmp1 protein	0.94	No hit
Q11136	Xaa-Pro dipeptidase	0.93	Binding & Catalytic activity & Nucleic acid binding transcription factor activity
E9QPI5	Sister chromatid cohesion protein PDS5 homolog A	0.92	Binding
Q811D0-3	Isoform 3 of Disks large homolog 1	0.92	No hit
P20060	Beta-hexosaminidase subunit beta	0.92	Catalytic activity
D3YU56	Inner nuclear membrane protein Man1	-0.9	No hit
Q9CWX2	Complex I intermediate-associated protein 30 mitochondrial	-0.9	No hit
O70200	Allograft inflammatory factor 1	-0.88	Binding
Q8BK67	Protein RCC2	-0.87	Binding & Catalytic & Enzyme regulator activity
Q8BHL5	Engulfment and cell motility protein 2	-0.87	Binding
Q80SZ6	Nuclear RNA export factor 7	-0.87	Binding
O35066	Kinesin-like protein KIF3C	-0.86	Catalytic activity & Structural molecule activity
P68040	Guanine nucleotide-binding protein subunit beta-2-like 1	-0.85	No hit

Protein ID	Protein Name	Ln Expression Ratio	GO Term
Q9ERG0	LIM domain and actin-binding protein 1	-0.85	Binding & Catalytic activity & Nucleic acid binding transcription factor activity & Structural molecule activity
B1AR39	Protein 2810408A11Rik	-0.85	No hit
E9QAF9	Protein TANC1	-0.84	No hit
Q9CR98	Protein FAM136A	-0.84	No hit
G3UYY1	Serine hydroxymethyltransferase (Fragment)	-0.84	No hit
Q63918	Serum deprivation-response protein	-0.84	Binding & Nucleic acid binding transcription factor activity
E9Q7C4	Protein Prr14l	-0.83	No hit
Q9R0H0-2	Isoform 2 of Peroxisomal acyl-coenzyme A oxidase 1	-0.83	Catalytic activity
Q684R7-3	Isoform 3 of FRAS1-related extracellular matrix protein 1	-0.83	Transporter activity
Q9D7S7	60S ribosomal protein L22-like 1	-0.82	Binding & Structural molecule activity
Q8C561	LMBR1 domain-containing protein 2	-0.82	No hit
Q61526	Receptor tyrosine-protein kinase erbB-3	-0.82	No hit
E9PXK1	Cone-rod homeobox protein	-0.82	No hit
E9PW52	Protein Gm3149	-0.81	No hit
Q9JIL4	Na(+)/H(+) exchange regulatory cofactor NHE_RF3	-0.79	No hit
Q7TPD1	F-box only protein 11	-0.79	No hit
B1AVK0	Protein FAM161A	-0.79	No hit
Q56A10	Zinc finger protein 608	-0.79	No hit
P51125	Calpastatin	-0.78	No hit
Q4KWH5	1-phosphatidylinositol 4-5-bisphosphate phosphodiesterase eta-1	-0.78	Binding & Catalytic activity & Enzyme regulator activity
Q91X46	Rho guanine nucleotide exchange factor 3	-0.77	Binding & Catalytic activity & Enzyme regulator activity
Q9D8U8	Sorting nexin-5	-0.77	No hit
Q9D117	MACRO domain containing 2	-0.77	No hit
P28481-2	Isoform 3 of Collagen alpha-1(II) chain	-0.77	Receptor activity & Structural molecule activity & Receptor activity
P48754	Breast cancer type 1 susceptibility protein homolog	-0.77	Catalytic activity
Q9CWL8	Beta-catenin-like protein 1	-0.77	No hit
P09411	Phosphoglycerate kinase 1	-0.76	Catalytic activity
Q9EQS9-3	Isoform 3 of Immunoglobulin superfamily DCC subclass member 4	-0.76	Catalytic activity & Receptor activity
Q9D0R2	Threonine--tRNA ligase, cytoplasmic	-0.76	Catalytic activity
D3YU82	Probable cation-transporting ATPase 13A5	-0.76	No hit
B2RXC5	Zinc finger protein 382	-0.75	Binding & Nucleic acid binding transcription factor activity
E9QNJ9	Fibroblast growth factor receptor 3	-0.75	No hit

Protein ID	Protein Name	Ln Expression Ratio	GO Term
Q9JII6	Alcohol dehydrogenase [NADP(+)]	-0.75	Catalytic activity & Transporter activity
Q9CZP7	Hsp90 co-chaperone Cdc37-like 1	-0.75	Binding & Catalytic activity & Enzyme regulator activity
H3BJZ2	Protein Cdhr4	-0.75	Binding & Receptor activity
P53996	Cellular nucleic acid-binding protein	-0.74	Binding
Q80U87	Ubiquitin carboxyl-terminal hydrolase 8	-0.74	Binding & Catalytic activity
E9Q1W0	Calcium/calmodulin-dependent protein kinase type II subunit beta	-0.74	No hit
J3QPC5	Protein Zfp850	-0.74	No hit
P29391	Ferritin light chain 1	-0.73	No hit
Q61771	Kinesin-like protein KIF3B	-0.73	Catalytic activity & Structural molecule activity
O89086	Putative RNA-binding protein 3	-0.72	Binding & Catalytic activity & Structural molecule activity
Q80US4	Actin-related protein 5	-0.72	Structural molecule activity
P53996-2	Isoform 2 of Cellular nucleic acid-binding protein	-0.72	Binding
Q64331	Unconventional myosin-VI	-0.72	No hit
Q61176	Arginase-1	-0.72	Catalytic activity
P97313	DNA-dependent protein kinase catalytic subunit	-0.71	Binding & Catalytic activity
Q8K3P5	CCR4-NOT transcription complex subunit 6	-0.71	Binding & Catalytic activity
O08677	Kininogen-1	-0.71	No hit

Table 2.4 Passive membrane properties of iPSCMNs

Weeks in culture	N	C_m (pF)	R_m (MΩ)	V_m (mV)
1-2	16	45.25 ± 26.91 **	666.38 ± 573.95**	-45.19 ± 9.47
3-4	9	121.33 ± 45.15 **	189.33 ± 104.37^	-47.33 ± 6.19
5-6	16	80.19 ± 21.10 **	195.69 ± 59.54^	-50.44 ± 7.84

Values = Mean ± SD

** = statistically significant difference from all other means (one-way ANOVA, $p<0.05$)

^ = statistically significant difference from only the first mean (one-way ANOVA, $p<0.05$)

CHAPTER 3: INDUCED MOTONEURONS POSSESS FUNCTIONAL CHARACTERISTICS OF ENDOGENOUS MOTONEURONS

Contribution statement

I would like to acknowledge the laboratory of Kevin Eggan for supplying the fully differentiated and purified iMNs; Caitlin Jackson-Tarlton and Alex Nelson for assistance with harvesting myotubes. This chapter contains portions of text written by Esther Son, Justin Ichida and Kevin Eggan; the portions co-written by Victor Rafuse and me include the methods section pertaining to the experiments performed in this chapter, as well as the majority of the results section. I designed and performed all experiments described in this chapter. Portions of this chapter have been published elsewhere (Son EY, Ichida JK, Wainger BJ, Toma JS, Rafuse VF, Woolf CJ, Eggan K. Conversion of mouse and human fibroblasts into functional spinal motor neurons. *Cell Stem Cell*. 2011 Sep 2;9(3):205–18) and are reprinted here with permission.

Abstract

The mammalian nervous system comprises many distinct neuronal subtypes, each with its own phenotype and differential sensitivity to degenerative disease. Although specific neuronal types can be isolated from rodent embryos or engineered from stem cells for translational studies, transcription factor-mediated reprogramming might provide a more direct route to their generation. Here we report that the forced expression of select transcription factors is sufficient to convert mouse and human fibroblasts into induced motoneurons (iMNs). iMNs displayed the functional characteristics of spinal motoneurons including the abilities to 1) form functional neuromuscular junctions *in vitro* when co-cultured with myotubes and 2) integrate into the ventral spinal cord and extend axons into the periphery when implanted into the developing chick spinal cord. Our findings demonstrate that fibroblasts can be converted directly into a specific differentiated and functional neural subtype, the spinal motoneuron.

Introduction

The mammalian central nervous system (CNS) is assembled from a diverse collection of neurons, each with its own unique properties. These discrete characteristics underlie the proper integration and function of each neuron within the circuitry of the brain and spinal cord. However, their individual qualities also render particular neurons either resistant or sensitive to particular degenerative stimuli. Thus, for each neurodegenerative disease, a stereotyped set of neuronal subtypes is destroyed, causing the hallmark presentation of that condition. Therefore, if we are to comprehend the mechanisms that underlie the development, function and degeneration of the CNS, we must first deeply understand the properties of individual neuronal subtypes.

Physiological and biochemical studies of individual neuronal types have been greatly facilitated by the ability to isolate distinct classes of neurons and interrogate them in vitro. Most studies have focused on neurons isolated from the developing rodent CNS. However, it is not routinely possible to isolate analogous populations of human neurons or to isolate and fully study differentiated central neurons. Pluripotent stem cells, such as embryonic stem cells (ESCs), may provide an inexhaustible reservoir of diverse neural subtypes, offering an attractive approach for *in vitro* studies (Wichterle et al., 2002). Although stem cells have shown great promise, to date, only a handful of neural subtypes have been produced in this way. Furthermore, in many cases the neuronal populations produced from stem cells have not been shown to possess refined subtype specific properties and may only superficially resemble their counterparts from the CNS (Peljto and Wichterle, 2011). Experiments using the reprogramming of one set of differentiated cells directly into another suggest an alternative approach for the generation of precisely defined neural subtypes.

Using distinct sets of transcription factors, it is possible to reprogram fibroblasts into pluripotent stem cells (Takahashi and Yamanaka, 2006), blood progenitors (Szabo et al., 2010), cardiomyocytes (Ieda et al., 2010) as well as functional, post-mitotic neurons (Caiazzo et al.; Pfisterer et al., 2011; Vierbuchen et al., 2010). We have therefore considered the idea that by using factors acting on cells intrinsically, rather than relying on morphogens that act extrinsically, it might be possible to more precisely specify the exact properties of a wide array of neuronal types. Most reprogramming studies have so

far only produced induced neurons (iNs) with an unknown developmental ontogeny and a generic phenotype (Pang et al., 2011; Pfisterer et al., 2011; Vierbuchen et al., 2010). Recently, two studies have generated cells that resemble dopaminergic neurons based on the production of tyrosine hydroxylase (Caiazzo et al.; Pfisterer et al., 2011). However, it is unclear whether these cells are molecularly and functionally equivalent to embryo- or ESC-derived dopaminergic neurons. In particular, it has yet to be determined whether any type of neuron made by reprogramming can survive and properly integrate into the CNS. If neuronal reprogramming is to be successfully applied to the study of CNS function or degeneration, then it must be capable of producing specific neuronal types that possess the correct phenotypic properties both *in vitro* and *in vivo*.

To determine whether transcription factors can bestow a precise neural subtype identity, we sought factors that could reprogram fibroblasts into spinal motoneurons. Motoneurons control the contraction of muscle fibres actuating movement. Damage to motoneurons caused by either injury or disease can result in paralysis or death; consequently, there is significant interest in understanding how motoneurons regenerate after nerve injury and why they are selective targets of degeneration in diseases such as spinal muscular atrophy (SMA) and amyotrophic lateral sclerosis (ALS). We therefore attempted induction of motoneurons both because of their significant translational utility and because the developmental origins and functional properties of this neural subtype are among the most well understood.

Here we show that when mouse fibroblasts express factors previously found to induce reprogramming toward a generic neuronal phenotype (Vierbuchen et al., 2010), they also respond to components of the transcription factor network that act in the embryo to confer a motoneuron identity on committed neural progenitors. Thus, we found that forced expression of these transcription factors converted mouse fibroblasts into induced motoneurons (iMNs). Importantly, we found that the resulting iMNs had a gene expression program, electrophysiological activity, synaptic functionality, *in vivo* engraftment capacity and sensitivity to disease stimuli that are all indicative of a motoneuron identity. We also show that the converting fibroblasts do not transition through a proliferative neural progenitor state before becoming motoneurons, indicating they are formed in a manner that is distinct from embryonic development. Finally, we

demonstrate that this same approach can convert human fibroblasts into motoneurons. In the present chapter, I will focus solely on functional aspects of both mouse and human iMNs; specifically, their abilities to form neuromuscular junctions (NMJs) and integrate into the developing nervous system.

Methods

Molecular cloning, isolating embryonic and adult fibroblasts, viral transduction, and cell culture

HB9::GFP$^+$ iMNs were developed in the laboratory of Dr. Kevin Eggan at Harvard University before being sent to Dalhousie University for further study (i.e. iMN/myotube co-cultures and *in ovo* transplantation studies described below). In brief, iMNs were generated using complementary DNAs for 7 reprogramming factors, each cloned into the pMXs retroviral expression vector using Gateway technology (Invitrogen). Reprogramming factors for mouse iMNs included Ascl1, Brn2, Myt1l, Lhx3, Hb9, Isl1, and Ngn2. Human iMNs were generated with all of the same factors except Hb9 and with the addition of NeuroD1. Hb9**::**GFP-transgenic mice (Jackson Laboratories) were mated with ICR mice (Taconic) and mouse embryonic fibroblasts (MEFs) were harvested from Hb9**::**GFP E12.5 embryos under a dissection microscope (Leica). Tail tip fibroblasts were isolated from Hb9**::**GFP-transgenic adult mice as previously described (Vierbuchen et al., 2010). The fibroblasts were passaged at least once before being used for experiments. Human adult fibroblasts were isolated and transduced with a lentivirus containing an Hb9::GFP construct. Retroviral transduction was performed as described (Ichida et al., 2009). Glial cells isolated from P2 ICR mouse pups were added to infected fibroblasts two days after transduction. The next day, medium was switched either to mouse motoneuron medium containing F-12 (Invitrogen), 5% horse serum, N2 and B27 supplements, glutamax and penicillin/streptomycin, or to N3 medium (Vierbuchen et al., 2010). Both media were supplemented with GDNF, BDNF and CNTF, all at 10 ng/ml. Efficiency of iMN generation was estimated by counting the number of Hb9**::**GFP$^+$ cells with neuronal morphologies using a fluorescence microscope (Nikon).

Induced motoneuron/myotube co-cultures: intracellular recordings and immunocytochemistry

Myoblasts were isolated from external adductor muscles of E10 White Leghorn chick embryos and plated in 24-well plates at a density of 100,000 cells/well. Cultures were maintained at 37^{0}C in F10 media (Gibco) supplemented with 0.44 mg/ml calcium chloride, 10% horse serum, 5% chicken serum and 2% penicillin:streptomycin. iMNs

were added to the myotubes 5 days later in Neurobasal media (Gibco) supplemented with B27 (Gibco), 1% L-glutamine and 1% penicillin:streptomycin. Co-cultures were supplemented with 10ng/mL CNTF and GDNF every two days for the first week following the addition of the iMNs. For intracellular recordings, experiments were performed as described in Chapter 2 for iPSCMN-myotube co-cultures. Co-cultures were maintained for up to 3 weeks when they were prepared for immunocytochemistry. Antibody staining was performed as previously described (Soundararajan et al., 2006). A rabbit anti-GFP (Chemicon, 1:2000) primary antibody was used to visualize the iMNs and rhodamine-conjugated α-bungarotoxin (Invitrogen, 1:500) was used to visualize the AChRs. Images were acquired on a laser scanning-confocal microscope (Zeiss LSM 510). Orthogonal images were rendered and edited with LSM imaging software (Zeiss) and further contrast and brightness adjustments were performed on Photoshop version 7.0.

In ovo transplantation of induced motoneurons and immunohistochemistry

In ovo transplantations and immunohistochemistry were performed as previously described (Soundararajan et al., 2006). Briefly, E2.5 chick embryos were exposed; the vitelline membrane and amnion were cut to allow surgical access to the neural tube. An incision of 1-1.5 somites in length was made along the midline of the neural tube at the rostral extent of the developing hind limb bud (T7-L1) using a flame-sterilized tungsten needle (0.077mm wire, World Precision Instruments). A sphere of iMNs containing approximately 200 cells was then guided into the resultant hole using a tungsten needle. The eggs were sealed, returned to the incubator. Five days later, the chick embryos were harvested, fixed in 4% paraformaldehyde/PBS, cut on a cryostat and then processed for immunohistochemistry. The following primary antibodies were used: rabbit anti-GFP (Chemicon, 1:1000) and mouse anti-Tuj1 (Covance, 1:1000). Images were captured with a digital camera (C4742; Hamamatsu Photonics, Hamamatsu, Japan) in conjunction with digital imaging acquisition software (IPLab; Version 4.0; BD Biosciences, Rockville, MD, USA).

Results

As described in Chapter 1, seven factors were determined to be essential for transdifferentiation of mouse fibroblasts into iMNs, with eight factors being essential for the generation of human iMNs. The human (h)iMNs used in this study were generated with all of the factors described by Son et al. (2011) except Hb9. Once a protocol was established to generate presumptive motoneurons, a series of assays were conducted to determine whether iMNs possess functional characteristics of motoneurons.

In order to directly visualize NMJ formation in iMN cultures, we first co-cultured mouse iMNs with primary chick myotubes (Figure 3.1; Figure 3.2). After one week of co-culture, we found that many Hb9::GFP$^+$ iMNs survived, even following withdrawal of neurotrophic support, suggesting that they had formed synapses with the muscle. Three weeks after co-cultures had been initiated, staining with α-bungarotoxin (α-btx) revealed acytelcholine receptor (AChR) clustering on the myofibres (Figures 3.1 A-G). As occurs in ESCMN/chick myotube co-cultures (Miles et al., 2004; Soundararajan et al., 2007), AChRs clustered preferentially near the iMN axons (Figure 3.1 C), although the clustering was not always clearly opposed to Hb9::GFP$^+$ axons. This phenomenon is similar to what occurs during chick (Dahm and Landmesser, 1988) and mouse (Lupa and Hall, 1989) neuromuscular development where receptor clustering first appears near the innervating motor axons, but not always in direct contact. Imaging in the x–z and y–z orthogonal planes verified that ACh receptors clustered near iMN axons superimposed with the Hb9::GFP$^+$ axons (Figure 3.1 D). These results indicate that iMNs signal to the post-synaptic muscle fibre to induce appropriate receptor clustering which is necessary for neuromuscular transmission. We then conducted the same experiment with hiMNs. We found that hiMNs, similar to mouse iMNs, associated with AChR clusters twelve days after initiation of co-culture (Figure 3.2 A-C). Additionally, much like previously observed with ESCMNs (Miles et al., 2004) and iPSCMNs (Chapter 2), iMNs generated post-synaptic endplate potentials that were detected by sharp electrode intracellular recordings at motor endplates (Figure 3.2 D). Together, these data indicate that iMNs can make functional synaptic junctions with muscle.

Previous studies have shown that transplantation of stem cells derived motoneurons into the developing chick spinal cord rigorously tests whether they develop

the same cellular phenotypes enabling them to migrate appropriately within the spinal cord, and to respond to axon guidance cues directing their axons to extend out of the spinal cord through the ventral root (Peljto et al., 2010; Soundararajan et al., 2006; Wichterle et al., 2002). To examine whether iMNs develop these properties, we transplanted FACS-sorted iMNs into the neural tube of HH st. 17 chick embryos at 12–16 days post-transduction (Figure 3.3). Although the injection of the iMNs along the dorsal-ventral axis was not precisely controlled, we observed that Hb9::GFP$^+$ iMNs engrafted in the ventral horn of the spinal cord in the location where endogenous motor neurons reside at HH st. 31 (Figure 3.3 A). Like transplanted embryonic stem cell derived motor neurons (ESCMNs) (Soundararajan et al., 2006; Wichterle et al., 2002), the Hb9::GFP$^+$ cells maintained Tuj1 expression and exhibited extensive dendritic arbors (Figure 3.3 A). Next, we examined whether iMNs projected axons out of the CNS. Indeed, we found that 80% (n=5) of the transplanted Hb9::GFP$^+$ iMNs normally projected axons out of the neural tube through the ventral root (Figure 3.3 A,B). Taken together, these data demonstrate that iMNs are able to engraft, migrate to appropriate sites of integration, and correctly respond to guidance cues that direct their axons out of the developing CNS.

Discussion

This study shows that a small set of transcription factors can convert embryonic and adult fibroblasts into functional motoneurons. These cholinergic iMNs also possessed many defining hallmark of motoneurons such as ability to form synapses at – and make functional connections with – muscle fibres. In addition, fibroblasts derived from adult humans were capable of transdifferentiation into iMNs that made functional connections with chick myotubes. One of the more important findings of this study is the ability of hiMNs to develop NMJs that are morphologically and physiologically similar to endogenous NMJs, as this factor is critical if iMNs are to be used for therapeutic purposes. Using intracellular recording techniques, EPPs were recorded from muscle fibres suggesting that activity is generated by iMNs in a manner similar to that described in previous studies of iPSCMNs (Chapter 2) or ESCMNs (Miles et al., 2004). Future investigations will need to be undertaken to determine to what degree hiMNs form functional NMJs, and whether transmission at these NMJs responds to pharmacological agents such as TTX or curare in a manner similar to that of the NMJs formed by ESCMNs or iPSCMNs.

Other promising results in this chapter show that iMNs are able to contribute to the developing CNS *in vivo*, migrating appropriately to the ventral horn and sending out axonal projections through the ventral root. While these results are encouraging, there were some limitations of the functionality of iMNs as compared to that of either iPSCMNs or ESCMNs. Unlike the case with transplanted iPSCMNs or ESCMNs, none of the transplanted iMNs projected axons through peripheral nerves towards muscle targets, suggesting that iMNs have a limited ability to project axons towards a peripheral target. The reasons for this are unknown, but may relate to the absence of adequate expression of appropriate guidance factors or levels of intrinsic activity within the iMN cell bodies (see discussion, Chapter 5).

In conclusion, although there are some noted differences in the functionality of iMNs as compared to motoneurons derived from iPSCs and ESCs, we provide several lines of evidence that iMNs are functional motoneurons with consequent utility for the study of motoneuron physiology and disease susceptibility.

Finally, it is critical to note that we cannot rule out the possibility that other motoneuron-inducing factors have been overlooked, or that varying the cocktail of genetic factors might further enhance the frequency or even accuracy of conversion. Such a reprogramming approach would greatly facilitate the production of patient-specific motoneurons for therapeutic uses in regenerative medicine as well as for disease-related studies.

Chapter 3 Figures

Figure 3.1 Mouse iMNs induce acetylcholine receptor clustering and form anatomical endplates on cultured myotubes

A, Fluorescence image of GFP$^+$ iMNs after 7 weeks of co-culture with chick myotubes. **B**, Rhodamine-conjugated α-btx staining showed ACh receptor clustering occurred on the chick myotubes. **C**, Merged image of (**A**) and (**B**) showed ACh receptors clustering preferentially occurred near the GFP$^+$ axons and at the end of the neurites at putative endplate regions (arrows). ACh receptor clusters were less pronounced on myotubes not associated with axons (arrowhead). **D**, Confocal image depicting a GFP$^+$ axon co-localized with acetylcholine receptors at a putative endplate in a 3-week co-culture. Imaging in both the x–z and y–z orthogonal planes confirms the close proximity of the receptors to the axon terminal. **E-G**, NMJ shown in **D**, α-btx$^+$ endplate (**E**), GFP$^+$ motor terminal, and merge (**G**). Scale bars represent 50 μm (**D**) and 5 μm (**E**).
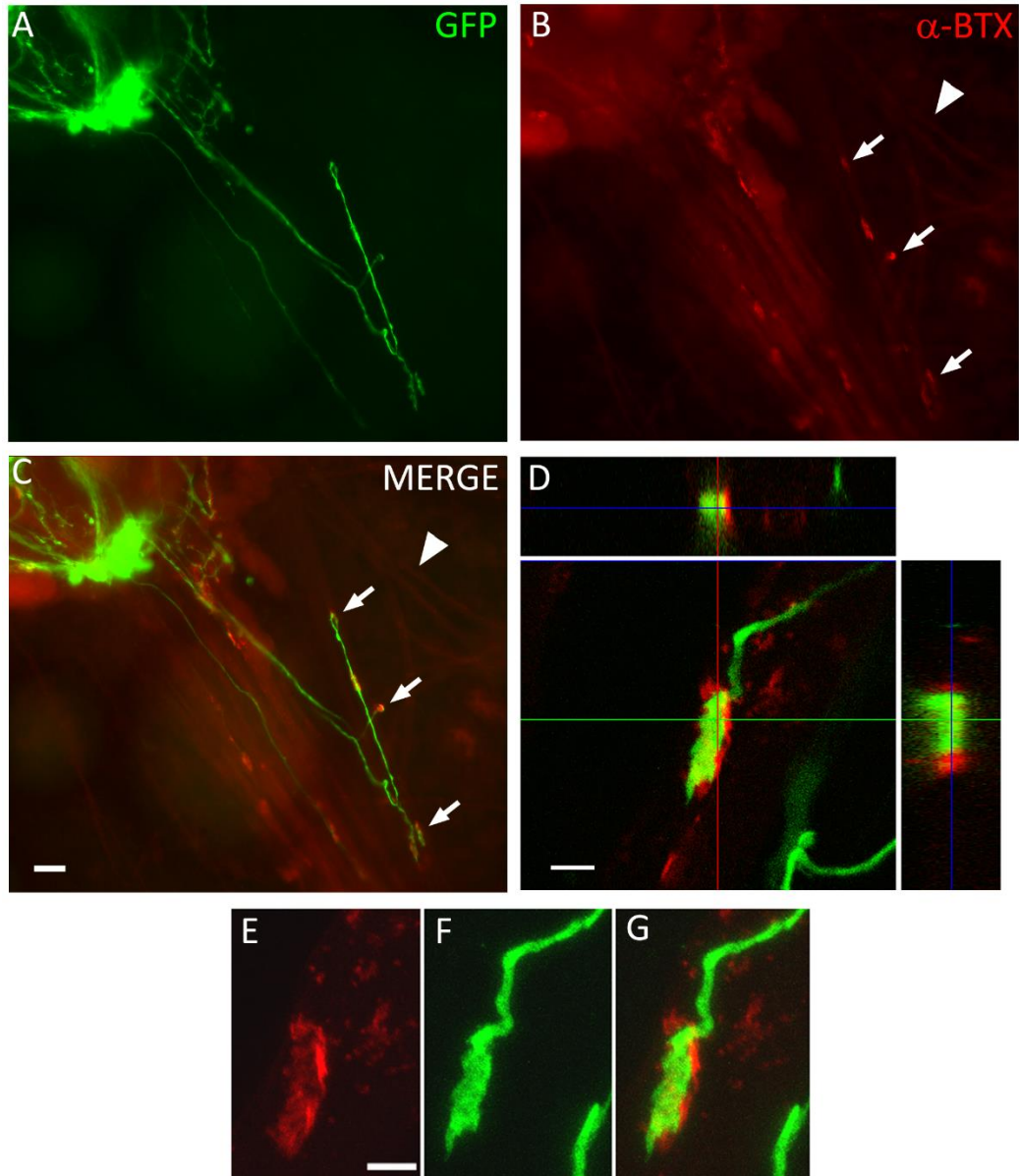
Figure 3.2 Human iMNs form functional NMJs on chick myotubes

A, hiMNs project GFP$^+$ axons along chick myotubes (**A**) and are associated with clusters of ACh receptors (arrowheads in **B**, **C**). ACh receptor clustering is largely absent on myotubes lacking contact with axons (asterisk). Scale bar = 20 μm. 12d. co-culture. **D**, A sample trace from a sharp electrode, post-synaptic intracellular recording of a 12d. hiMN-myotube co-culture. The black arrowheads indicate miniature endplate potentials (spontaneous events, single quantum) and the white arrowhead indicates a presumptive evoked endplate potential (multi-quanta event, > 1mV). Resting membrane potential = -50mV.
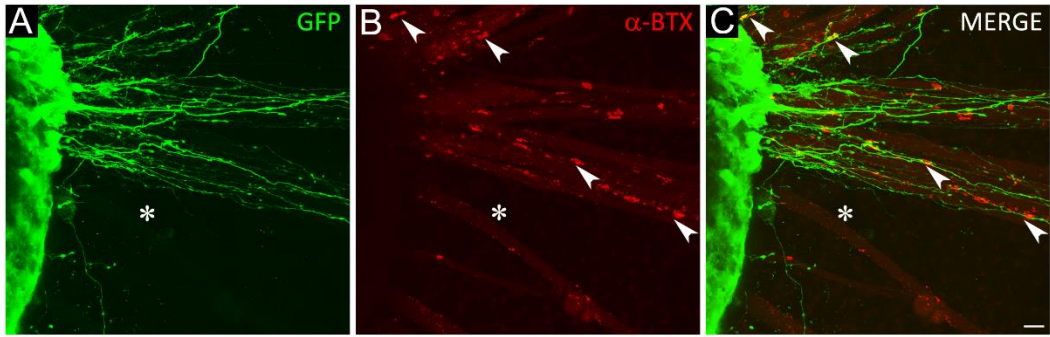
Figure 3.3 iMNs integrate into the developing chick spinal cord and project axons into the periphery

iMNs were transplanted into the neural tube of the HH st. 17 chick embryo and transverse sections of iMN-injected chick neural tube 5 days after transplantation are shown in (**A**) and (**B**). Asterisk indicates iMN in ventral horn in (**A**). Arrows in (**A**) and (**B**) indicate the same axon of an iMN exiting the spinal cord through the ventral root. SC: spinal cord, D: dorsal, V: ventral, VR: ventral root. red = neuronal specific microtubule protein Tuj1, green = GFP.
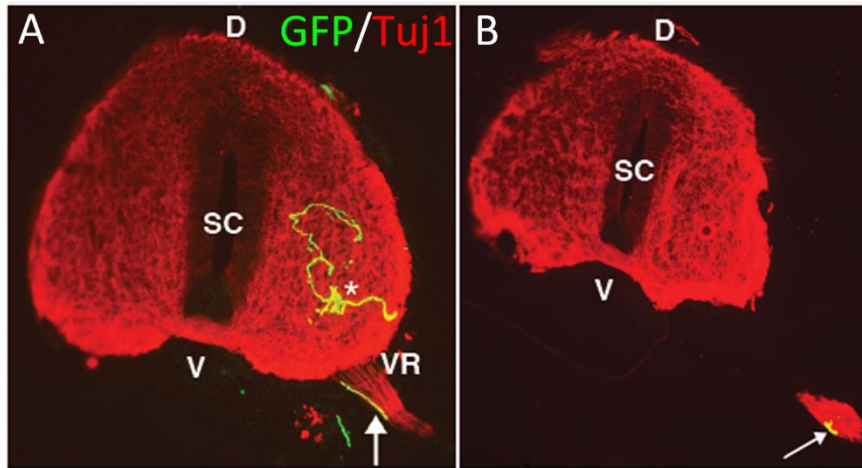
CHAPTER 4: THE EFFECTS OF EXTENDED RETINOIC ACID TREATMENT ON EMBRYONIC STEM CELL DERIVED MOTONEURONS: A PHENOTYPIC ANALYSIS OF LHX1$^+$ MOTONEURONS

Contribution statement

Abstract

Retinoic acid (RA) is known to be an important factor for the differentiation of embryonic stem cell derived motoneurons (ESCMNs), however its use in ESCMN differentiation protocols results largely in the generation of motoneurons that develop the characteristics of medial motor column motoneurons which innervate postural muscles. Here, we demonstrate that extended treatment of ESCMNs with RA for up to 3 days following results in increased expression of genes and proteins expressed by motoneurons of the lateral division of the lateral motor column (LMC_l) – large, limb-innervating motoneurons that are susceptible to degeneration and death in motoneuron diseases such as amyotrophic lateral sclerosis (ALS). We found that 70-80% of all ESCMNs expressed Lhx1 and FoxP1, transcription factors necessary for the formation of LMCl motoneurons. We then go on to show that ESCMNs decrease their expression of Lhx1 through what is likely a cell-autonomous manner as they mature. ESCMNs exposed to extended RA treatment on myotubes were found to be larger on average than motoneurons that did not receive RA treatment after weeks in culture, which may be a result of a gene expression program similar to that of large limb-innervating, LMC_l motoneurons. In contrast, the average cell soma size of ESCMNs that harbour a genetic mutation in the SOD1 gene (which results in ALS) decreased in response to RA, suggesting that the larger motoneurons may be degenerating and dying, as occurs in ALS. We conclude that extended RA treatment may provide an important role in generating the high yields of LMCl ESCMNs necessary for both developmental studies of limb-innervating motoneurons and for the potential development of therapeutics for motoneuron diseases such as ALS.

Introduction

Embryonic stem cell-derived motoneurons (ESCMNs) are currently widely used to model motoneuron diseases, such as amyotrophic lateral sclerosis (ALS), and to investigate the molecular mechanisms regulating motoneuron development (reviewed by Chipman et al., 2012). To date, most studies have directed embryonic stem (ES) cells to differentiate into motoneurons using retinoic acid (RA) and a sonic hedgehog pathway agonist (smoothened agonist, SAG). Using this technique, ESCMNs differentiate into a very specific subset of motoneurons that express the homeodomain factor Lhx3 and reside in the medial aspect of the medial motor column (MMC_m). Both $Lhx3^+$ ESCMNs and their endogenous counterparts selectively innervate epaxial muscles lining the vertebral column because they express axon guidance molecules appropriate for MMC_m motoneurons (Wichterle et al., 2002; Soundararajan et al., 2006, 2007, 2010). $Lhx3^+$ motoneurons are smaller than limb-innervating motoneurons and they develop electrophysiological/molecular characteristics that are appropriate to their size (Soundararajan et al., 2006).

It is now well established that large motoneurons die before smaller ones in both patients with ALS and in mouse models of the disease (Amoroso et al., 2013; Frey et al., 2000, Pun et al., 2006, reviewed by Kanning et al., 2010). As a result, recent efforts have been made to generate large limb-innervating ESCMNs in order to study how the two classes of motoneurons develop and why large motoneurons are more susceptible to disease. For example, using only endogenous stem cell mitogens, Peljto et al. (2010) generated a population of ESCMNs whereby 15% of them expressed FoxP1. FoxP1 is a transcription factor essential for the development of limb-innervating motoneurons residing in the LMC (Dasen et al., 2008; Rousso et al., 2008). Amoroso et al. (2013) showed that 70% of human (h)ESCMNs express FoxP1 when treated with two different sonic hedgehog agonists – SAG and purmorphamine – along with RA. These $FoxP1^+$ ESCMNs selectively targeted limb musculature when transplanted *in ovo* indicating that they likely expressed axon guidance molecules appropriate for LMC motoneurons (Amoroso et al., 2013). More recently, a genetic approach to generating limb-innervating motoneurons has been developed whereby FoxP1 is constitutively expressed in developing ESCMNs (Adams et al., 2015). These cells preferentially targeted limb

muscles both *in vitro* and *in ovo*. Taken together, these results suggest that FoxP1$^+$ ESCMNs are developmentally similar to their endogenous counterparts, however it is not known whether they are more susceptible to disease compared to smaller Lhx3$^+$ motoneurons.

The LMC is subdivided into two motor columns that differ in transcription factor expression patterns and axonal projection patterns. Motoneurons in the medial aspect of the LMC (LMC$_m$) express FoxP1 and Isl1 and innervate muscles (mostly flexor) derived from the ventral muscle mass (Dasen et al., 2008; Rousso et al., 2008; Tsuchida et al., 1994; Landmesser, 1978). Motoneurons in the lateral aspect of the LMC (LMC$_l$) express FoxP1 and the LIM homeodomain factor Lhx1 (Dasen et al, 2008; Rousso et al, 2008; Tsuchida et al., 1994). These motoneurons innervate muscles arising from the dorsal muscle mass (largely extensor muscles) (Landmesser, 1978). Thus, the LMC is composed of two distinctly different types of motoneurons, those innervating flexor muscles while another innervates predominantly extensor muscles. The molecular mechanisms governing the directed differentiation of the two cell types is not fully understood. However, developmental studies suggest that LMC$_l$ neurons acquire Lhx1 expression because they are exposed to retinoid signals for a longer period of time compared to MMC$_m$ or LMC$_m$ neurons (Sockanathan and Jessell, 1998). While efforts to generate Lhx1$^+$ ESCMNs utilizing pulses of RA have been attempted (Peljto et al., 2010; Amoroso et al., 2013; Adams et al., 2015), generation of high yields of ESCMNs that express Lhx1 has not yet been achieved.

In the present study, we describe a protocol for differentiating ES cells into Lhx$^+$ LMC$_l$ motoneurons using prolonged exposure to RA. This technique reliably generates high yields (~80%) of Lhx1$^+$ ESCMNs. We show that Lhx1$^+$ motoneurons express proteins characteristic of LMC$_l$ motoneurons (including FoxP1) and exhibit a larger soma size than Lhx3$^+$ ESCMNs. RA treated ESCMNs also exhibited enhanced survival rates *in vitro*, indicating a possible long-term trophic effect of RA on ESCMNs. In contrast to healthy ESCMNs exposed to RA, we show that RA treated ESCMNs harboring a mutation in the superoxide dismutase 1 (SOD1) gene (Di Giorgio et al., 2007), which results in ALS, decrease in size between 25d. and 40d. when co-cultured with chick myotubes. These results suggest that larger ESCMNs carrying the SOD1 mutations die

first, as occurs in ALS (reviewed by Kanning et al., 2010). When co-cultured long term (up to 40d.) in co-culture with chick myotubes, RA treated ESCMNs develop larger motor endplates indicating that Lhx1 expression leads to an increased ability to form large neuromuscular junctions because they generate larger 'fast' motoneurons that typically innervate large fast contracting muscle fibres (Suzuki et al., 2009). In conclusion, we demonstrate that extended RA exposure induces phenotypic properties in ESCMNs reminiscent of LMC_1 motoneurons and that these cells may be useful to study motoneuron development and disease.

Methods

Generation of ESCMNs

The methods used to generate and maintain ES cell colonies and differentiation of ESCMNs were similar to those previously reported. Modified excerpts from "Chipman PH, Zhang Y, Rafuse VF (2014) A Stem-Cell Based Bioassay to Critically Assess the Pathology of Dysfunctional Neuromuscular Junctions. PLoS ONE 9(3): e91643. doi:10.1371/journal.pone.0091643" are reprinted with permission below.

Three ES cells lines were used in this study. First, HBG3 mouse ES cells (a kind gift provided by Tom Jessell, Columbia University, New York NY) were originally derived from Hb9::GFP transgenic mice (Jackson Labs, Bar Harbour, Maine). Second, a mouse ES cell line possessing the human SOD1G93A mutation (HBSOD1) and express GFP under the Hb9 promoter were provided by Kevin Eggan (Harvard University, Cambridge MA). ESCMNs expressing tdtomato (termed HBR1) were generated in the lab by crossing mice expressing Hb9::Cre with mice expressing a loxP-stop-loxP-tdtomato construct under the ubiquitously-expressed Gt(ROSA)26Sor locus (Jackson Labs, Bar Harbour, Maine). Hb9::tdtomato ES cells were isolated from the inner cell mass of a mouse blastocysts using standard techniques. Briefly, pregnant females were sacrificed on the 3rd day of pregnancy when embryos are at the 8–16 cell stage. The uterine horn was extracted and placed in warmed M2 media (Sigma M7167). Blastocysts were flushed from the uterine horn and transferred to a 4 well plate containing a confluent monolayer of mitomycin C treated (Sigma) primary mouse embryonic fibroblasts (PMEFs). The inner cell mass (ICM) was allowed to expand for approximately 4 days then fed every two days with embryonic stem cell media (ESC media) containing DMEM (Gibco 11995-073), ESC grade fetal bovine serum (FBS; 15% by volume; Millipore ES-009-B), penicillin/streptomysin (1% by volume; Gibco 5140-122), 2-mercaptoethanol (1% by volume; Millipore ES-007-E), non-essential amino acids (1% by volume; Millipore TMS-001-C) and ESGRO LIF (leukaemia inhibitory factor; 1000 u/ml; Millipore ESG1106). After another 4–6 days, the ICM was mechanically separated from the blastocyst using a tungsten needle and 2.5% trypsin. Cells were further dissociated into small clumps and transferred onto a 4 well plate containing a confluent monolayer of

PMEFs and ESC media where they were allowed to expand into ES colonies and were passaged as needed to avoid confluence. This cell line was generated at Dalhousie University with the approval of the Dalhousie University Committee on Laboratory Animals. Isolated ES cell colonies were differentiated into motoneurons as described previously (Wichterle et al 2002; Miles et al 2004; Soundararajan et al 2006). In brief, ES cells were grown as aggregate cultures in DFK10 media to form free floating embryoid bodies. DFK10 medium consisted of DMEM (Gibco 11995-073) and Ham's F-12 media (Specialty Media) in a 1:1 ratio supplemented with knock-out serum replacement (10% by volume; Invitrogen, Burlington, Ontario, Canada), penicillin/streptomycin (1% by volume; Sigma, St. Louis, MO), N2 supplement (2.4% by volume; Invitrogen), glucose (4500 mg/l), L-glutamine (200 mM), heparin (1 u/l; Sigma), and β-mercaptoethanol (0.1 mM; Sigma). After 2 days, the embryoid bodies were treated with a smoothened agonist (SAG, 500 nM, Enzo) and RA (1 μM; Sigma, St. Louis, MO) and cultured as free-floating cells for an additional 4 days. On day 2 or 3 of differentiation, approximately half of the media was removed and fresh media supplemented with RA and SAG was added. GFP expression was monitored as an assessment of differentiation and only embryoid bodies with robust and homogenous GFP expression were used for further assessment.

All procedures in this study were conducted in accordance with the guidelines of the Canadian Council on Animal Care and specifically approved by the Dalhousie University Committee on Laboratory Animals.

ESCMN cultures

ESCMNs that were treated for 4 days with RA and SAG and then dissociated with TrypLe (Invitrogen) and 1 x DNAse for approximately 15 min. at room temperature and plated on coverslips coated with one of the following substrates: Matrigel (BD Biosciences), Poly-d-lysine (1mg/mL, Millipore), C6 glioma cells (ATCC) or PMEFs (isolated from ~e15 mouse embryos) (see results, Figure 4.1). ESCMNs were treated with DFK10 media supplemented with 10 ng/μl GDNF (Gibco) and CNTF (Gibco) for 2-3 days prior to fixation and immunocytochemical analysis. 1 μM of RA was added at the

time of plating ESCMNs in the RA treated group, cells receiving only GDNF and CNTF are referred to as growth factor (GF) only controls.

ESCMN/myotube co-cultures

Control and hSOD1G93A$^+$ ESCMNs were dissociated in TrypLe (Invitrogen) 4 days after initial RA and SAG treatment and plated on chick myotubes harvested 2-3 days earlier (as described in Chapter 2). ESCMNs were added to the myotubes with DFK10 supplemented with the growth factors GDNF (10 ng/μl) and CNTF (5 ng/μl) following removal of F10 media present in the myotube cultures. DFK10 was replaced with growth factor-supplemented Neurobasal media (Gibco) after 2 d. in co-culture. Growth factor-free Neurobasal was used after 1 week of co-culture. Approximately 50,000 GFP$^+$ ESCMNs were added to each co-culture. Approximately ½ of the Neurobasal media (~500 μl) was replaced every 2 days. 1 μM of RA was added at the time of plating ESCMNs in RA treated co-cultures. For experiments involving coverslips overlying myotubes (see results, Figure 4.5), cells were treated with either DFK10 or Neurobasal media. No differences were noted in Lhx1 expression in ESCMNs cultured in either media (data not shown). α-bungarotoxin (α-btx) (Life Technologies) was used at a final concentration of ~ 2 μg/ml and applied daily for experiments described in Figure 4.5.

Immunocytochemistry and quantification of immunoreactivity

ESCMN cultures and co-cultures were fixed in 4% formaldehyde for approximately 15 min., washed multiple times in PBS for approximately 30 min. and immunocytochemistry was performed as described in Chapter 2. The following 1^0 antibodies were used: mouse anti-Lhx1 (supernatant, 1:2, DSHB), rabbit anti-HoxC6 (Abcam, 1:200), guinea pig anti-HoxA5 (a kind gift from Tom Jessell's lab, 1:10 000), and rabbit anti-FoxP1 (Abcam, 1: 20 000). 2^0 antibodies include goat anti-guinea pig Alexa Fluor 488 (Molecular Probes), goat anti-rabbit Alexa Fluor 488 (Molecular Probes), goat anti-rabbit Cy3 (Jackson ImmunoResearch) goat anti-mouse Alexa Fluor 488 (Molecular Probes) and goat anti-mouse Cy3 (Jackson ImmunoResearch). For any cultures older than approximately 1 week, rabbit anti-GFP (Chemicon, 1:1000) was used to visualize motoneurons. All 2^0 antibodies were used at 1:500. Tetramethylrhodamine

conjugated α-btx (1:500, Invitrogen). Coverslips were mounted onto slides and immunocytochemistry was analyzed as described in Chapter 2.

For quantification of ESCMN survival or immunoreactivity, 4 counting regions were established for each coverslip. Each counting region was defined by a field of view under 20x objective magnification. Typically 2 coverslips were used per experimental condition and counts were summed across counting regions and coverslips (i.e. 8 counting regions/ experimental condition). Cell count values reported in Figure 4.10 M were estimated by extrapolating the value determined in the 8 counting regions over the total area of 2 coverslips. Cell counts were highly variable depending on experimental conditions. For hSOD1G93A$^+$ ESCMN survival on matrigel experiments (Figure 4.9), 2 regions were counted per coverslip and cell numbers were summed across 2 coverslips to obtain the values reported in the figure. Images of ESCMNs were taken on a laser scanning-confocal microscope (Zeiss LSM 510) and contrast and brightness adjustments were made on Adobe photoshop CS5 software. Some images of ESCMNs (Figures 4.5, 4.6 and 4.11) were acquired using a Photometrics Cool Snap HQ2 camera mounted to a Zeiss Axio Examiner D1 microscope.

Analysis of ESCMN cell soma and endplate area

For each RA treated and untreated GF only group, cell soma area values were pooled across 4 separate experiments. Endplate areas for healthy ESCMNs were pooled across 4 experiments and values were pooled across 2 experiments for hSOD1G93A$^+$ ESCMNs. For each experiment, a maximum of 30 ESCMN cell bodies and 40 endplates were analyzed per treatment group (GF only and RA treated) per timepoint per condition (healthy or hSOD1G93A$^+$). ESCMNs and endplates were captured using a Photometrics Cool Snap HQ^2 camera mounted to a Zeiss Axio Examiner D1 microcope. Cell soma and endplate areas were measured using 3i Software: Slidebook 6 (64 bit). Endplate areas = area of α-btx labelling (See Figures 4.7 and 4.12).

Statistical Analyses

All statistics were analyzed using Sigma Plot 11 (Systat Software) and XLSTAT 2014 (Addinsoft). All details are reported in the text. Plots were constructed using Sigma Plot 11 or GraphPad Prism version 5.01 (GraphPad Sofware).

Results

Mouse ES cells can be directed to express Lhx1

Previous work, using chick neural tube explants, suggests that LMC_l neurons express Lhx1 because they are exposed to retinoid signals from neighbouring cells for a longer period of time compared to MMC_m or LMC_m neurons (Sockanathan and Jessell, 1998). Inspired by these results we sought to determine whether prolonged treatment of mouse ES cells to RA directs them to differentiate into $Lhx1^+$ LMC_l motoneurons. Typically, mouse HBG3 ES cells form clusters of cells, called embryoid bodies that preferentially differentiate into $eGFP^+$ MMC_m, $Lhx3^+$ ESCMNs when exposed to RA and a SAG for 5 days *in vitro* (Wichterle et al., 2002; Soudararajan et al., 2006; 2010). To expose HBG3 to RA for a longer period of time we treated HBG3 embryoid bodies for 4 days *in vitro* (DIV) with RA (1 μM) and SAG (500nM), before dissociating them into a single cell suspension that was subsequently plated on matrigel coated coverslips. The media was supplemented with GDNF (10 ng/μl) and CNTF (5 ng/μl) to promote better cell survival. Half of the cultures were treated with RA (1 μM) for 1-4 more days while the other half received only the two growth factors. Figure 4.1 (A-F) shows that the number of GFP^+ motoneurons expressing Lhx1 was dramatically higher in cultures treated for 3 days with RA compared to those cultured in growth factors only. Indeed, approximately 80% of the GFP^+ motoneurons expressed Lhx1 when exposed to RA for 2-4 days after plating (Figure 4.1 G). While the percentage of ESCMNs expressing Lhx1 was significantly higher in RA treated cells versus untreated controls at all of the time points studied, there was greater variability in the number of $Lhx1^+$ motoneurons after only 1 day of RA treatment (Figure 4.1 G). The percentage of ESCMNs expressing Lhx1 in cultures containing only growth factors (~15%; Figure 4.1 G) was similar to that observed in previous studies where embryoid bodies were treated for 5 DIV with RA and SAG (Wichterle et al., 2002; Soundararjan et al., 2006). Interestingly, if we simply treated embryoid bodies with RA for an additional 2 days (i.e. a total of 7 DIV), the percentage of ESCMNs expressing Lhx1 remained low (~26%). This surprising result suggest that growth on matrigel is required for Lhx1 expression or some factor associated with embryoid bodies inhibits its expression.

To determine if there is a substrate effect on the expression of Lhx1, we plated dissociated ESCMNs on two cell-free adherent substrates (poly-d-lysine and matrigel) and three cell-based substrates (PMEFs, C6 rat glioma cells, and chick myotubes) after treating them with RA and SAG for 4 DIV. The plated cells were treated with growth factors and RA for an additional 2 DIV prior to fixation. Interestingly, only 3 substrates (matrigel, poly-d-lysine and myotubes) provided conditions conducive to maximize the expression of Lhx1$^+$ by ESCMNs (Figure 4.1 H). Indeed, the percentage of ESCMNs expressing Lhx1 was not significantly different from one another when cultured on matrigel, poly-d-lysine or chick myotubes. Interestingly, however, GFP$^+$ ESCMNs plated on PMEFs and C6 cells contained significantly fewer Lhx1$^+$ ESCMNs than those cultured on matrigel, poly-d-lysine or myotubes (Figure 4.1 H). The reasons for this is unclear but may reflect paracrine inhibition of Lhx1 expression by PMEFs and C6 glioma cells.

Three ES cell lines were used in this study (HBG3, HBR1 and HBSOD1). In every line investigated, the percentage of Lhx1 was approximately 80% when dissociated and cultured on matrigel or chick myotubes in the presence of RA for an additional 2-3 DIV. Although not the focus of this study, the vast majority of motoneurons derived from mouse induced-pluripotent stem cells also expressed Lhx1 when cultured in this manner (data not shown). Taken together, these results indicate that pluripotent stem cells differentiate into Lhx1$^+$ motoneurons when treated with RA and SAG for 4 DIV and then dissociated and plated for an additional 2 days in the presence of RA, GDNF and CNTF. For convenience, we will refer to this differentiation protocol as "growth factors and RA (GF+RA)" while the dissociated cultures treated with only growth factors will be referred to as "GF" throughout the remainder of this chapter.

Protein expression patterns in Lhx1$^+$ ESCMNs

We next sought to determine if prolonged RA treatment produces Lhx1$^+$ ESCMNs with characteristics typical of LMC$_l$ motoneurons. Because FoxP1 is essential for the development of limb-innervating LMC$_l$ motoneurons (Dasen et al., 2008; Rousso et al., 2008) we immunolabeled tdtomato$^+$ ESCMNs derived from HBR1 ES cells (see

Methods for details) for FoxP1 (Figure 4.2). We found that the percentage of ESCMNs expressing FoxP1 was significantly higher when the cells received GF+RA compared to GF (Figure 4.2 G) (mean ± standard deviation, GF = 27 ± 8%, n = 3; GF+RA = 71 ± 6%, n = 4, p < 0.001, Student t-test). Because Hox genes are essential for initiating gene expression programs responsible for determining motoneuron identity (Dasen et al., 2003; 2005; reviewed by Dasen and Jessell, 2009) we next investigated whether expression of Hox transcription factors differed between the two differentiation protocols (i.e. GF+RA, GF only) Previous studies have shown that mouse ES cells differentiate into motoneurons with a cervical spinal cord fate identity, marked by HoxA5 expression, when differentiated as embryoid bodies in the presence of RA and Shh or SAG (Wichterle et al., 2002, Peljto et al., 2010). Figure 4.3 shows that not only did the majority of GFP$^+$ ESCMNs express HoxA5, but both differentiation protocol yielded the same number of HoxA5$^+$ motoneurons (Figure 4.3 G) (mean ± standard deviation, GF = 74 ± 14%, GF+RA treated = 81 ± 3%, n = 3/group, p = 0.413, Student t-test). In contrast, Figure 4.4 shows that the number of ESCMNs expressing HoxC6 was significantly higher in cultures treated with GF+RA compared to GF only (Figure 4.4 G) (mean ± standard deviation, GF only = 0.8 ± 0.4%, GF+RA = 5 ± 2%, n = 3/group, p = 0.025, Student t-test). While the reasons for this latter result is unclear, the combinatorial expression of Lhx1, FoxP1, HoxA5 and HoxC6 suggest that GF+RA treatment produces limb-innervating, cervical motoneurons.

Profile of Lhx1 expression in ESCMNs

LIM homeodomain proteins, such as Lhx1, are typically down-regulated in motoneurons after they form mature synaptic connections with muscle fibres late in development (Tsuchida et al., 1994). Based on this correlation, we sought to examine whether the formation of mature neuromuscular junctions (NMJs) triggers the down-regulation of Lhx1 in ESCMNs. To this end, we compared Lhx1 expression in ESCMNs co-cultured with chick myofibres (Figure 4.5, A-I) to those plated on matrigel (Figure 4.5, J-R). Because previous studies have shown that ESCMNs make functional synaptic contacts with chick muscle fibres after 7 DIV (Miles et al., 2004; Chipman et al., 2014), we

quantified Lhx1-expressing motoneurons before (2 and 4 DIV) and after (8 DIV) this time point. Figure 4.5 S shows that the number of motoneurons expressing Lhx1 decreased significantly when the neurons were co-cultured with myofibres as compared to motoneurons plated on matrigel, but only after 8 DIV (mean ± standard deviation, value at 8d. on matrigel = 75 ± 5%; on myotubes = 37 ± 9%, n = 3/group, p = 0.003, Student t-test). The number of Lhx1^{+} ESCMNs also decreased by 8 DIV when the post-synaptic AChRs were blocked with α-btx indicating that neurotransmission at the NMJ is not required for its down-regulation (mean ± standard deviation, value at 8d. on matrigel = 75 ± 5%; on myotubes treated with α-btx = 42 ± 9%, n = 3/group, p = 0.005, Student t-test; Figure 4.5 S). To test whether myotubes secrete a factor regulating Lhx1 expression we plated motoneurons onto matrigel-coated coverslips mounted on a plastic ring placed over the myotubes. This prevented direct contact between motoneurons and myotubes while allowing media (and any secreted factors) to flow freely between them. We found that the percentage of Lhx1^{+} motoneurons on coverslips suspended over myotubes was the same as those plated on matrigel only (mean ± standard deviation, value at 8d. on matrigel = 75 ± 5%, at 8d. on matrigel over myotubes = 76 ± 4%, n = 3/group, p = 0.885, Student t-test, Fig. 4.5 S). These results suggest that the regulation of RA-induced Lhx1 expression in motoneurons does not involve secreted factors from muscle, however the possibility remains that a muscle-derived factor expressed on the surface of muscle fibres may contribute to the decline of Lhx1 in motoneurons.

Motoneuron cell soma size increased in response to RA treatment
Next we investigated whether extended GF+RA treatment resulted in any phenotypic changes to the motoneurons that would resemble a more LMC$_l$-like, limb-innervating phenotype, such as larger cell soma, which are characteristic of fast-fatigable limb-innervating motoneurons (Cullheim et al., 1987). To test whether extended RA would affect soma size, we plated motoneurons on myotubes with RA treatment for 2 days and replaced the media with RA-free neurobasal as described in the Methods section. Up to 10 DIV, there was no difference in cell soma area between GF+RA treated and GF control ESCMNs (Figure 4.6 A-B, E-J; Two-Sample Kolmogorov-Smirnov Test, p =

0.564 at 2d. and p = 0.165 at 10d., n = 120/group). However, by 25 DIV, the population of GF+RA ESCMNs grew significantly larger than GF ESCMNs (Two-Sample Kolmogorov-Smirnov Test, p = 0.001, GF, n = 78; GF+RA, n = 98, Figure 4.6 M). This trend was maintained up to 40d. (Two-Sample Kolmogorov-Smirnov Test, p = 0.001, GF, n = 80; GF+RA, n = 94, Figure 4.6 P).

The distribution of cell soma areas for each condition at each time point is shown in histograms in Figure 4.6. The distribution in sizes remains fairly similar between GF+RA and GF ESCMNs at 2 and 10 DIV (compare E to F and H to I, respectively, Figure 4.6). As well, there was no significant change in cell soma area between 25 and 40 DIV in either the GF+RA treated or GF ESCMNs (p > 0.05 for each comparison, Mann-Whitney Rank Sum Test). However, by 25 DIV, there is an increase in a subset of larger motoneurons in the GF+RA ESCMNs as compared to GF controls that is maintained up to 40 DIV (compare K to L and N to O respectively, Figure 4.6). We defined a large motoneuron as being greater than 400 μm^2, which is based on the area of an average motoneuron with a diameter of ~20 μm. This definition is based on previous studies where motoneurons of the mouse lumbar spinal cord with a circular diameter of > 20 μm were considered large by McHanwell and Biscoe (1981). The percentage of ESCMNs with soma areas > 400 μm^2 increased in the GF ESCMNs until 25 DIV, where these values were similar at 25 and 40 DIV between both RA treated and untreated healthy control ESCMNs (% cells > 400 μm^2, untreated controls at 25d. = 36%, at 40d. = 40%; RA treated at 25d. = 61%, at 40d. = 66%) with the percentage being ~ 25% greater in RA treated ESCMNs at both time points. We then investigated cell soma area changes between 25d. and 40d. in the largest motoneurons (as defined by having a soma area > 600 μm^2) and found that they increased modestly in GF+RA ESCMNs while remaining similar in the GF group from 25d to 40d. in co-culture (untreated controls at 25d. = 13%, at 40d. = 12%; RA treated at 25d. = 21%, at 40d. = 27%). The largest ESCMNs at 40 DIV were the GF+RA treated ESCMNs, suggesting that 2d. of extended RA treatment may play a role in promoting characterisitics of large, limb-innervating LMC$_l$-like ESCMNs. Importantly, the range of cell soma areas of GF+RA ESCMNs on myotubes, by 25 DIV, was comparable to α-motoneuron soma size ranges measured in the lumbar

spinal cord of 8 to 12 week old mice, suggesting that cell sizes on myotubes are relevant to those measured *in vivo* (range reported by McHanwell and Biscoe (1981) = 200 – 1100 μm^2).

Motor endplate sizes increase in ESCMNs in response to extended RA treatment
Measurements of motor endplate area were then conducted to determine if extended (2d.) RA treatment would alter the size of NMJs formed by ESCMNs on myotubes. Endplate area is well correlated with motoneuron size *in vivo* (Suzuki et al., 2009), and thus it seemed reasonable to determine if this was reflected *in vitro* using ESCMNs. Endplate sizes were measured at 25 and 40 DIV, times when mature NMJs have been formed in co-culture between ESCMNs and chick myotubes (Chipman et al., 2014). Endplate sizes were significantly larger in the GF+RA ESCMN group as compared to GF ESCMNs at both 25 and 40 DIV, coinciding with the larger soma size of the GF+RA treated ESCMNs (Two-Sample Kolmogorov-Smirnov Test at 25d.: p = 0.007, GF, n = 135; GF+RA, n = 140; Two-Sample Kolmogorov-Smirnov Test at 40d.: GF, n = 78; GF+RA, n = 129, p = 0.016, Figure 4.7 A-L). Endplate area remained the same between 25 and 40 DIV, however, in both GF and GF+RA ESCMN groups (median values for ESCMNs: GF at 25d. = 99 μm^2, n = 135; at 40d. = 127 μm^2, n = 78, p = 0.491, Mann-Whitney Rank Sum Test; GF+RA at 25d. = 136 μm^2, n = 140; at 40d. = 157 μm^2, n = 129, p = 0.204, Mann-Whitney Rank Sum Test). These results support the hypothesis that RA treatment promotes larger endplate sizes due to the development of larger motoneurons.

Lhx1 expression in a cellular model of ALS: hSOD1G93A[+] ESCMNs
We next chose to investigate whether Lhx1 is expressed in this cellular model of ALS, as previous work shown that larger motoneurons (such as those that express Lhx1 during development) die before smaller motoneurons typically innervating slow, Type I muscle fibres (Frey et al., 2000, Pun et al., 2006, reviewed by Kanning et al., 2010). To test this hypothesis, we treated mouse ESCMNs carrying a human SOD mutation (hSOD1G93A) (Di Giorgio et al., 2007) with GF+RA and compared changes over time in Lhx1 expression to healthy mouse ESCMNs. The number of Lhx1^{+} cells declined significantly from 2 to 10 DIV on myotubes in both the GF+RA treated healthy ESCMNs (labelled

"control" in Figure 4.8) and GF+RA hSOD1G93A$^+$ ESCMNs (values = mean ± standard deviation; healthy ESCMNs: at 2 DIV = 68 ± 4%, at 10 DIV = 23 ± 14%, n = 5/group, p < 0.001; hSOD1G93A$^+$ ESCMNs: at 2 DIV = 67 ± 14%, at 10 DIV = 31 ± 10%, n = 5/group; Student t-test, Figure 4.8 A-M). Both control and hSOD1G93A$^+$ GF+RA treated ESCMNs had significantly more Lhx1$^+$ motoneurons than GF control groups at both 2 and 10 DIV (n = 5/group except GF healthy ESCMNs at 10d., n = 4; Mann-Whitney Rank Sum Test; asterisks in Figure 4.8 M over control bars). The initial percentage of, and subsequent decline in, Lhx1$^+$ motoneurons was similar in both the GF+RA treated healthy and hSOD1G93A$^+$ ESCMNs, with values for both groups being statistically similar at 2 and 10 DIV (at 2d., median values: healthy ESCMNs = 68%, hSOD1G93A$^+$ ESCMNs = 70%, n = 5/group, p = 1.000, Mann-Whitney Rank Sum Test; at 10d., mean values ± standard deviation: healthy control ESCMNs = 23 ± 14%, hSOD1G93A$^+$ ESCMNs = 31 ± 10%, n = 5/group, p = 0.312, Student t-test, Figure 4.8 M). As expected, GF treated ESCMNs in both groups expressed very low levels of Lhx1 (Figure 4.8 M).

Lhx1$^+$ ESCMNs possessing the hSOD1G93A mutation are not primed to die faster than Lhx$^-$, hSODG93A$^+$ ESCMNs

Because hSOD1G93A$^+$ ESCMNs expressed Lhx1 in similar patterns to healthy ESCMNs when treated with GF+RA we next examined whether Lhx1$^+$ expression in motoneurons carrying the SOD1 G93A mutation would die faster in culture compared to motoneurons not expressing Lhx1. To test this hypothesis, we cultured GF+RA treated hSOD1G93A$^+$ ESCMNs (labelled SOD in Figure 4.9) for an additional 2 or 4 days in the absence of growth factors in order to challenge motoneuron survival (Figure 4.9 A). As expected, GF+RA treated hSOD1G93A$^+$ ESCMNs died rapidly within the first week in culture with significant declines in motoneuron numbers after 2d. and 4d. in GF free media (Figure 4.9 K, mean values ± standard deviation, 463 ± 115 at 3 d. vs. 104 ± 6 at 5 d., p = 0.006, Student t-test, n = 3/group) and 5 and 7 DIV (104 ± 6 at 5 d. vs. 42 ± 11 at 7 d., p = 0.001, Student t-test, n = 3/group). Interestingly, the percentage of Lhx1$^+$ motoneurons remained constant throughout the timecourse investigated (mean values between 67% to 78%, for all 3 time points, n = 3/group, p = 0.139, one-way ANOVA, Figure 4.9 B-J, L),

indicating that Lhx1 expression did not predispose hSOD1G93A-expressing motoneurons to die earlier than Lhx1$^-$ motoneurons. It is possible that because ALS is a progressive neurodegenerative disease whereby motoneurons degenerate and die long after subtype-specific LIM-homeodomain factors are downregulated that we were unable to detect any differences in cell death rates between Lhx1$^+$ and Lhx1$^-$ hSOD1G93A-expressing motoneurons. Furthermore, neuromuscular contact, which is recognized as a factor in ALS pathophysiology, was not taken into consideration in this assay (reviewed by Kanning et al., 2010).

Survival of RA-treated healthy and hSOD1G93A$^+$ ESCMNs in long-term co-culture with myofibres

To further investigate the possibility that GF+RA treatment would increase the probrability that hSOD1G93A$^+$ ESCMNs will die at later time points, along with the potential role of motoneuron-muscle interaction in motoneuron survival, we plated ~50,000 GF+RA and GF treated hSOD1G93A-expressing GFP$^+$ motoneurons and GF+RA and GF treated control ESCMNs on chick myotubes for up to 40 DIV (see Methods). To challenge survival, motoneurons were cultured in the absence of growth factors. Figure 4.10M shows that there was no significant difference between the number of hSOD1G93A$^+$ ESCMNs and control ESCMNs after 2 DIV (mean values, p = 0.342, one-way ANOVA, n = 5/hSOD1G93A$^+$ ESCMN group and 4 for each healthy ESCMN group). While the vast majority of the motoneurons died in each group over the next 10-25 DIV (Figure 4.10N-O) there was no significant differences between groups until 40 DIV (Figure 4.10 P). At this time point, the numbers of GF+RA treated healthy ESCMNs were significantly greater than GF ESCMN controls, indicative of a possible trophic effect of RA in healthy motoneurons (Figure 4.10 P, p < 0.001, one-way ANOVA, Student-Newman-Keuls Method for multiple pairwise comparisons, n = 3/group). However, RA treatment did not result in an increase of hSOD1G93A$^+$ motoneurons, possibly due to the deleterious effects of the SOD1 transgene (Figure 4.10 P). Significantly fewer hSOD1G93A$^+$ ESCMNs were present compared to healthy ESCMNs by 40 DIV (Figure 4.10 P, p = 0.037, one-way ANOVA, Student-Newman-Keuls Method for multiple pairwise comparisons, n = 3 for healthy ESCMNs, n = 4 for hSOD1G93A$^+$ ESCMNs) which was expected based on previous observations of

decreases in hSOD1G93A$^+$ ESCMNs over weeks in culture (Di Giorgio et al., 2007). It is possible that significant differences in survival between treatment groups were present prior to 40 DIV that were not detected due to low sample sizes. Ongoing experiments are being conducted to determine if significant differences exist between treatment groups at earlier timepoints, and whether these differences become more pronounced by 40 DIV.

Motoneuron cell soma size declines over time in hSOD1G93A$^+$ ESCMNs in response to RA treatment

We then sought to investigate the effects of GF+RA treatment on hSOD1G93A$^+$ ESCMNs (Figure 4.11) and compare them to the effects present with healthy ESCMNs (Figure 4.6). Cell soma area measurements were compared at 25 and 40 DIV, times at which RA-induced phenotypic changes in size were observed in healthy ESCMNs. At 25 DIV there was no difference in cell soma area between the population of hSOD1G93A$^+$ ESCMNs and control ESCMNs in the GF+RA treated group (Two-Sample Kolmogorov-Smirnov Test, p = 0.432, healthy control, n = 98; hSOD1G93A$^+$ ESCMNs, n = 113). However, by 40 DIV, soma areas of GF+RA treated hSOD1G93A$^+$ ESCMNs were smaller than those of GF+RA treated healthy ESCMNs (median values: hSOD1G93A$^+$ ESCMNs GF+RA = 324 μm^2, n = 38; healthy ESCMNs GF+RA = 487 μm^2, n = 95, p < 0.001, Mann-Whitney Rank Sum Test). This was not paralleled by a significant difference at 40 DIV between the GF control groups of the hSOD1G93A$^+$ ESCMNs and healthy ESCMNs (p = 0.955, Mann-Whitney Rank Sum Test).

By 40 DIV, there was a dramatic decline in the cell soma area of GF+RA treated hSOD1G93A$^+$ ESCMNs as compared to 25 DIV (Two-Sample Kolmogorov-Smirnov Test, p < 0.001, at 25 DIV, n = 113; at 40 DIV, n = 38; Figure 4.11 D). This was not accompanied by a statistically significant decrease in cell size in the GF treated control group between 25 and 40 DIV (Two-Sample Kolmogorov-Smirnov Test, p = 0.258, at 25 DIV, n = 107; at 40 DIV, n = 36; Figure 4.11 C). These results suggest that hSOD1G93A$^+$ motoneurons receiving RA treatment were possibly declining in size due to deteriorating health as a result of the hSOD1G93A transgene (Di Giorgio et al., 2007). The fact that far fewer hSOD1G93A$^+$ ESCMNs were counted at 40 versus 25 DIV (see n

values above for 25 versus 40 DIV; see also Figure 4.10 O and P) also supports this hypothesis.

As described above (Figure 4.6), we investigated the effect of RA treatment on the largest healthy ESCMNs. Intriguingly, RA treatment maintained the presence of the largest motoneurons in the healthy ESCMNs from 25 to 40 DIV (Figure 4.6), which could reflect a general trophic effect of RA on the health of ESCMNs, as well as possibly contributing to the generation of large, limb-innerving LMC_l-like motoneurons. We then sought to further investigate the effects of RA treatment on the largest hSOD1G93A$^+$ ESCMNs, as large, limb-innervating motoneurons are the most susceptible to dysfunction and death in ALS (Frey et al., 2000; Pun et al., 2006; reviewed by Kanning et al., 2010). We defined a large motoneuron as being greater than 400 μm^2 (as described above). We found that the percentage of hSOD1G93A$^+$ ESCMNs larger than 400 μm^2 was very similar between GF+RA treated and untreated groups at 25 DIV, with a decrease in both groups between 25 and 40 DIV reflecting the overall decline in cell size in these ESCMNs (GF at 25d. = 54%, at 40d. = 42%; GF+RA at 25d. = 58%; at 40d. = 32%). These results suggest that any possible trophic effect supplied by RA treatment is overwhelmed in hSOD1G93A$^+$ ESCMNs by the toxic effects of the mutated SOD transgene. As well, as there was a greater proportion of large motoneurons dying in GF+RA hSOD1G93A$^+$ ESCMNs from 25 to 40 DIV (26%) as compared to GF hSOD1G93A$^+$ ESCMNs (12%), suggesting a possible susceptibility of large GF+RA hSOD1G93A$^+$ ESCMNs to death as occurs in ALS. We then investigated cell soma area changes between 25 and 40 DIV in the largest motoneurons (as defined by having a soma area > 600 μm^2). As expected, these values were very low in the hSOD1G93A$^+$ ESCMNs (untreated controls at 25d.= 16%, at 40d. = 14%; RA treated at 25d. = 17%, at 40d. = 11%) with a small decline in the largest cells of the GF+RA treated group. These results further indicate that loss of the largest motoneurons in GF+RA hSOD1G93A$^+$ ESCMNs may represent their susceptibility to death.

Motor endplate sizes increase in hSOD1G93A$^+$ ESCMNs in response to extended RA treatment

While endplate size increased with GF+RA treatment in control ESCMNs (Figure 4.7), this effect was not present in the hSOD1G93A$^+$ ESCMN cells, where endplate sizes were not significantly different between GF+RA treated and GF groups at either 25 or 40 DIV (Two-Sample Kolmogorov-Smirnov Test at 25d.: GF group, n = 72; GF+RA group, n = 66, p = 0.951; Two-Sample Kolmogorov-Smirnov Test at 40d.: GF group, n = 26; GF+RA group, n = 28, p = 0.992, Figure 4.14 A-L). Interestingly, endplate area significantly increased in size in the hSOD1G93A$^+$ ESCMN groups (GF and GF+RA groups) between 25 and 40 DIV, varying inversely with cell soma size over the same period (Figure 4.11) (median values for hSOD1G93A$^+$ ESCMNs: GF at 25d. = 71 μm^2, n = 72; at 40d. = 132 μm^2, n = 26, p = 0.01, Mann-Whitney Rank Sum Test; GF+RA at 25d. = 68 μm^2, n = 66; at 40d. = 139 μm^2, n = 28, p = 0.006, Mann-Whitney Rank Sum Test).

At 25 DIV, endplates were significantly larger in both the GF+RA treated and GF groups of the healthy ESCMNs compared to the hSOD1G93A$^+$ ESCMNs (median values: GF healthy ESCMNs at 25d. = 99 μm^2, n = 135; GF hSOD1G93A$^+$ ESCMNs at 25d. = 71 μm^2, n = 72, p = 0.047, Mann-Whitney Rank Sum Test; GF+RA treated healthy ESCMNs at 25d. = 136 μm^2, n = 140; GF+RA treated hSOD1G93A$^+$ ESCMNs = 68 μm^2, n = 66, p < 0.001, Mann-Whitney Rank Sum Test). However, due to the increase in endplate sizes in the hSOD1G93A$^+$ ESCMN groups between 25 to 40 DIV, endplate sizes were no longer significantly different between the healthy ESCMNs and the hSOD1G93A$^+$ ESCMN by 40 DIV (median values: GF healthy ESCMNs at 40d. = 127 μm^2, n = 78; GF hSOD1G93A$^+$ ESCMNs at 40d. = 132 μm^2, n = 26, p = 0.36, Mann-Whitney Rank Sum Test; GF+RA treated healthy ESCMNs at 40d. = 157 μm^2, n = 129; GF+RA treated hSOD1G93A$^+$ ESCMNs = 139 μm^2, n = 28, p = 0.376, Mann-Whitney Rank Sum Test). Correspondingly, the percentage of large endplates (arbitrarily defined as those with areas over 100 μm^2) increased substantially in both the GF+RA treated and GF groups of the hSOD1G93A$^+$ ESCMNs from ~35% of the total endplates at 25 DIV to ~60-65% of the total endplates at 40 DIV. The percentage of large endplates did not

change nearly as dramatically in healthy ESCMNs from 25 to 40 DIV in either the GF group (from 47% at 25d. to 59% at 40d.) or the GF+RA treated group (from 65% at 25d. to 71% at 40d.). In summary, endplates in both healthy and hSOD1G93A$^+$ ESCMNs increased in size between 25 and 40 DIV, suggesting that the motoneurons that survived were able to form stable and strong synapses with myotubes. The largest endplates were formed by RA treated healthy ESCMNs, possibly emphasizing a role for RA in establishing and maintaining healthy synapses in ESCMN-myotube co-cultures.

Discussion

Extended RA treatment promotes expression of proteins associated with LMC_l motoneuron fate in ESCMNs

In the present study we found that exposing ESCMNs to RA for up to 3 days following the standard RA and SAG motoneuron differentiation protocol resulted in expression of LMC markers Lhx1 and FoxP1 in the vast majority (~70-80%) of motoneurons. Our study is the first to report such a high percentage of LMC_l markers in ESCMNs, although Amoroso and colleagues were recently able to generate a majority of hESCMNs that expressed FoxP1 using a combination of the sonic hedgehog signalling agonists purmorphamine and SAG (~70%) (Amoroso et al., 2013). The percentage of FoxP1 expressing hESCMNs receiving standard RA and sonic hedgehog agonist treatment in this study was also comparable to the control ESCMNs in our study (~30% of ESCMNs). It is interesting to note that such divergent techniques using ESCMNs derived from different species were able to elicit similar FoxP1 expression profiles, indicating that multiple differentiation protocols may be used to generate LMC-like ESCMNs across species.

While the FoxP1 expression profile of ESCMNs receiving extended RA treatment was comparable to previous work, the percentage of ESCMNs expressing Lhx1 was much higher than that cited by previous studies. Only a small percentage of ESCMNs expressed Lhx1 following a late pulse of RA in an otherwise retinoid-free differentiation protocol (Peljto et al., 2010). Likewise, the majority of hESCMNs treated with SAG and purmorphamine with a pulse of RA late in the protocol failed to differentiate into Lhx1$^+$ motoneurons (Amoroso et al., 2013). Using an identical RA treatment protocol to the one used in our study, Adams et al. (2015) claimed that a maximum of 40% of ESCMNs generated with FoxP1 expressed under the Hb9 promoter (Hb9::FoxP1) are Lhx1$^+$. Interestingly, they report that only ~5% of control ESCMNs (Hb9::GFP) express Lhx1 under the same treatment paradigm – results that are at odds with the present study.

The reasons for these discrepancies in Lhx1 expression remain unknown, although differences in differentiation protocol (e.g. differences in amount of RA present throughout differentiation and timing of RA exposure) may be involved in some cases.

For example, while the concentration of RA used by our group and Peljto et al. (2010) was the same (1 μM), it was added 1 day later in our differentiation protocol. As well, their protocol was retinoid free up to the point of the pulse, which may also contribute to the discrepancy. Differences in Lhx1 expression may also be a result of modified culture conditions between studies. For example, the highest yields of Lhx1 expression in our study was noted after plating the ESCMNs. In contrast, Adams et al. (2015) treated the ESCMNs with RA while the cells were in suspension as embryoid bodies, which may result in reduced ability to express Lhx1, either due to inefficient exposure to RA or possible inhibitory signalling within embryoid bodies.

RA-induced Lhx1 expression in ESCMNs: effects of substrate and time
We found that Lhx1 expression in response to GF+RA treatment varied according to the substrate in which the ESCMNs were plated. Plating on matrigel, poly-d-lysine and myotubes elicited maximum percentage of Lhx1$^+$ ESCMNs (~70-80%) while PMEFs and C6 cells proved to be the least effective substrates (~40% Lhx1$^+$ ESCMNs, Figure 4.1). The causes of the differential effects of substrate on Lhx1 expression remain unknown, but it is interesting to speculate that the cells that make up the more inhibitory substrates interfere with the expression of Lhx1 either through direct cell-cell interactions with ESCMNs or through expression of secreted inhibitory factors. Whether the inhibitory nature of these substrates to Lhx1 expression is induced by GF+RA treatment remains unknown as well. Further investigation into these phenomena may provide unique insight into the signalling mechanisms required for expression of genes essential for differentiation of various motoneuron subtypes.

We also noted that the percentage of Lhx1$^+$ ESCMNs declined over time when cultured on myotubes while remaining constant on matrigel. While Lhx1 expression declined to levels matching that on myotubes over many weeks in culture (data not shown), these results implicate a possible role for muscle in influencing the regulation of Lhx1 in developing motoneurons. Lhx1 is required for directing motoneurons in the LMC$_l$ to project axons towards the dorsal component of the limb muscle mass. The appropriate guidance of these axons depends on Lhx1 and its control of EphA4

expression (Kania et al., 2000; Kania and Jessell 2003). By HH st.41, long after motor axons have reached their muscle targets, Tsuchida et al. (1994) showed that Lhx1 expression could no longer be detected in motoneurons. In vitro, by 8 days in co-culture, axons from ESCMNs make functional connections with chick muscle fibres (Chipman et al., 2014). This contact may initiate a program responsible for the decline of Lhx1 expression in motoneurons. While we were unable to show a role for post-synaptic activity in this process, it is possible that other muscle-derived signals may play a role in regulating the decline of Lhx1 expression.

For future studies, a reporter gene that would allow tracking of Lhx1 would aid in studies of its regulation. Further studies investigating the molecular factors involved in regulating Lhx1 expression in motoneurons may centre on transcription factors that bind either directly to the LIM domain or interact with other proteins (cofactors) that bind to the LIM domain, such as the ubiquitin ligase RLIM, which negatively regulates LIM homeodomain expression in the developing neural tube. RLIM has previously been shown to be present in Lhx3$^+$ and Isl1$^+$ motoneurons and is likely involved in regulating these LIM homeodomain proteins (Ostendorff et al, 2006). External factors controlling the expression of these regulatory proteins are not well understood and would be an interesting area of future study.

Effects of extended RA treatment on survival of Lhx1$^+$ hSOD1G93A$^+$ ESCMNs
Previous work has shown that SOD1G93A$^+$ ESCMNs die in culture gradually over weeks if supplied with trophic support, however these cells die rapidly (over days) if cultured in a trophic factor-free environment (DiGiorgio et al., 2007; Yang et al., 2013). We adapted the trophic factor withdrawal assay described by Yang et al. (2013) and found that the majority of hSOD1G93A$^+$ ESCMNs died 4 days after trophic factor withdrawal. We hypothesized that Lhx1$^+$ motoneurons, if they possess characteristics of limb-innervating motoneurons in cases of ALS would die at an accelerated rate compared to Lhx1$^-$ motoneurons, presumably non-limb-innervating motoneurons (reviewed by Kanning et al., 2010). However, the majority of the motoneurons that survived were Lhx1$^+$. It is possible that the ESCMNs expressing Lhx1 did not possess the necessary physiological

characteristics of limb-innervating motoneurons that promotes early degeneration in ALS. Alternatively, the hSOD1G93A$^+$ ESCMNs may not have reached appropriate physiological maturity to display differences in survival between limb-innervating and other motoneurons present. Finally, it is possible that this cell-death assay may not be an appropriate model of the pathophysiology of SOD mutations in ALS.

To test the role of neuromuscular activity in the survival of hSOD1G93A$^+$ ESCMNs treated with RA, we plated these cells on myotubes for up to 40 DIV. We found that healthy ESCMNs exposed to RA exhibited better long-term survival, as significantly more GF+RA treated ESCMNs remained at 40 DIV compared to untreated GF controls. These results suggest that, even after only 2 additional days of treatment, RA provides a neuroprotective or trophic effect on ESCMNs. This conclusion is supported by previous work, as activation of RA receptors with agonists has been shown to have neuroprotective effects in cultured rat motoneurons exposed to oxidative stress (Kolarcik and Bowser, 2012). Survival differences between healthy and hSOD1G93A$^+$ ESCMNs were evident by 40 DIV, where a greater proportion of healthy ESCMNs (both GF+RA and GF alone) had survived compared to hSOD1G93A$^+$ ESCMNs. These results are in line with previous work demonstrating impaired survival of hSOD1G93A$^+$ ESCMNs compared to healthy ESCMNs over weeks in culture (DiGiorgio et al., 2007). It is unknown why the effect of the SOD mutation on survival was not apparent earlier (e.g. by 25d.), although it is possible that the chick muscle fibres provide a neuroprotective milieu.

Effects of extended RA treatment on ESCMN morphology: healthy and hSOD1G93A$^+$ ESCMNs

We found that GF+RA treatment promoted development of large soma size in healthy ESCMNs. Interestingly, the effects of GF+RA were quite delayed as the ESCMNs did not exhibit larger somas compared to GF treated ESCMNs until at 25 DIV with myotubes. The median size increased even further over the next 15 days. The reason for this delay is not clear, however it suggests that the long-term effects of GF+RA treatment may be the result of an extensive program of gene expression involved in cellular

expansion. It is also not clear if this program involves genes associated with LMC_l motoneurons (such as Lhx1 or FoxP1) or is the result of other growth-promoting effects of RA. Identifying factors involved in this growth program could be beneficial in understanding factors involved in the maturation of motoneurons. In contrast to the growth of healthy ESCMNs in response to GF+RA, hSOD1G93A$^+$ ESCMNs declined in size between 25 and 40 DIV. It is likely that any growth-promoting effects of GF+RA were overcome by the toxic effects of the SOD transgene, resulting in either degeneration-induced reduction in size or survival of only the smallest motoneurons. If the latter is true, this would suggest that the model is accurately depicting events that occur in the etiology of ALS (reviewed by Kanning et al., 2010). It is also important to note that the growth of ESCMNs on myotube co-cultures resulted in motoneurons that had sizes within the range previously determined for young adult mice, adding support for this model as a valid representation of early motoneuron development (McHanwell and Biscoe, 1981). The motoneuron size measurements noted by McHanwell and Biscoe (1981) were of motoneurons that innervate the hindlimb, indicating that a large degree of variability exists in the size of LMC motoneurons *in vivo*. This variability in size is captured in our ESCMN-myotube co-culture system, with GF+RA treated healthy ESCMNs not only possessing a population of larger motoneurons as compared to GF treated ESCMNs, but also possessing a broader range of sizes as a result. Importantly, and consistent with the etiology of ALS, this variability decreases in the GF+RA treated hSOD1G93A$^+$ ESCMNs between 25 to 40 DIV, with only smaller motoneurons remaining.

Motor endplate area was another morphological feature investigated in this study. At both 25 and 40 DIV, healthy GF+RA treated ESCMNs had larger endplates than untreated controls. Larger endplates have been noted as a feature of fast-fatigable muscle, as Suzuki et al. (2009) established that endplates of fast type IIx/b muscle fibres of the rat diaphragm were larger than those of slow, type I muscle fibres. If GF+RA treated ESCMNs develop into large 'fast' motoneurons, it follows that the endplate size of the motoneuron should match its soma size.

Perhaps surprisingly, we found that endplate sizes of both healthy and hSOD1G93A[+] ESCMNs increased between 25 and 40 DIV despite the observation that soma sizes of hSOD1G93A[+] ESCMNs decreased across the same period. One possible explanation for these results is that a subpopulation of healthy but small hSOD1G93A[+] ESCMNs were able to sustain and even expand their synaptic connections. This would suggest that this subpopulation of hSOD1G93A[+] ESCMNs were either relatively resistant to mutant SOD-induced degeneration and death or that these cells were able to maintain survival due to synaptic activity. Further studies using this model system could involve time lapse imaging analysis of motoneurons to determine if connectivity is related to survival in hSOD1G93A[+] ESCMNs over weeks in co-culture with myotubes. As well, future studies should aim to investigate the degeneration process of hSOD1G93A[+] ESCMNs on myotubes to determine if the etiology of ALS is recapitulated in this model (i.e. motoneurons degenerate and axons retract from muscle prior to motoneuron death).

Further investigation of other morphological features of ESCMN-myotube co-cultures, such as complexity of dendritic branching of motoneurons and motor unit analysis, would be of interest to pursue using this model system. We were unable to analyze these features due to technical difficulties associated with identifying single motoneurons and their associated processes. Although these co-cultures were developed using dissociated ESCMNs, many motoneurons had large dendritic trees and axonal branches that overlapped with neighbouring motoneurons, making identification of motor units and extent of dendritic branching difficult, especially by 25-40 DIV. However, use of techniques such as neurobiotin labelling to identify motoneurons may overcome these experimental limitations and allow for assessment of these morphological aspects. It would be of interest to determine if large ESCMNs treated with GF+RA would develop larger motor units and possess a greater degree of dendritic branching, as these are characteristics of fast-fatigable, limb-innervating motoneurons (Cullheim et al., 1987; reviewed by Kanning et al., 2010).

Concluding remarks: RA signalling and the development of limb-innervating motoneurons

RA signalling is critical for the development of LMC_l motoneurons (Sockanathan and Jessell, 1998). Vermot et al. (2005) demonstrated that mice that lack the RA synthesizing enzyme Raldh2 exhibit absence of $Lhx1^+$ motoneurons. The authors also found that in the brachial spinal cord, the expression of Hoxc8 was found to be critical for the expression of retinoic acid receptor β. Mice that lacked Hoxc8 displayed a decline in Lhx1 expression, a phenotype similar to that seen in Raldh2 knockout mice (Vermot et al., 2005). It would be interesting to investigate whether ESCMNs that lack Hoxc8 function would be able to express $Lhx1^+$ when exposed to extended RA treatment.

Previous studies of the role of RA signalling in the mouse embryo have revealed that genes which respond to RA signalling (i.e. contain RA response elements) and a protein necessary for RA synthesis (RDH10) are present throughout the developing spinal cord at times of motoneurogenesis; they are not strictly localized to the LMC (Rossant et al., 1991; Sandell et al., 2007). It may be possible that all motoneurons have the capacity to respond to retinoid signalling and upregulate genes characteristic of LMC motoneurons (e.g. Lhx1 and FoxP1), but RA activity is tightly controlled in areas outside of the developing LMC, possibly through the activity of RA signalling inactivators such as the cyp26a1 enzyme (see discussion below). Therefore, our ability to generate high yields of $Lhx1^+$ motoneurons may result from the absence of such RA signalling inhibition *in vitro*.

ESCMNs generated using the GF+RA protocol possess protein expression patterns and morphological characteristics of LMC_l-like motoneurons without the need for genetic modification (e.g. misexpression of FoxP1). However, to further enhance the development of these motoneurons, another approach may involve modifying the function of enzymes associated with RA metabolism. Cyp26a1, an enzyme which inactivates RA signalling, has recently been demonstrated to play a role in ESCMN subtype development. Using ESCMNs from mice lacking this enzyme, Ricard and Gudas (2013) were able to generate motoneurons that had increased expression of HoxC6 and Raldh2, genes associated with LMC development, along with decreased Lhx3 expression.

These results suggest that removal of cyp26a1 can promote an LMC-like phenotype (Ricard and Gudas, 2013). Taken together with our results, RA signalling appears to be a critical factor in the differentiation of ESCMNs possessing characteristics of LMC motoneurons.

Chapter 4 Figures

Figure 4.1. Extended RA treatment induces Lhx1 expression in the majority of ESCMNs

Lhx1 expression is largely absent in growth factor (GF) only control ESCMNs (**A-C**, **G**) while the majority of ESCMNs treated with RA (GF+RA) for 3d. express Lhx1 (**D-G**). Asterisks indicate significant difference between means (± standard deviation) for treatment and control at each time point (**G**). **H**, Plating GF+RA ESCMNs on different substrates for 2d. resulted in variable amounts of Lhx1$^+$ motoneurons. MG = matrigel, PL = poly-d-lysine, myo = chick myotubes, C6 = C6 rat glioma cells, PMEFs = primary mouse embryonic fibroblasts. Values = mean ± standard deviation, n = 3/group, ANOVA with Holm-Sidak method for pairwise multiple comparisons, asterisk denotes significance, p < 0 .05. Scale bar = 50 μm.
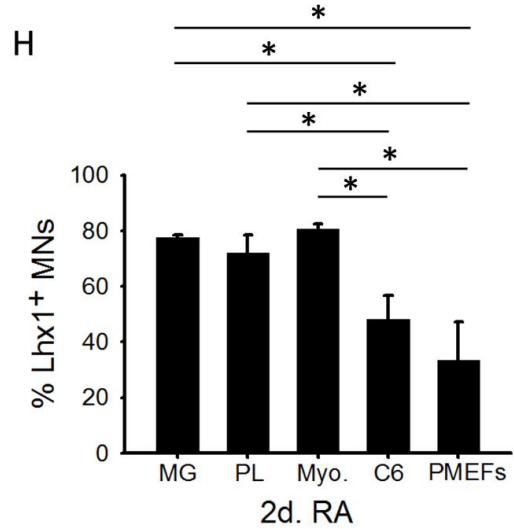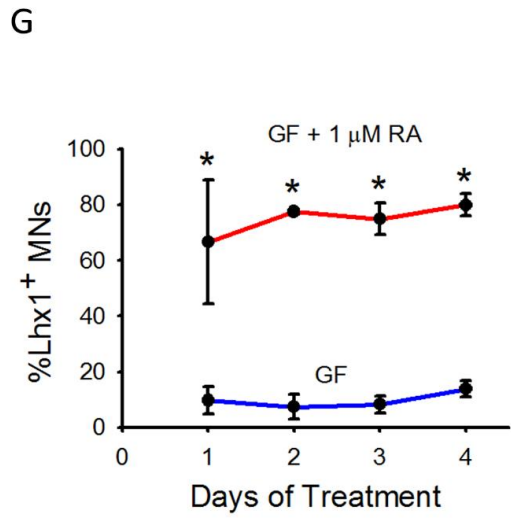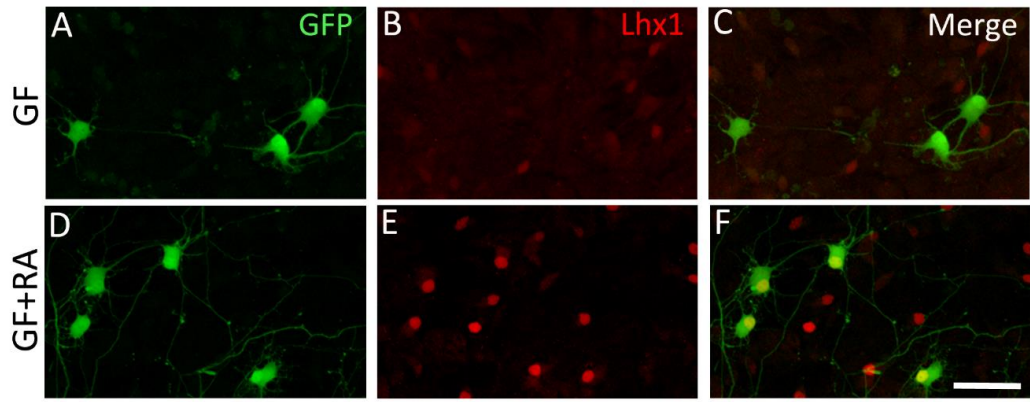
Figure 4.2. Extended RA treatment induces FoxP1 expression in ESCMNs

A-C, GF only controls. **D-F**, GF+RA treated cells. **G**, quantification of FoxP1 expression. Arrowheads in **A-C** indicates a FoxP1$^+$ ESCMN. Arrows in **D** and **F** indicate a FoxP1$^-$ ESCMN. Asterisk in **G** denotes significant difference between GF and GF+RA treated ESCMNs. Values = mean ± standard deviation. Scale bar = 50 μm.

A tdTomato   B FoxP1   C Merge
GF

D   E   F
GF+RA

G
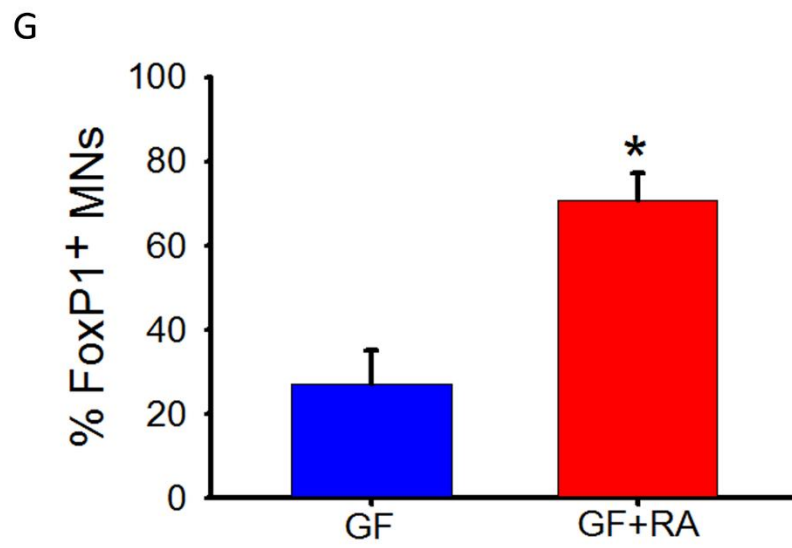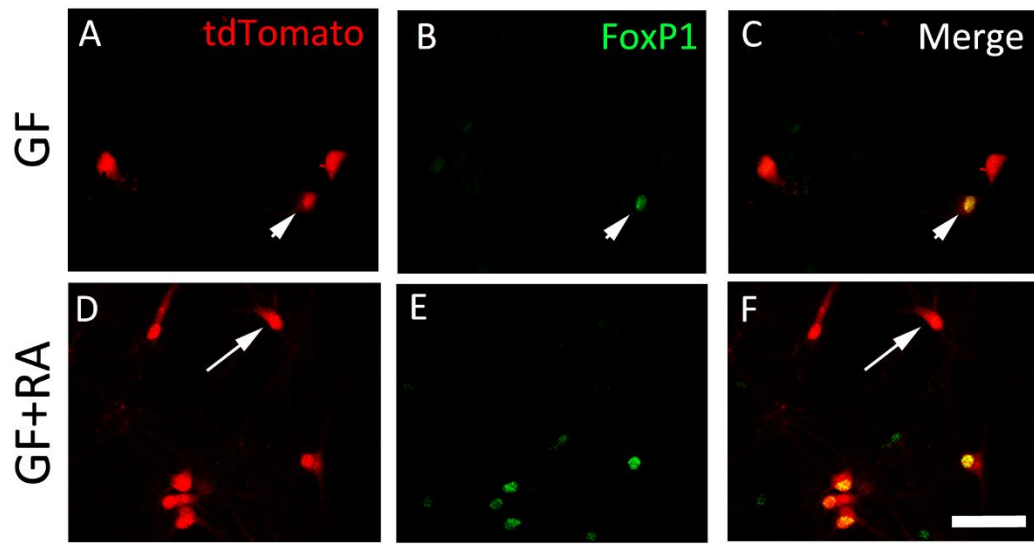
Figure 4.3. Extended RA treatment does not alter the number of HoxA5$^+$ ESCMNs
A-C, GF only controls. **D-F**, GF+RA treated ESCMNs. **G**, quantification of HoxA5 expression. Arrowheads in D-F indicate a HoxA5$^-$ ESCMN. Scale bar = 50 μm.
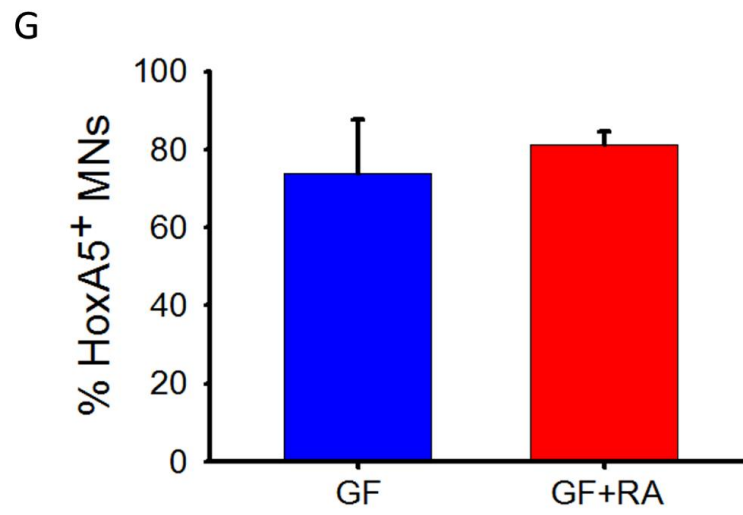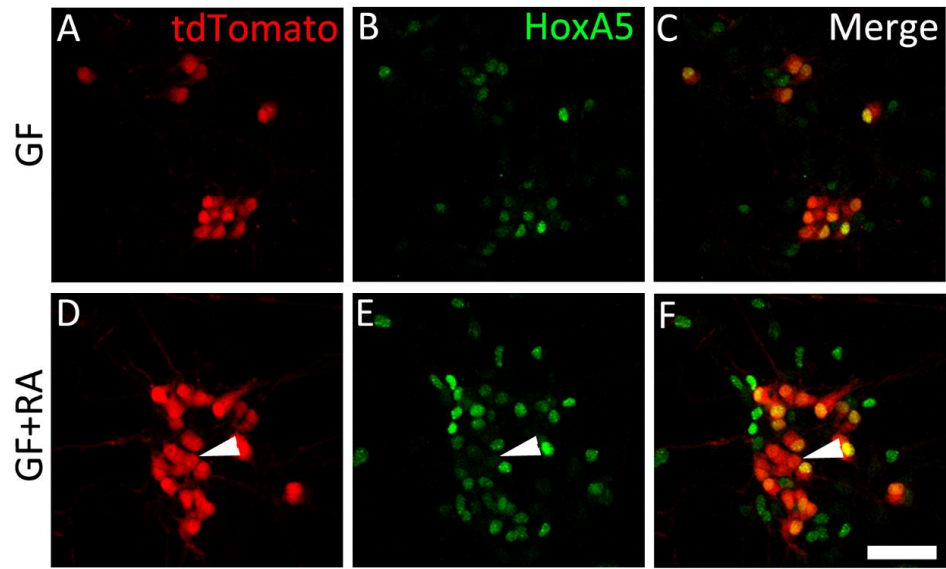
Figure 4.4. Extended RA treatment induces minor increases in HoxC6$^+$ ESCMNs
A-C, GF only controls. **D-F**, GF+RA treated ESCMNs. Arrow in **D-F** indicates a
HoxC6$^+$ motoneuron. **G**, quantification of HoxC6 expression. Values = mean ± standard
devation. Scale bar = 50 μm.
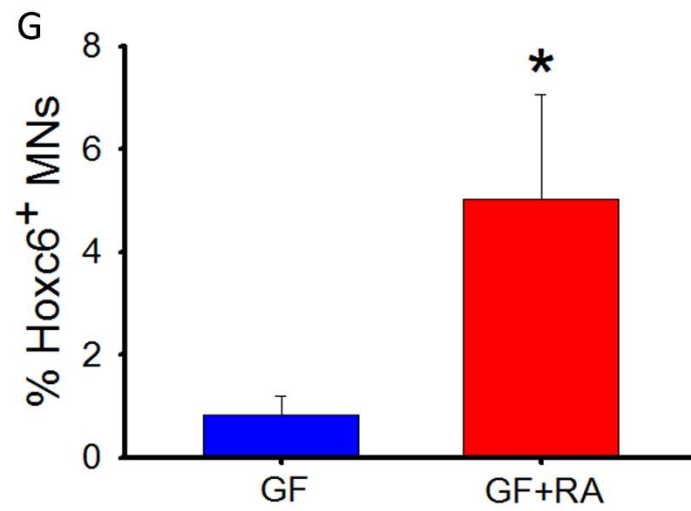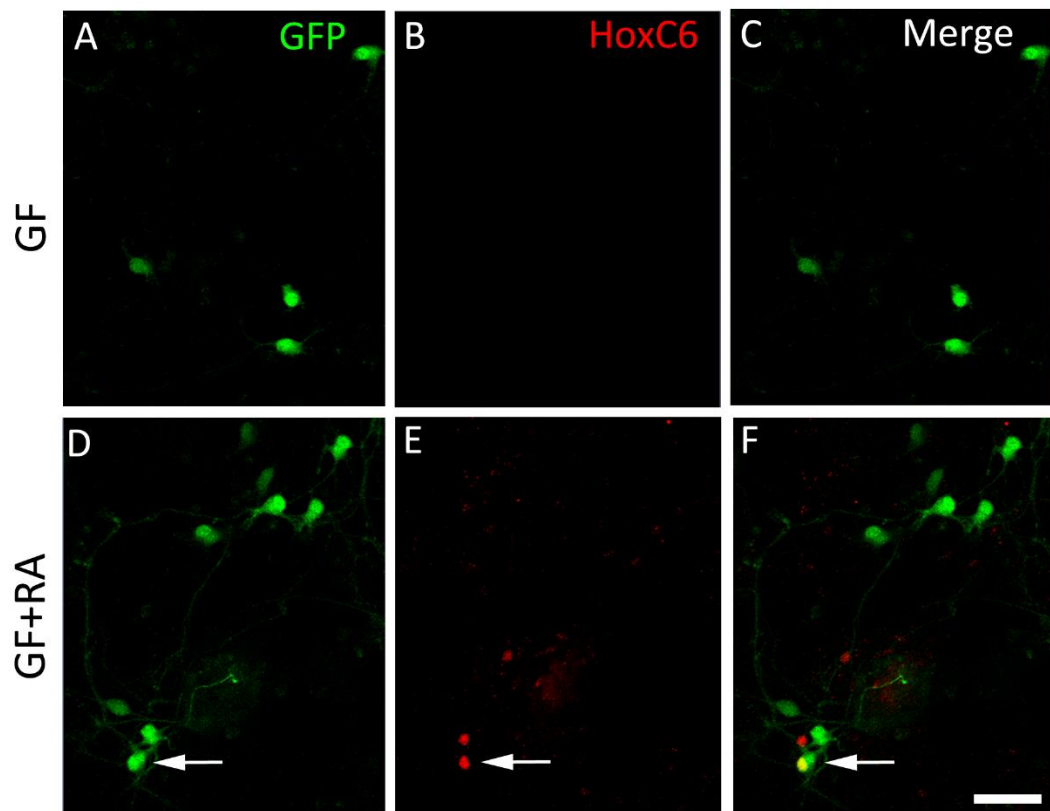
Figure 4.5. Expression profile of RA-induced Lhx1 expression in ESCMNs on matrigel and chick myotubes

Lhx1 expression after 2d. of extended RA treatment on myotubes (**A-C**), 4 DIV (2d. RA treatment, 2 d. media only, D-F) and 8 DIV (2d. RA treatment, 6d. media only, **G-I**). Lhx1 expression after 2d. of extended RA treatment on matrigel (**J-L**), 4 DIV (2d. RA treatment, 2 d. media only, **M-O**) and 8 DIV (2d. RA treatment, 6d. media only, **P-R**). **S**, Quantification of Lhx1$^+$ ESCMNs on myotubes and matrigel at 2, 4, and 8 DIV. ESCMNs were either plated directly on matrigel (control matrigel) or on a matrigel-coated coverslip suspended over myotubes (matrigel over myotubes). Other ESCMNs were plated directly on myotubes (control myotubes) and some were treated daily with α-bungarotoxin (α-btx myotubes). Arrowheads in **A-R** indicate Lhx1$^+$ ESCMNs. Asterisks in **S** denote significant differences, details of statistical analyses described in text. Values = mean ± standard deviation. Scale bars: in **F** and **O** = 10 μm; in **I** = 50 μm; in **R** = 50 μm.

Myotubes | Matrigel

| | GFP | Lhx1 | Merge | | GFP | Lhx1 | Merge |
2d. RA — A, B, C | J, K, L
4d. — D, E, F | M, N, O
8d. — G, H, I | P, Q, R

S

% Lhx1+ MNs vs. Days in Culture/Coculture

Legend:
- Control Myotubes (black)
- α-btx Myotubes (gray)
- Control Matrigel (red)
- Matrigel Over Myotubes (blue)
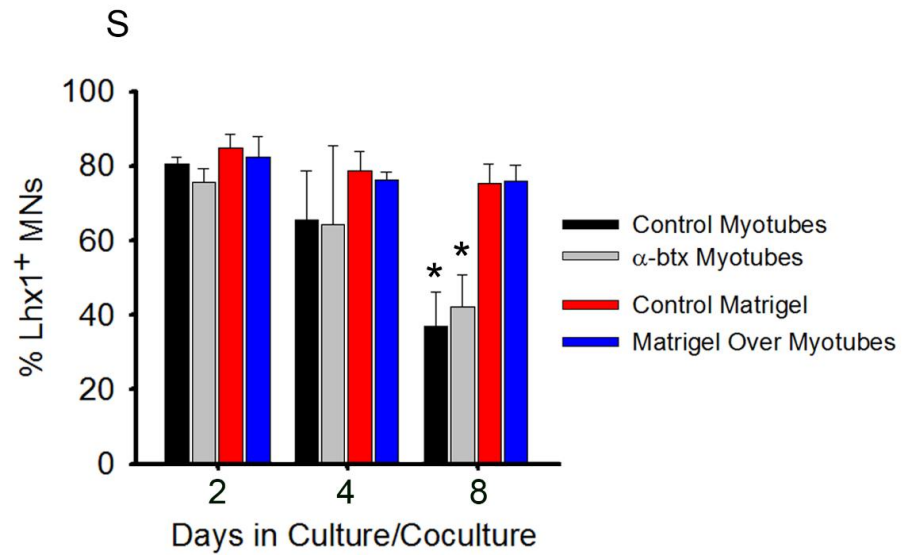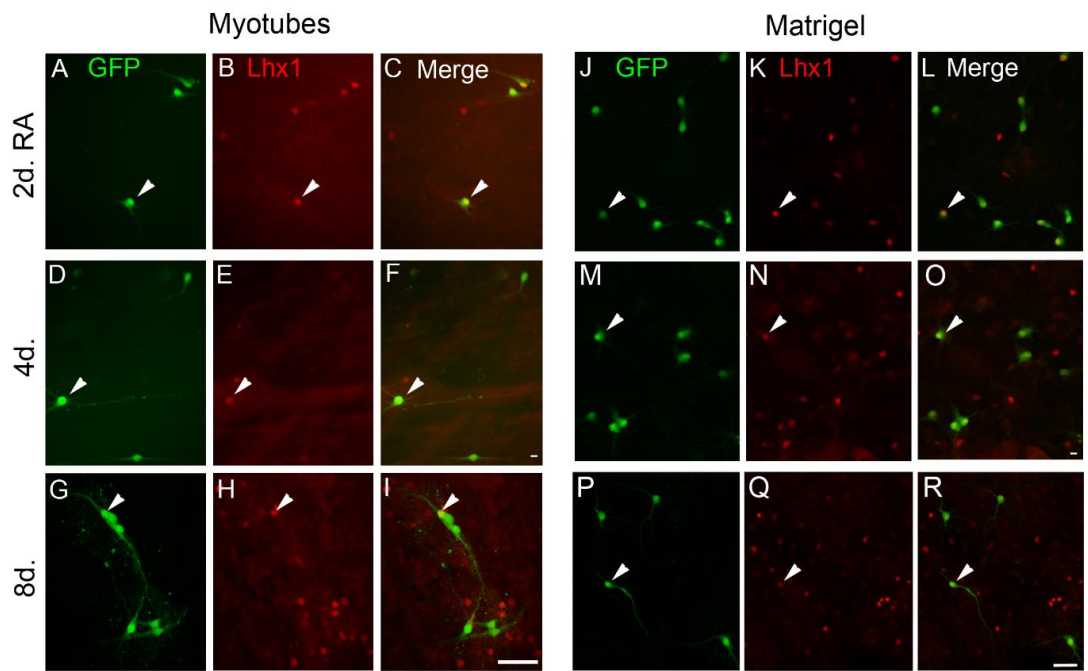
Figure 4.6. Effects of extended (2d.) RA treatment on soma area in ESCMNs on myotubes

Sample GFP$^+$ ESCMNs at 2d. (GF control, **A**; GF+RA treated, **B**) and at 40d. (GF control, **C**; GF+RA treated, **D**). Histograms of soma sizes at 2d. (GF control, **E**; GF+RA treated, **F**), 10d. (GF control, **H**; GF+RA treated, **I**), 25d. (GF control, **K**; GF+RA treated, **L**), and 40d. (GF control, **N**; GF+RA treated, **O**). Cumulative frequency plots comparing soma sizes of GF controls and GF+RA treated ESCMNs are shown at 2d. (**G**), 10d. (**J**), 25d. (**M**), and 40d. (**P**). Asterisks in **M** and **P** denote statistical difference, details in text. Scale bar = 20 μm.

GF GF+RA GF GF+RA

2d.

40d.

E   F   G

2d.

MN Count

GF   GF+RA

% Cumulative Frequency

2d. GF+RA
2d. GF

Soma Area (μm²)
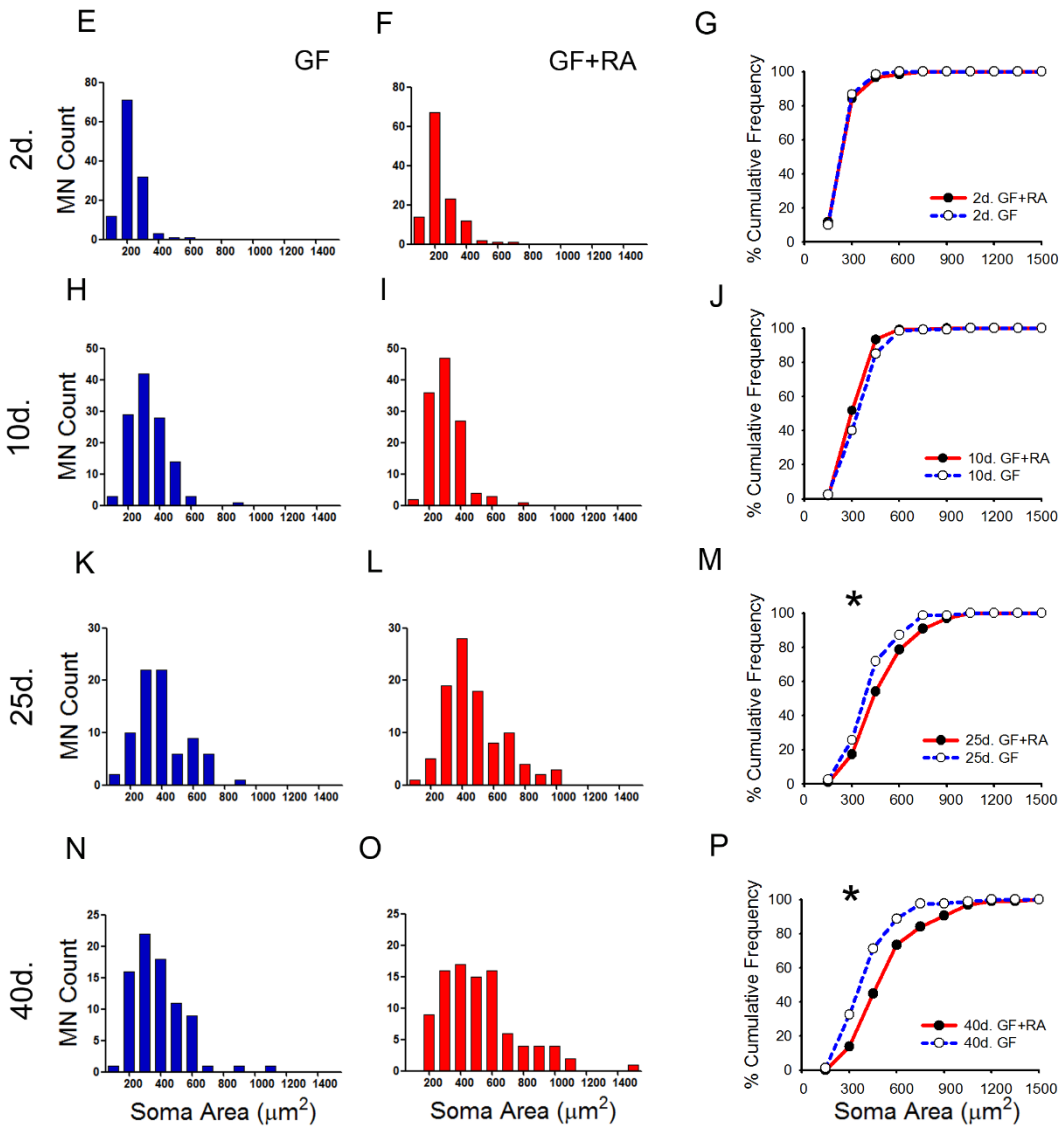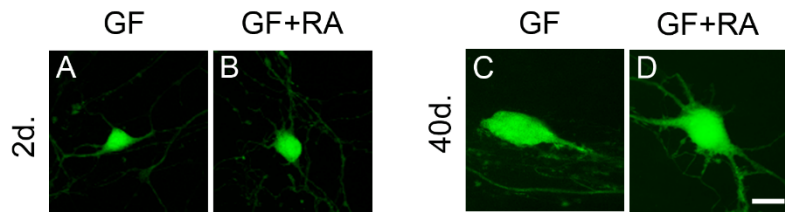
Figure 4.7. Effects of extended (2d.) RA treatment on endplate area in ESCMN-myotube co-cultures

Neuromuscular junctions with ESCMNs at 40 DIV (GF control, **A**; GF+RA treated, **D**) and highlighted endplates identified by rhodamine conjugated α-bungarotoxin (α-btx) (GF control, **B**; GF+RA treated, **E**; regions outlined in boxes are expanded in insets in **B** and **E**). Merges shown in **C** and **F** for GF controls and GF+RA treated ESCMNs, respectively. Histograms of soma sizes at 25d. (GF control, **G**; GF+RA treated, **H**), and 40d. (GF control, **J**; GF+RA treated, **K**). Cumulative frequency plots comparing endplate sizes of GF controls and GF+RA treated ESCMNs are shown at 25d. (**I**), and 40d. (**L**). Asterisks in **I** and **L** denote statistical difference, details in text. Scale bar = 20 μm.

GF

A GFP   B α-BTX   C MERGE

GF+RA

D   E   F

G   H   I
GF   GF+RA

J   K   L
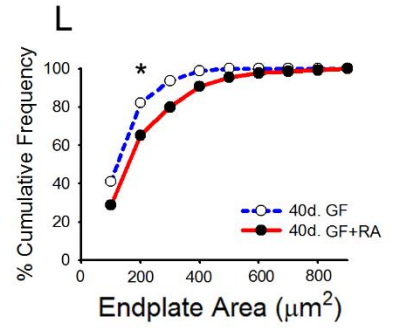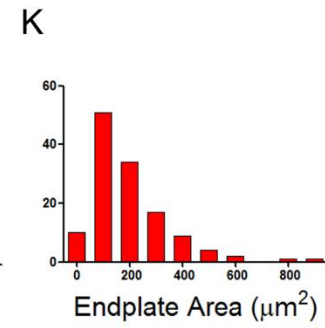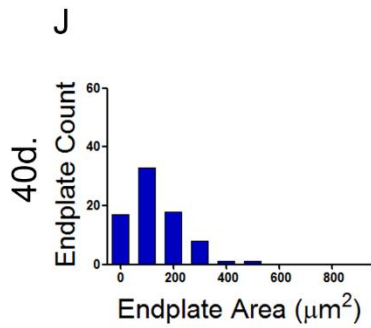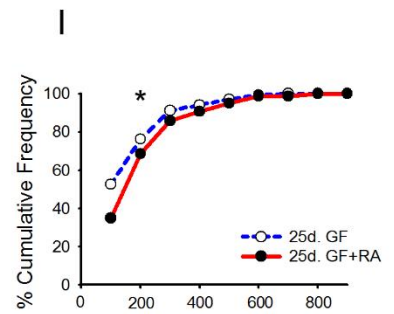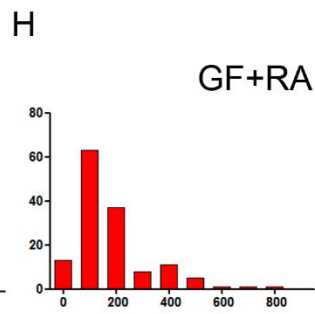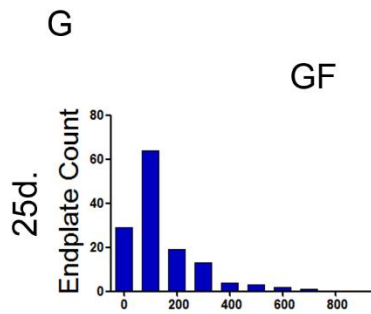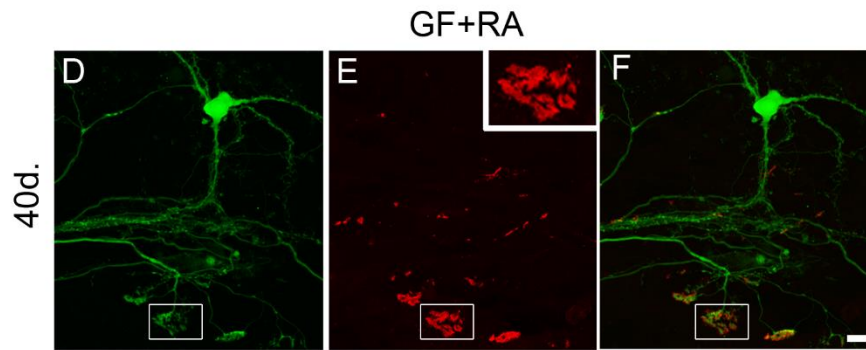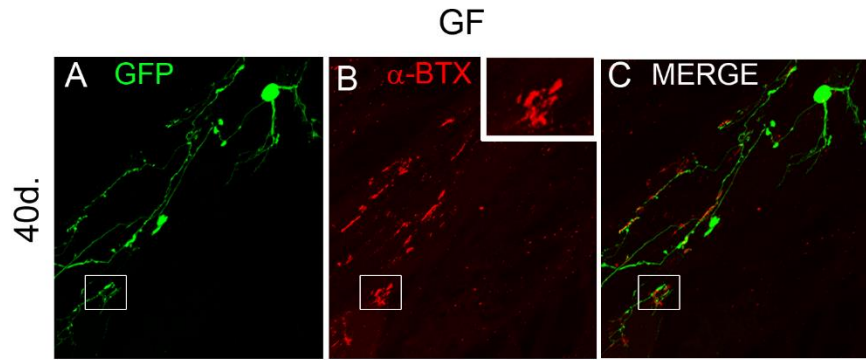
Figure 4.8. Lhx1 expression in healthy and hSOD1G93A$^+$ ESCMNs on myotubes following extended RA treatment

Lhx1 expression in healthy (control) ESCMNs and hSOD1G93A$^+$ (SOD) ESCMNs after 2d. of RA treatment (control, **A-C**; SOD, **G-I**) and 10 DIV (control, **D-F**; SOD, **J-L**). **M**, Quantification of Lhx1 expression in each group. Values = mean ± standard deviation. Asterisks in **D-F** and **J-L** indicate faintly Lhx1$^+$ ESCMNs. Asterisks in **M** denote statistical difference, details in text. Scale bar = 20 μm.

Control
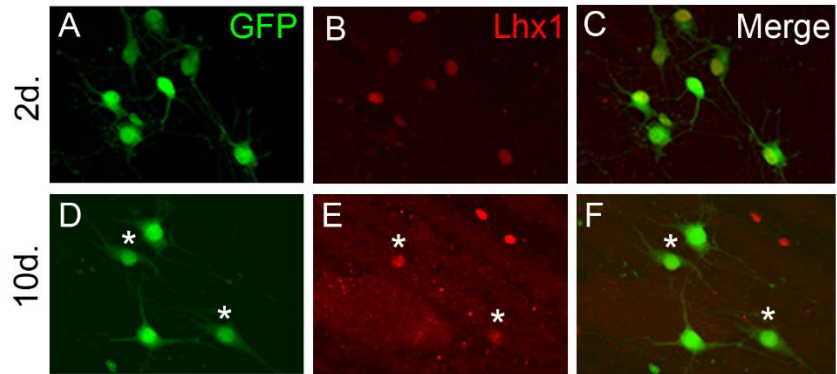
SOD
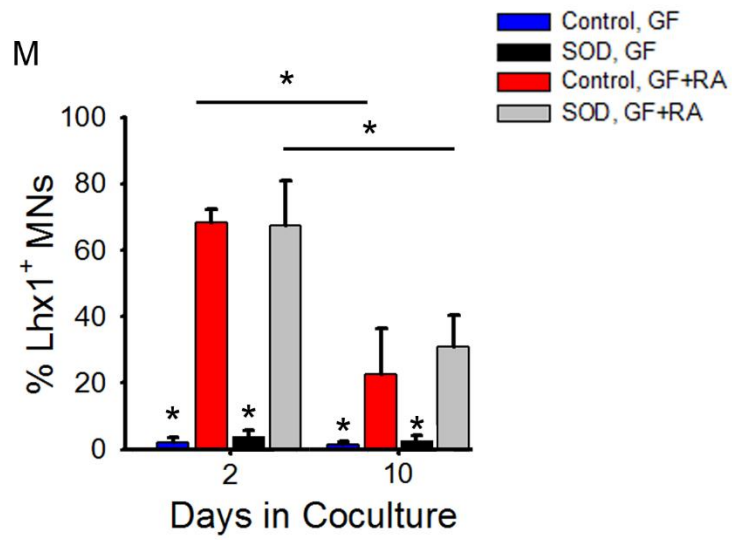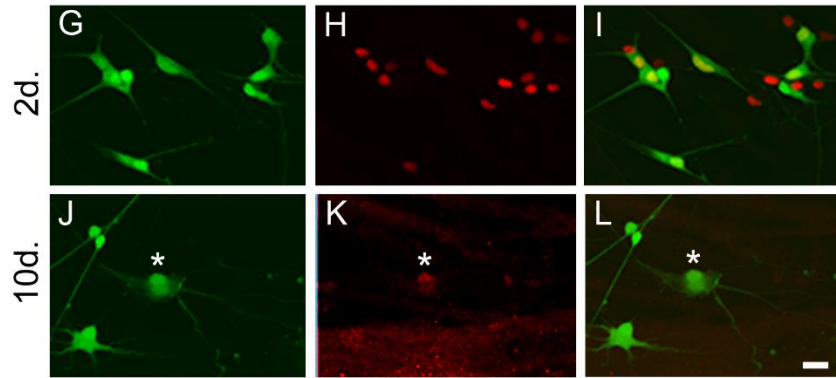
Figure 4.9. Lhx1$^+$ hSOD1G93A$^+$ ESCMNs do not die faster than Lhx$^-$ hSOD1G93A$^+$ ESCMNs

A, Treatment protocol. Lhx1 expression in hSOD1G93A+ ESCMNs after 3d. of GF+RA treatment in media containing serum and growth factor support (**B-D**). Lhx1 expression after another 2d. (**E-G**) and 4d. (**H-J**) in growth factor and serum free culture media without RA (GF+RA free media). **K**, Counts of motoneurons over the 3 time points. **L**, Quantification of Lhx1+ motoneurons at each of the 3 time points. Values = mean ± standard devation. Asterisks in **K** denote statistical difference, details of statistical analyses described in text. Scale bar = 50 μm.

A

3d.
GF+RA
SOD MNs → Replace with → +2d. → Fix MNs, → +2d. → Fix MNs,
GF+RA free media   stain for Lhx1   stain for Lhx1

3d. GF+RA

B GFP   **C** Lhx1   **D** Merge

+ 2d. GF+RA free media

E   **F**   **G**

+ 4d. GF+RA free media

H   **I**   **J**

K

L
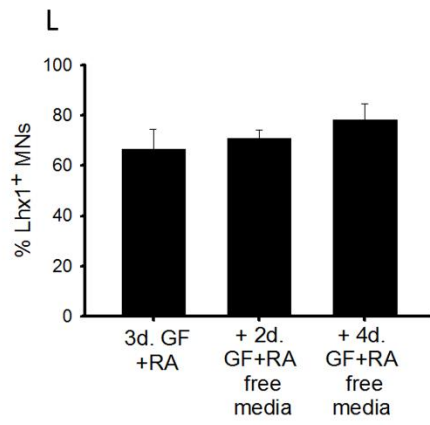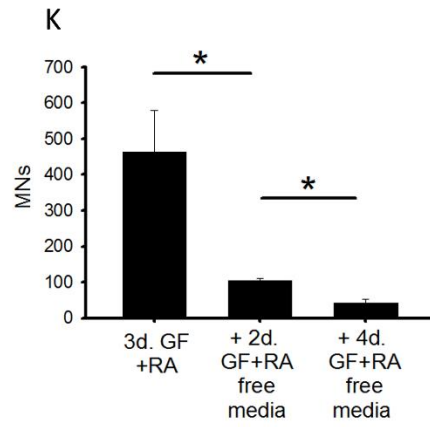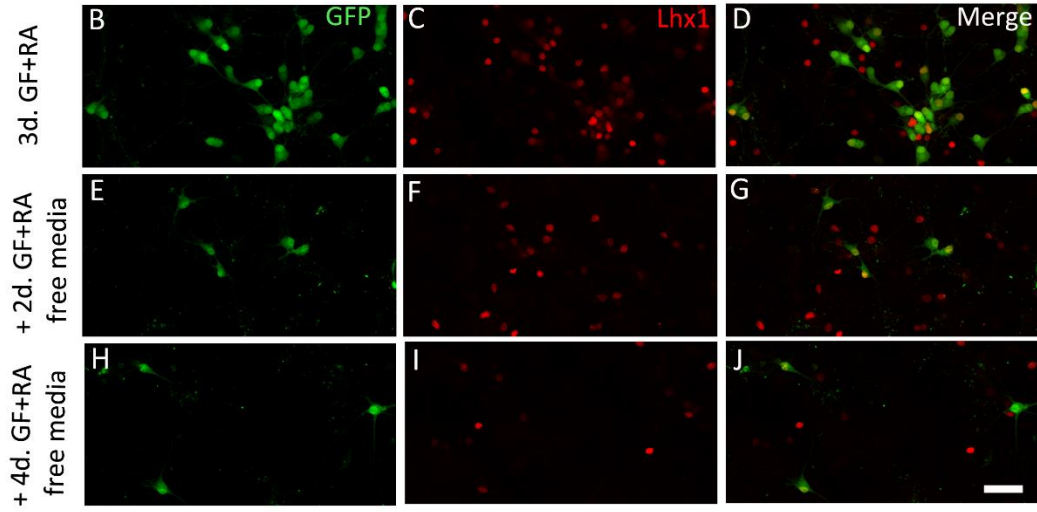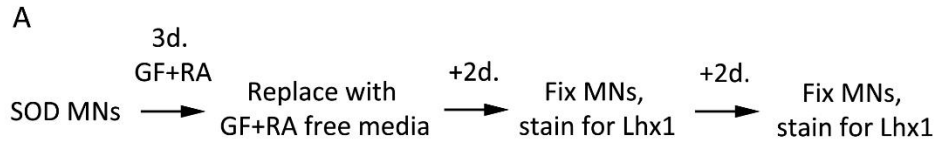
Figure 4.10. Survival of hSOD1G93A$^+$ and healthy ESCMNs on myotubes following extended RA treatment

Healthy (control) ESCMNs plated on myotubes and treated for 2d. with RA (GF+RA) and GF controls (**A**, **B**). hSOD1G93A$^+$ (SOD) ESCMNs plated on myotubes and treated for 2d. with RA (GF+RA) and GF controls (**C**, **D**). **E**, GF control ESCMNs at 10d. **F**, GF+RA treated control ESCMNs at 10d. **G**, GF hSOD1G93A$^+$ ESCMNs at 10d. **H**, GF+RA hSOD1G93A$^+$ ESCMNs at 10d. **I**, GF control ESCMNs at 40d. **J**, GF+RA control ESCMNs at 40d. **K**, GF hSOD1G93A$^+$ ESCMNs at 40d. **L**, GF+RA hSOD1G93A$^+$ ESCMNs at 40d. **M**, ESCMN counts at 2d. Percent survival of ESCMNs of each group at 10 (**N**), 25 (**O**) and 40 (**P**) DIV, values normalized to counts at 2d. Values = mean ± standard devation. Scale bar = 20 μm.
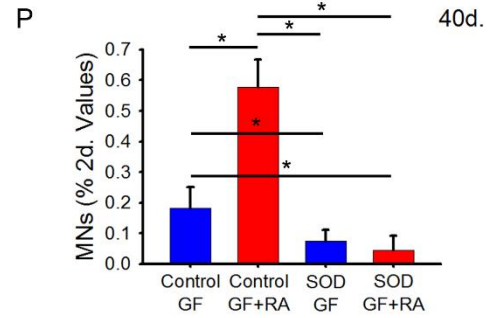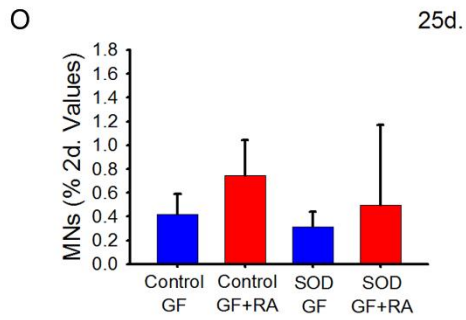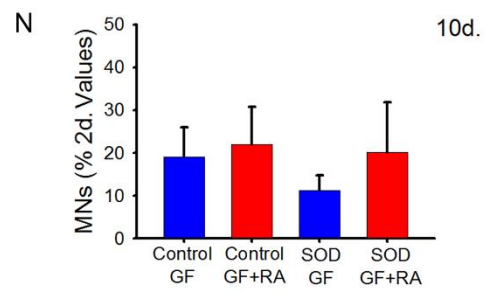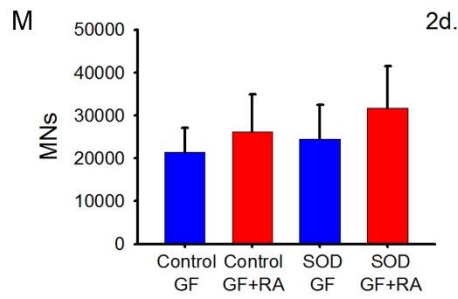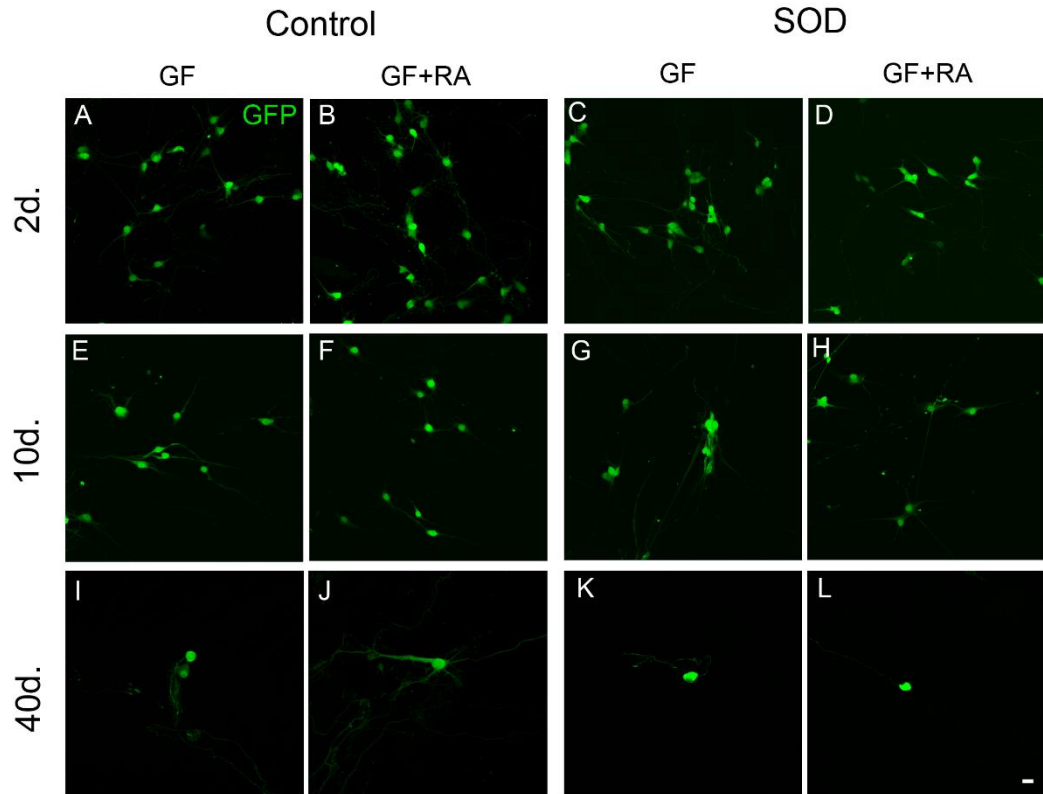
Figure 4.11. Effects of extended (2d.) RA treatment on soma area in hSOD1G93A$^+$ ESCMNs on myotubes

Sample GFP$^+$ ESCMNs at 25d. (GF control, **A**; GF+RA treated, **B**). Cumulative frequency plots comparing soma sizes of GF controls (at 25d. and 40d., **C**) and GF+RA treated cells (at 25d. and 40d., **D**). Asterisk in **D** denotes statistical difference, details in text. Scale bar = 20 μm.

GF

A

25d.

B

GF+RA

C

% Cumulative Frequency

100
80
60
40
20
0

0   200   400   600   800   1000

Soma Area (μm^2)

SOD 25d. GF
SOD 40d. GF

D

% Cumulative Frequency

*

100
80
60
40
20
0

0   200   400   600   800   1000

Soma Area (μm^2)

SOD 25d. GF+RA
SOD 40d. GF+RA
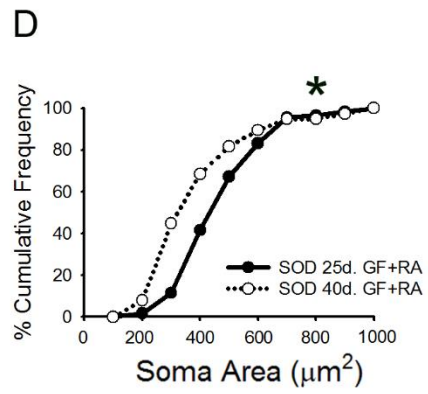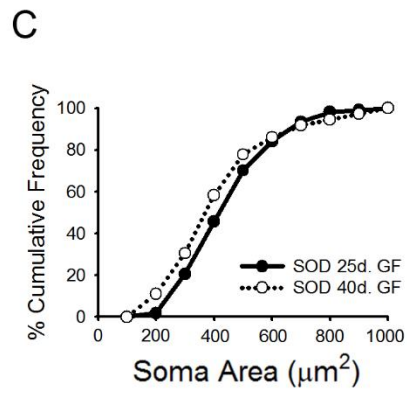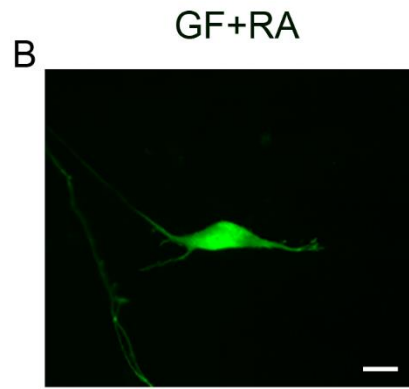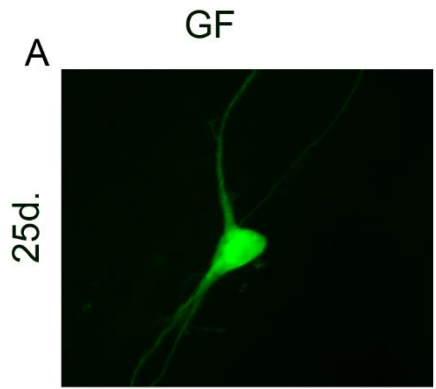
Figure 4.12. Effects of extended (2d.) RA treatment on endplate area in hSOD1G93A$^+$ ESCMN-myotube co-cultures

Neuromuscular junctions with ESCMNs at 25 DIV (GF control, **A**; GF+RA treated, **D**) and highlighted endplates identified by rhodamine conjugated α-bungarotoxin (α-btx) (GF control, **B**; GF+RA treated, **E**; regions outlined in boxes are expanded in insets in **B** and **E**). Merges shown in **C** and **F** for GF controls and GF+RA treated ESCMNs, respectively. Histograms of endplate sizes at 25d. (GF control, **G**; GF+RA treated, **H**) and 40d. (GF control, **I**; GF+RA treated, **J**). Cumulative frequency plots comparing endplate sizes of GF controls (at 25d. and 40d., **K**) and GF+RA treated cells (at 25d. and 40d., **L**). Asterisks in **K** and **L** denote statistical difference, details in text. Scale bar = 50 μm.

GF

A GFP   B α-BTX   C MERGE

25d.

GF+RA

D   E   F

25d.

G GF   H GF+RA   I

25d.

J   K   L

40d.

M   N
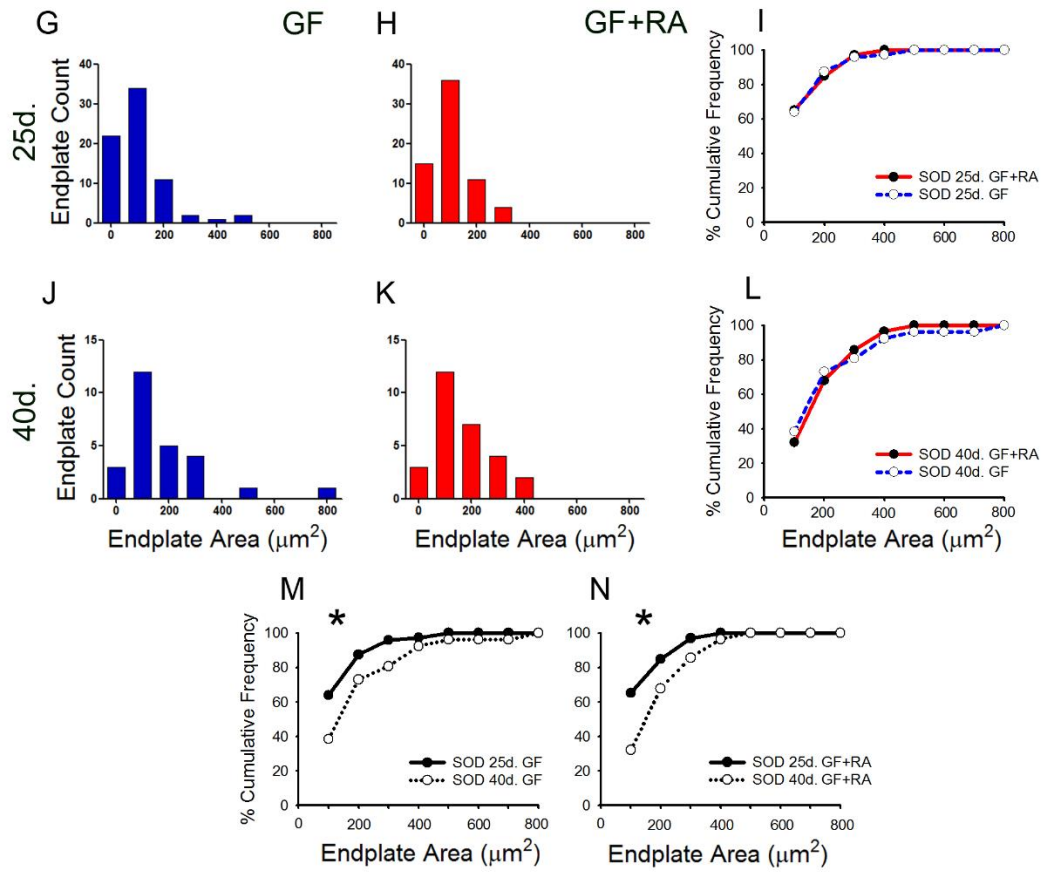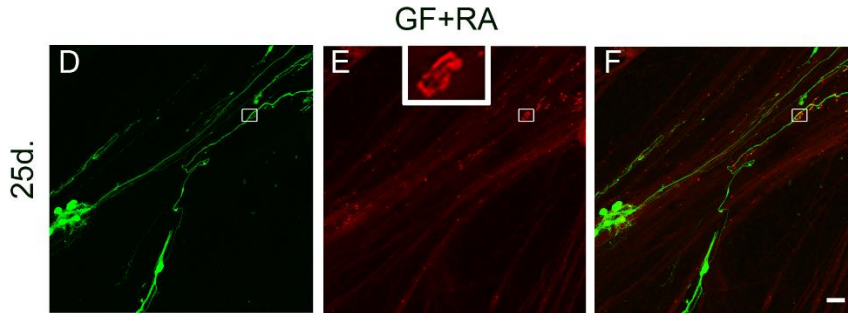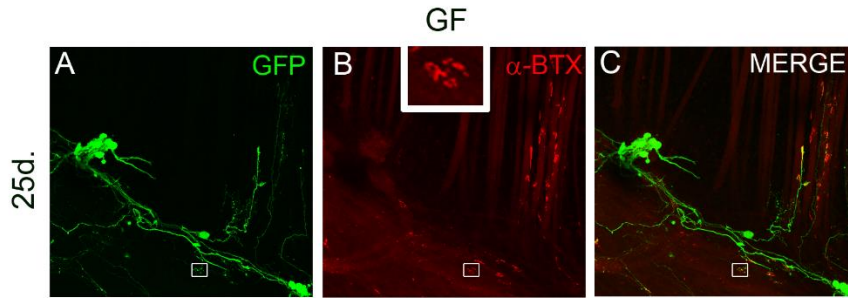
CHAPTER 5: DISCUSSION

Our abilities to model the nervous system have come a long way since the initial *in vitro* experiments performed by Ross Harrison. We are now able to generate a technically inexhaustible supply of specific cell types, such as motoneurons, for *in vitro* modelling. The two main areas for which pluripotent stem cell-derived motoneurons (along with iMNs) can be used *in vitro* are for 1) investigations concerning motoneuron development and 2) utilizing these cells for modelling motoneuron disease. I will now discuss how the data presented in this thesis relate to these two areas in the context of current research and what possible avenues further research could take. This discussion will be followed by an in-depth comparison of the abilities of the three cell types described in this thesis (ESCMNs, iPSCMNs and iMNs) to model spinal motoneurons *in vitro*.

5.1 Pluripotent stem cell-derived motoneurons and modelling motoneuron development *in vitro*

The ability to generate a theoretically limitless supply of purified ESCMNs/iPSCMNs is critical for studies requiring large numbers of motoneurons. For example, studies of gene or protein expression changes following treatment with factors involved in promoting the phenotypic characteristics of motoneurons of a specific subtype. One example of this is described in Chapter 4, whereby thousands of motoneurons were required for assessing expression of proteins influenced by extended RA treatment. The study I present in Chapter 4 illustrates the advantage of using ESCMN technology. For example, the large number of motoneurons generated allowed for a large population of motoneurons that resulted in a population of motoneurons with a broad soma size range. It is important to note that this range resembled previously reported for endogenous mouse spinal motoneurons (McHanwell and Biscoe, 1981). This finding validates the use of ESCMNs for use in investigations of developmental size differences in motoneurons, and using ESCMNs may allow for further research into the factors governing cell size in developing motoneurons (i.e. intrinsic genetic factors versus environmental cues). It is worth noting that other studies have generated large quantities of motoneurons from either iPS cells or ES cells for investigations of motoneuron soma size, but these were used for comparing healthy motoneurons versus motoneurons with a mutation conferring

SMA (Corti et al., 2012) or motoneurons exposed to toxins from mutated-SOD1 astrocytes (Nagai et al., 2007). For the purposes of studying motoneuron growth and development *in vitro*, soma sizes have yet to be investigated in depth.

The downregulation of developmentally-important LIM homeodomain proteins coincides with motoneuron size increases (Chapter 4). Whether these developmental events are related or are occurring concomitantly through independent mechanisms as part of an overall trend towards maturity is currently unknown. LIM homeodomain proteins are involved in a variety of developmental processes in neuronal populations throughout the spinal cord. For example, Lhx1 regulates genes involved in axon guidance in both motoneurons and spinal dorsal interneurons (Kania and Jessell, 2003; Avraham et al., 2009). Lhx1 plays other important roles in neuronal development of the spinal cord, including promoting a GABAergic inhibitory phenotype in interneurons of the dorsal horn of the spinal cord (Pillai et al., 2007) and modulating signals essential for appropriate migration of motoneurons to the LMC (Palmesino et al., 2010).

What drives the genetic programs essential for maturation of motoneurons (including for example, appropriate ion channel expression for mature firing properties) is still not completely understood, however it is known that spontaneous rhythmic activity in the spinal cord is essential for motoneuron development, and this activity has an effect on the expression of LIM homeodomain factors (Hanson and Landmesser, 2004). Hanson and Landmesser (2004) showed that pharmacological blockade of early rhythmic activity in the developing chick spinal cord results in decreases in the LIM homeodomain factors Lim1 (i.e. Lhx1 protein in chick) and Isl1. Blocking activity also caused axon pathfinding errors that may have been attributed to altered expression of guidance molecules including EphA4, however these effects occurred earlier in development than the noted decline in LIM homeodomain factors, indicating that this decline was not responsible for the pathfinding errors or alteration in guidance factor expression. Further work by Benjumeda et al. (2013) utilized a genetic approach to block spontaneous activity in developing chick motoneurons through ectopic expression of an inwardly rectifying potassium channel (Kir2.1). The results of this study found that silencing activity in motoneurons did not affect FoxP1 or Lim1 expression in LMC motoneurons. Blocking activity also had no measurable effect on EphA4 expression and

activity in LMC$_l$ axons, as they correctly targeted the dorsal limb muscle mass. The only noted effects of silencing spontaneous activity in motoneurons were disrupted branching and pruning once axons had reached their appropriate target tissues. The authors concluded that motoneuron specification, EphA4 expression and function and guidance of LMC motor axons are independent of spontaneous activity. While it is not completely understood, the discrepancies between the findings of Hanson and Landmesser (2004) and Benjemuda et al. (2013) may relate to the methods used to silence motoneurons, as the pharmacological blockade as used by Hanson and Landmesser may have less specific effects on motoneuron development by affecting activity in other cells within the spinal cord (e.g. interneurons).

Factors that normally regulate the decline in LIM homeodomain factors in motoneurons remain unknown, however the results of our *in vitro* investigations in Chapter 4 suggests that it may be a cell-autonomous mechanism, which may or may not be related to activity. It is also unknown how well our findings extrapolate to other cell populations that express Lhx1 in the spinal cord, including interneurons of the dorsal horn (Pillai et al., 2007). It is intriguing to speculate that if activity is involved in regulation of LIM homeodomain expression in motoneurons (Hanson and Landmesser et al., 2004), it could result from the changing nature of the activity of maturing motoneurons (altered ion channel expression for example). This possibility could be tested *in vitro* with the addition of the pharmacological agents used by Hanson and Landmesser (2004) including picrotoxin (the GABAergic Cl$^-$ channel blocker used to block excitation of embryonic motoneurons) or strychnine (which inhibits glycinergic transmission) to ESCMNs in embryoid bodies. Axon outgrowth could also be assessed in culture. Potential links between ion channel expression and Lhx1 immunoreactivity could be investigated as well.

Declines in Lhx1 expression in ESCMNs were found to be due, at least in part, to interaction with muscle, thus demonstrating that the ESCMN-chick myotube co-culture system can be used for investigating developmentally-relevant gene expression changes in motoneurons. Further *in vitro* experiments illustrating the role of the muscle in gene expression in motoneuron maturation can be tested using this model system, possibly involving subtype-specific motoneuron-muscle interactions.

In line with the role of activity in promoting outgrowth, we noted an inability of iMNs to successfully extend axons out of the chick spinal cord all the way to peripheral muscle following implantation, as described in Chapter 3. This may be due to the fact that the iMNs implanted into the spinal cord are lacking other neurons that may contribute to generating the activity necessary for promoting outgrowth following FACS purification of the iMNs. As described in Chapter 2, embryoid bodies containing iPSCMNs were implanted into the developing chick spinal cord and successfully projected axons to peripheral muscle, as previously demonstrated with ESCMNs (Peljto et al., 2010; Soundarajan et al., 2006; 2007; 2010). In these studies as well as the study presented in Chapter 2, ESCMNs/iPSCMNs were maintained as aggregates composed of motoneurons as well as any other cell types present in the embryoid bodies including astrocytes and other neurons (unpublished observations, Rafuse laboratory). It would be interesting to test the hypothesis that inhibiting activity (as described above for *in vitro* culture) in the embryoid bodies would decrease motor axon outgrowth into the periphery following intraspinal transplantation.

Pluripotent stem cell-derived motoneurons can also be used to investigate mechanisms related to motor axon guidance. For example, when transplanted far from the normal settling position within the spinal cord, iPSCMNs and ESCMNs will still project axons towards appropriate muscle targets (Chapter 2; Soundararajan et al., 2006). For example, as demonstrated in Figure 2.3, iPSCMNs transplanted dorsal to the ventral horn were capable of projecting axons to epaxial muscles and limbs. This suggests that these cells possess the intrinsic capacity to project axons despite improper localization within the spinal cord. It is possible that these cells are responding to cues within the spinal cord that direct their axons outside of the cord, and once present in the peripheral nerves, local guidance cues direct them towards their appropriate muscle targets. It may be possible to use transplanted pluripotent stem cell-derived motoneurons to further investigate the nature of axonal projections both within and outside the spinal cord, perhaps by transplanting cells that lack candidate guidance genes and monitoring axon growth could provide unique insights into the factors that govern motor axon guidance. Along these lines, recent work has demonstrated a role for ESCMNs in investigating the intracellular mechanisms of motor axon guidance in response to cues. Nedelec et al. (2012)

demonstrated that local protein synthesis within the motor axon is not essential for appropriate axon guidance in response to ephrin-A5, however it is for response to low concentrations of semaphorins. Further investigations using ESCMNs could demonstrate the role of local protein synthesis to appropriate motor axon guidance in response to other cues as well as reveal more intracellular pathways involved in the guidance process.

5.2 The utility of iPSCMNs for disease modelling *in vitro*

The results I present in this thesis support the use of iPSCMNs for use in studies of *in vitro* motoneuron disease modelling. iPSCMNs were found to possess the phenotypical characteristics of endogenous motoneurons, a necessary prerequisite if iPSCMNs are to be useful for therapeutic purposes (see results, Chapter 2). iPSCMNs are ideal for patient-specific, personalized drug treatment, which is an especially critical aspect of this technology for modelling a disease such as ALS. The multiple underlying causes of ALS suggest that a single drug target useful in treating all cases of the disease is unlikely, and given the fact that the majority of cases are sporadic, a therapeutic approach tailored to individuals will likely provide the most effective treatment strategy. However, these approaches are appropriate for therapeutics targeted towards familial ALS as well, as more genetic underpinnings of the disease are continuously being discovered (as described in Chapter 1, see review by Ajroud-Driss and Siddique, 2014). For example, recent work has shown that some forms of familial ALS are associated with mutations in a gene involved in cytoskeletal integrity, i.e. the tubulin gene TUBA4A (Smith et al., 2014), in addition to the more heavily studied genes involved in ALS such as SOD1 and TDP-43. Given the wide array of functions of the panoply of genes associated with ALS, different drug targets are almost certainly required for different forms of the disease.

Another promising use of iPS cell technology is a cell source for autologous transplantation, as cells derived from an individual could be differentiated into motoneurons and transplanted into the same individual, perhaps to treat peripheral nerve damage (see Figure 1.1; reviewed in Chipman et al., 2012). In the case of transplantations of iPSCMNs as well as ESCMNs into peripheral nerves following injury, much work remains to overcome issues of tumorogenesis that occur as a result of transplantation of undifferentiated cells alongside motoneurons (Rafuse lab, unpublished results). With

regard to the therapeutic potential of iPSCMNs, it is in my estimation that, at present, the strength of this technology lies in the ability to generate high yields of homogeneous iPSCMNs for drug screening purposes rather than the use of iPS cells for transplantation, as the risks associated with the latter treatment far outweigh those of *in vitro* manipulations.

Although cell replacement therapy involving iPSCMNs may be useful for treatment of peripheral nerve injuries, is unlikely to yield promising results for patients of ALS as the disease does not only affect motoneurons. Therefore, cell replacement involving 1) motoneurons derived from an ALS patient that have either been genetically-corrected using gene editing technologies such as the recently developed CRISPR technique (Barrangou, 2014) or 2) motoneurons derived from healthy individuals in conjuction with immune suppressants is not likely to promote long-term benefits as these cells will be placed within a diseased cellular environment. One aspect where gene-editing technology may be useful with respect to ALS therapeutics is in *in vitro* modelling as new genetic targets of ALS are unveiled from clinical studies. Using CRISPR, motoneurons could be induced to harbour newly-discovered genetic mutations associated with ALS. These motoneurons could theoretically be generated from any set of human iPSCs or ESCs thus overcoming any issues related to obtaining patient tissue or specific iPSC lines derived from patient tissue. Large numbers of high-throughput screening assays of motoneurons harbouring these ALS-associated mutations could then be performed to determine if candidate therapeutic drugs could offer increased cell survival benefits or increased ability of motoneurons to remain connected to muscle in a motoneuron-myofibre co-culture assay.

5.3 Functional comparisons between ESCMNs, iPSCMNs, and iMNs

Surprisingly few exogenous cues are necessary to initiate a program of motoneurogenesis from pluripotent stem cells. Treatment of pluripotent stem cells with two factors, Shh signalling agonists and RA, result in postmitotic motoneurons that possess the functional characteristics of mature spinal motoneurons. The process of virally-transduced genetic transdifferentiation was used to generate motoneurons directly from fibroblasts – a novel technique for the development of motoneurons that does not rely on the classic

morphogen-based differentiation protocol used to generate motoneurons from ESCs or iPSCs. The following section will compare and contrast the functionality of ESCMNs, iPSCMNs, and iMNs.

All three of these cell types are capable of extending neurites in culture, as well as the ability to generate one single axon from these neurites when plated on myofibres. The degree to which these cells generate other morphological features of motoneurons, such as functional dendrites for example, is still not well characterized. One characteristic aspect of spinal motoneurons is the NMJ, which requires specialized synaptic machinery and morphological features that are essential to provide an effective functional interface with muscle. ESCMNs, iPSCMNs and iMNs are all capable of forming NMJs *in vitro* when plated on chick myotubes, but the degree to which they form functional motoneurons may vary. Both iPSCMNs (Chapter 2) and ESCMNs (Chapter 4 and elsewhere; e.g. Miles et al., 2004 and Chipman et al., 2014) form NMJs that possess the essential synaptic components for normal transmission, including active vesicular cycling as demonstrated by FM4-64 dye labelling experiments. These NMJs also respond appropriately to pharmacological intervention, as revealed through intracellular recordings from endplates of the postsynaptic muscle. Glutamate treatment increases the frequency of EPPs and treatment with either curare or TTX inhibit neurotransmission at NMJs of both iPSCMNs and ESCMNs (Chapter 2; Miles et al., 2004). While muscle contractions in iMN-myofibre co-cultures were blocked by curare, no direct endplate recordings were undertaken (Son et al, 2011). While iMNs were found to be capable of generating EPPs when co-cultured with chick myofibres (Chapter 3), further investigations of the functionality of the NMJs formed by iMNs will be essential if these cells are to prove useful for therapeutic purposes. In line with the appropriate functionality of the NMJs formed by these three cell types, the morphological development of these NMJs approximates that seen *in vivo*, as described throughout this thesis and elsewhere. Clustering of AChRs is associated with developing NMJs formed by ESCMNs, iPSCMNs and iMNs (Chapters 2, 3; Miles et al., 2004; Chipman et al., 2014). The transition of plaque-like endplate formations to mature pretzel-like formations is evident in co-cultures formed from either iPSCMNs (Chapter 2) or ESCMNs (Chapter 4; Chipman et al., 2014), suggesting that these cells have activated a gene expression

program characteristic of developing spinal motoneurons. We did not specifically note the transition from plaque to pretzel shaped endplates in iMN-myofibre co-cultures, which may be indicative of differences in functional capabilities (possibly due to slight differences in gene expression programs) between iMNs and ESCMNs or iPSCMNs. Another component essential to the function of motoneurons is the ability to fire action potentials in a manner capable of generating muscle contractions. In terms of developing appropriate firing properties, both ESCMNs and iPSCMNs are capable of firing repetitive action potentials and developing mature firing properties characteristic of endogenous spinal motoneurons, such as spike frequency adaptation (Miles et al., 2004; Chapter 2). The characterization of developing firing properties of iMNs was not as complete as that carried out for both ESCMNs and iPSCMNs, however evidence suggests that iMNs are capable of firing (Son et al., 2011). Further investigation of firing properties of iMNs should be conducted in order to evaluate the utility of iMNs for therapeutic purposes, especially cell replacement therapy, as appropriate activation of muscle contractions is essential for this therapeutic strategy.

Of the three cell types investigated in this thesis (i.e. iPSCMNs, iMNs and ESCMNs), iMNs appeared to be the least capable of demonstrating the properties of mature motoneurons. Although following transdifferentiation of fibroblasts, these cells became cholinergic, expressed appropriate ion channels and were capable of inducing AChR (Chapter 3; Son et al., 2011), there were characteristic of normal motoneurogenesis that were absent. For example, upon transplantation into the developing chick spinal cord, iMNs were incapable of extending axons towards peripheral muscle targets (as demonstrated in Chapter 3). Whether this inability is related to the viral reprogramming procedure *per se* remains to be determined, however evidence suggests that viral transduction of iPSCs and ESCs with appropriate transcription factors is capable of generating functional motoneurons from human cells. Hester et al. (2011) have shown that hESCs and human iPSCs transduced with neurogenin-2, Lhx3, and islet-1, factors known to be essential for motoneuron differentiation, exhibit firing properties characteristic of mature motoneurons. Utilizing viral transduction instead of traditional RA and Shh differentiation, Hester et al. (2011) were able to dramatically decrease the amount of time (by ~ 30 days) required to generate functional motoneurons. These results

suggest that viral transduction of appropriate transcription factors can yield functional motoneurons, at least from pluripotent stem cells. Whether motoneurons generated by this approach possess other abilities characteristic of mature motoneurons, such as the ability to form physiologically-relevant NMJs when co-cultured on myofibres, remains to be investigated.

Upon transduction of motoneurogenic factors, there was evidence that transdifferentiating fibroblasts quickly transitioned to a post-mitotic stage in order to generate iMNs, as incorporation of BrdU, a label for dividing cells, was found to decline in the days following transduction (Son et al., 2011). As well, these cells did not express Nestin, a protein associated with neural progenitors (Son et al., 2011). While Son et al. (2011) claim that iMNs did not transition through a neural progenitor state, expression of factors essential for the endogenous development of motoneurons such as Olig2 or Nkx6.1 was not directly compared with expression levels in developing ESCMNs or iPSCMNs. Whether the inability of iMNs to develop the same properties as iPSCMNs and ESCMNs results from the absence of an environment that allows for particular gene expression programs or an epigenetic landscape that only can be provided by progressive differentiation of neural progenitors into motoneurons is not fully understood. Along these lines, neurogenin-2, one of the transduced reprogramming factors that is essential for normal motoneuron development, was found to be expressed at somewhat lower levels in iMNs as compared to ESCMNs (Son et al., 2011). The functional relevance of this differential expression is not known. It is worth noting, however, that reprogramming of fibroblasts into iMNs did result in the activation of a motoneuron-like gene expression program, as genes essential for motoneurogenesis and motoneuron function that were not transduced were upregulated in these cells, such as islet-1 and ChAT.

While Son et al. (2011) did investigate the global gene expression profile of iMNs and found that it was more similar to endogenous motoneurons than fibroblasts or ESCs, the possibility still remains that gene regulatory mechanisms are different between iMNs and ESCMNs (or iPSCMNs). Regulation of the transgenic expression of the cocktail of motoneuron genes may not take place in a fashion similar to endogenous motoneurons. For example, the regulation of factors that are necessary for early establishment of motoneuron subtype identity, such as Lhx3, may not occur as effectively as in

endogenous motoneurons or those generated from ESCs or iPSCs, and this may not be ideal for the development of mature motoneurons. Clearly, iMNs do not seem to respond to exogenous axon guidance clues as readily as iPSCMNs and ESCMNs following transplantation into the developing spinal cord, so subtle differences in the expression of essential guidance factors (such as FGFR1, a guidance factor expressed by Lhx3$^+$ MMC motoneurons (Shirasaki et al., 2006), for example) could partially account for this variability.

5.4 Conclusions and future considerations

The pluripotent stem cell technology that has given rise to ESCMNs and iPSCMNs, and the newly-developed iMN technology, have allowed for the reliable generation of large numbers of motoneurons for the purposes of *in vitro* modelling. Stem cell technology allows for easy development of motoneurons from transgenic stem cell lines (including gene knockouts and conditional knockouts), thus opening the door for many possible aspects of motoneuron development and physiology to be investigated *in vitro*. For example, coculturing genetically altered ESCMNs or iPSCMNs with multiple cell types of the spinal cord may shed light on mechanisms involved in developing spinal circuitry, as it may be possible to gain insight into how only a small subset of developing spinal neurons interact. Indeed, ongoing efforts to model V3 spinal interneuron development *in vitro* using ES cell technology, and to co-culture these cells with ESCMNs are currently underway (unpublished results, laboratories of Victor Rafuse and Ying Zhang, Dalhousie University).

As for disease modelling, iPSCMNs show much promise, as the results I present in Chapter 2 demonstrate. Despite concerns regarding epigenetic memory in cells derived from iPS cells (Kim et al., 2010; Ma et al., 2014), iPS cells appear as capable of generating functional motoneurons as ES cells. This is encouraging news, as use of iPS cell technology has the potential to generate breakthroughs for identifying potential therapeutic targets for motoneuron diseases such as ALS. Also encouraging are the developments in iPS cell technology as they relate to *in vitro* modelling and generating therapies for other neurodegenerative diseases such as Alzheimer's, Parkinson's and Huntington's disease (reviewed by Kaye and Finkbeiner, 2013; Cao et al., 2014). By

utilizing a common approach to developing therapeutics for these diseases, which share some etiological features such as protein aggregation and faulty protein clearance (reviewed by Ajroud-Driss and Siddique, 2014), it is possible that a drug that treats many if not all of these diseases could arise. In summary, stem-cell derived motoneurons are likely to continue to be a powerful tool for *in vitro* modelling of both motoneuron development and disease that will complement (and possibly direct) future *in vivo* studies.

REFERENCES

Adams KL, Rousso DL, Umbach JA, Novitch BG (2015) Foxp1-mediated programming of limb-innervating motor neurons from mouse and human embryonic stem cells. Nat Commun 6:6778.

Ajroud-Driss S, Siddique T (2015) Sporadic and hereditary amyotrophic lateral sclerosis (ALS). Biochim Biophys Acta 1852:679-684.

Alami NH, Smith RB, Carrasco MA, Williams LA, Winborn CS, Han SS, Kiskinis E, Winborn B, Freibaum BD, Kanagaraj A, Clare AJ, Badders NM, Bilican B, Chaum E, Chandran S, Shaw CE, Eggan KC, Maniatis T, Taylor JP (2014) Axonal transport of TDP-43 mRNA granules is impaired by ALS-causing mutations. Neuron 81:536-543.

Alaynick WA, Jessell TM, Pfaff SL (2011) SnapShot: spinal cord development. Cell 146:178.

Amoroso MW, Croft GF, Williams DJ, O'Keeffe S, Carrasco MA, Davis AR, Roybon L, Oakley DH, Maniatis T, Henderson CE, Wichterle H (2013) Accelerated high-yield generation of limb-innervating motor neurons from human stem cells. J Neurosci 33:574-586.

Arbab M, Baars S, Geijsen N (2014) Modeling motor neuron disease: the matter of time. Trends Neurosci 37:642-652.

Arber S, Han B, Mendelsohn M, Smith M, Jessell TM, Sockanathan S (1999) Requirement for the homeobox gene Hb9 in the consolidation of motor neuron identity. Neuron 23:659-674.

Avraham O, Hadas Y, Vald L, Zisman S, Schejter A, Visel A, Klar A (2009) Transcriptional control of axonal guidance and sorting in dorsal interneurons by the Lim-HD proteins Lhx9 and Lhx1. Neural Dev 4:21.

Bain G, Kitchens D, Yao M, Huettner JE, Gottlieb DI (1995) Embryonic stem cells express neuronal properties in vitro. Dev Biol 168:342-357.

Balice-Gordon RJ, Chua CK, Nelson CC, Lichtman JW (1993) Gradual loss of synaptic cartels precedes axon withdrawal at developing neuromuscular junctions. Neuron 11:801-815.

Barrangou R (2014) RNA events. Cas9 targeting and the CRISPR revolution. Science 344:707-708.

Bellefroid EJ, Bourguignon C, Hollemann T, Ma Q, Anderson DJ, Kintner C, Pieler T (1996) X-MyT1, a Xenopus C2HC-type zinc finger protein with a regulatory function in neuronal differentiation. Cell 87:1191-1202.

Benjumeda I, Escalante A, Law C, Morales D, Chauvin G, Muca G, Coca Y, Marquez J, Lopez-Bendito G, Kania A, Martinez L, Herrera E (2013) Uncoupling of EphA/ephrinA signaling and spontaneous activity in neural circuit wiring. J Neurosci 33:18208-18218.

Bennett MR, Lai K, Nurcombe V (1980) Identification of embryonic motoneurons in vitro: their survival is dependent on skeletal muscle. Brain Res 190:537-542.

Berg DK, Fischbach GD (1978) Enrichment of spinal cord cell cultures with motoneurons. J Cell Biol 77:83-98.

Berghs S, Aggujaro D, Dirkx R Jr, Maksimova E, Stabach P, Hermel JM, Zhang JP, Philbrick W, Slepnev V, Ort T, Solimena M. (2000) betaIV spectrin, a new spectrin localized at axon initial segments and nodes of ranvier in the central and peripheral nervous system. J Cell Biol 151:985-1002.

Betz WJ, Bewick GS (1992) Optical analysis of synaptic vesicle recycling at the frog neuromuscular junction. Science 255:200-203.

Bezakova G, Ruegg MA (2003) New insights into the roles of agrin. Nat Rev Mol Cell Biol 4:295-308.

Bilican B, Serio A, Barmada SJ, Nishimura AL, Sullivan GJ, Carrasco M, Phatnani HP, Puddifoot CA, Story D, Fletcher J, Park IH, Friedman BA, Daley GQ, Wyllie DJ, Hardingham GE, Wilmut I, Finkbeiner S, Maniatis T, Shaw CE, Chandran S (2012) Mutant induced pluripotent stem cell lines recapitulate aspects of TDP-43 proteinopathies and reveal cell-specific vulnerability. Proc Natl Acad Sci U S A 109:5803-5808.

Boillee S, Vande Velde C, Cleveland DW (2006) ALS: a disease of motor neurons and their nonneuronal neighbors. Neuron 52:39-59.

Bolliger MF, Zurlinden A, Luscher D, Butikofer L, Shakhova O, Francolini M, Kozlov SV, Cinelli P, Stephan A, Kistler AD, Rulicke T, Pelczar P, Ledermann B, Fumagalli G, Gloor SM, Kunz B, Sonderegger P (2010) Specific proteolytic cleavage of agrin regulates maturation of the neuromuscular junction. J Cell Sci 123:3944-3955.

Boulting GL, Kiskinis E, Croft GF, Amoroso MW, Oakley DH, Wainger BJ, Williams DJ, Kahler DJ, Yamaki M, Davidow L, Rodolfa CT, Dimos JT, Mikkilineni S, MacDermott AB, Woolf CJ, Henderson CE, Wichterle H, Eggan K (2011) A functionally characterized test set of human induced pluripotent stem cells. Nat Biotechnol 29:279-286.

Boyer JG, Deguise MO, Murray LM, Yazdani A, De Repentigny Y, Boudreau-Lariviere C, Kothary R (2014) Myogenic program dysregulation is contributory to disease pathogenesis in spinal muscular atrophy. Hum Mol Genet 23:4249-4259.

Briscoe J, Ericson J (2001) Specification of neuronal fates in the ventral neural tube. Curr Opin Neurobiol 11:43-49.

Briscoe J, Pierani A, Jessell TM, Ericson J (2000) A homeodomain protein code specifies progenitor cell identity and neuronal fate in the ventral neural tube. Cell 101:435-445.

Bruijn LI, Becher MW, Lee MK, Anderson KL, Jenkins NA, Copeland NG, Sisodia SS, Rothstein JD, Borchelt DR, Price DL, Cleveland DW (1997) ALS-linked SOD1 mutant G85R mediates damage to astrocytes and promotes rapidly progressive disease with SOD1-containing inclusions. Neuron 18:327-338.

Buganim Y et al. (2014) The developmental potential of iPSCs is greatly influenced by reprogramming factor selection. Cell Stem Cell 15:295-309.

Burkhardt MF et al. (2013) A cellular model for sporadic ALS using patient-derived induced pluripotent stem cells. Mol Cell Neurosci 56:355-364.

Caiazzo M, Dell'Anno MT, Dvoretskova E, Lazarevic D, Taverna S, Leo D, Sotnikova TD, Menegon A, Roncaglia P, Colciago G, Russo G, Carninci P, Pezzoli G, Gainetdinov RR, Gustincich S, Dityatev A, Broccoli V (2011) Direct generation of functional dopaminergic neurons from mouse and human fibroblasts. Nature 476:224-227.

Camu W, Henderson CE (1992) Purification of embryonic rat motoneurons by panning on a monoclonal antibody to the low-affinity NGF receptor. J Neurosci Methods 44:59-70.

Cao L, Tan L, Jiang T, Zhu XC, Yu JT (2014) Induced Pluripotent Stem Cells for Disease Modeling and Drug Discovery in Neurodegenerative Diseases. Mol Neurobiol.

Chambers SM, Fasano CA, Papapetrou EP, Tomishima M, Sadelain M, Studer L (2009) Highly efficient neural conversion of human ES and iPS cells by dual inhibition of SMAD signaling. Nat Biotechnol 27:275-280.

Chen JA, Huang YP, Mazzoni EO, Tan GC, Zavadil J, Wichterle H (2011) Mir-17-3p controls spinal neural progenitor patterning by regulating Olig2/Irx3 cross-repressive loop. Neuron 69:721-735.

Chen XL, Zhong ZG, Yokoyama S, Bark C, Meister B, Berggren PO, Roder J, Higashida H, Jeromin A (2001) Overexpression of rat neuronal calcium sensor-1 in rodent

NG108-15 cells enhances synapse formation and transmission. J Physiol 532:649-659.

Chipman PH, Toma JS, Rafuse VF (2012) Generation of motor neurons from pluripotent stem cells. Prog Brain Res 201:313-331.

Chipman PH, Zhang Y, Rafuse VF (2014) A stem-cell based bioassay to critically assess the pathology of dysfunctional neuromuscular junctions. PLoS One 9:e91643.

Corti S, Nizzardo M, Simone C, Falcone M, Nardini M, Ronchi D, Donadoni C, Salani S, Riboldi G, Magri F, Menozzi G, Bonaglia C, Rizzo F, Bresolin N, Comi GP (2012) Genetic correction of human induced pluripotent stem cells from patients with spinal muscular atrophy. Sci Transl Med 4:165ra162.

Crain SM (1964) Electrophysiological studies of cord-innervated skeletal muscle in long-term tissue cultures of mouse embryo myotomes. Anat Rec. 148:273–274.

Crain SM (1968) Development of functional neuromuscular connections between separate explants of fetal mammalian tissues after maturation in culture. Anat Rec. 160:466.

Crain SM, Alfei L, Peterson ER (1970) Neuromuscular transmission in cultures of adult human and rodent skeletal muscle after innervation in vitro by fetal rodent spinal cord. J Neurobiol. 1(4):471-89.

Cullheim S, Fleshman JW, Glenn LL, Burke RE (1987) Membrane area and dendritic structure in type-identified triceps surae alpha motoneurons. J Comp Neurol 255:68-81.

Dahm LM, Landmesser LT (1988) The regulation of intramuscular nerve branching during normal development and following activity blockade. Dev Biol 130:621-644.

Dahm LM, Landmesser LT (1991) The regulation of synaptogenesis during normal development and following activity blockade. J Neurosci 11:238-255.

Dasen JS, Jessell TM (2009) Hox networks and the origins of motor neuron diversity. Curr Top Dev Biol 88:169-200.

Dasen JS, Liu JP, Jessell TM (2003) Motor neuron columnar fate imposed by sequential phases of Hox-c activity. Nature 425:926-933.

Dasen JS, Tice BC, Brenner-Morton S, Jessell TM (2005) A Hox regulatory network establishes motor neuron pool identity and target-muscle connectivity. Cell 123:477-491.

Dasen JS, De Camilli A, Wang B, Tucker PW, Jessell TM (2008) Hox repertoires for motor neuron diversity and connectivity gated by a single accessory factor, FoxP1. Cell 134:304-316.

Davis-Dusenbery BN, Williams LA, Klim JR, Eggan K (2014) How to make spinal motor neurons. Development 141:491-501.

de Boer AS, Koszka K, Kiskinis E, Suzuki N, Davis-Dusenbery BN, Eggan K (2014) Genetic validation of a therapeutic target in a mouse model of ALS. Sci Transl Med 6:248ra104.

DeJesus-Hernandez M et al. (2011) Expanded GGGGCC hexanucleotide repeat in noncoding region of C9ORF72 causes chromosome 9p-linked FTD and ALS. Neuron 72:245-256.

Delestree N, Manuel M, Iglesias C, Elbasiouny SM, Heckman CJ, Zytnicki D (2014) Adult spinal motoneurones are not hyperexcitable in a mouse model of inherited amyotrophic lateral sclerosis. J Physiol 592:1687-1703.

Deng HX, Zhai H, Bigio EH, Yan J, Fecto F, Ajroud K, Mishra M, Ajroud-Driss S, Heller S, Sufit R, Siddique N, Mugnaini E, Siddique T (2010) FUS-immunoreactive inclusions are a common feature in sporadic and non-SOD1 familial amyotrophic lateral sclerosis. Ann Neurol 67:739-748.

Deng HX et al. (2011) Mutations in UBQLN2 cause dominant X-linked juvenile and adult-onset ALS and ALS/dementia. Nature 477:211-215.

Di Giorgio FP, Boulting GL, Bobrowicz S, Eggan KC (2008) Human embryonic stem cell-derived motor neurons are sensitive to the toxic effect of glial cells carrying an ALS-causing mutation. Cell Stem Cell 3:637-648.

Di Giorgio FP, Carrasco MA, Siao MC, Maniatis T, Eggan K (2007) Non-cell autonomous effect of glia on motor neurons in an embryonic stem cell-based ALS model. Nat Neurosci 10:608-614.

Dimos JT, Rodolfa KT, Niakan KK, Weisenthal LM, Mitsumoto H, Chung W, Croft GF, Saphier G, Leibel R, Goland R, Wichterle H, Henderson CE, Eggan K (2008) Induced pluripotent stem cells generated from patients with ALS can be differentiated into motor neurons. Science 321:1218-1221.

Durston AJ, van der Wees J, Pijnappel WW, Godsave SF (1998) Retinoids and related signals in early development of the vertebrate central nervous system. Curr Top Dev Biol 40:111-175.

Durston AJ, Timmermans JP, Hage WJ, Hendriks HF, de Vries NJ, Heideveld M, Nieuwkoop PD (1989) Retinoic acid causes an anteroposterior transformation in the developing central nervous system. Nature 340:140-144.

Ebert AD, Yu J, Rose FF, Jr., Mattis VB, Lorson CL, Thomson JA, Svendsen CN (2009) Induced pluripotent stem cells from a spinal muscular atrophy patient. Nature 457:277-280.

Echelard Y, Epstein DJ, St-Jacques B, Shen L, Mohler J, McMahon JA, McMahon AP (1993) Sonic hedgehog, a member of a family of putative signaling molecules, is implicated in the regulation of CNS polarity. Cell 75:1417-1430.

Egawa N et al. (2012) Drug screening for ALS using patient-specific induced pluripotent stem cells. Sci Transl Med 4:145ra104.

Esmaeili MA, Panahi M, Yadav S, Hennings L, Kiaei M (2013) Premature death of TDP-43 (A315T) transgenic mice due to gastrointestinal complications prior to development of full neurological symptoms of amyotrophic lateral sclerosis. Int J Exp Pathol 94:56-64.

Fallini C, Bassell GJ, Rossoll W (2012) Spinal muscular atrophy: the role of SMN in axonal mRNA regulation. Brain Res 1462:81-92.

Fischbach GD (1970) Synaptic potentials recorded in cell cultures of nerve and muscle. Science 169:1331-1333.

Fischbach GD (1972) Synapse formation between dissociated nerve and muscle cells in low density cell cultures. Dev Biol 28:407-429.

Fischbach GD, Cohen SA (1973) The distribution of acetylcholine sensitivity over uninnervated and innervated muscle fibers grown in cell culture. Dev Biol 31:147-162.

Fischer LR, Culver DG, Tennant P, Davis AA, Wang M, Castellano-Sanchez A, Khan J, Polak MA, Glass JD (2004) Amyotrophic lateral sclerosis is a distal axonopathy: evidence in mice and man. Exp Neurol 185:232-240.

Frey D, Schneider C, Xu L, Borg J, Spooren W, Caroni P (2000) Early and selective loss of neuromuscular synapse subtypes with low sprouting competence in motoneuron diseases. J Neurosci 20:2534-2542.

Fulton BP, Walton K (1986) Electrophysiological properties of neonatal rat motoneurones studied in vitro. J Physiol 370:651-678.

Gaffield MA, Betz WJ (2006) Imaging synaptic vesicle exocytosis and endocytosis with FM dyes. Nat Protoc 1:2916-2921.

Gao BX, Ziskind-Conhaim L (1998) Development of ionic currents underlying changes in action potential waveforms in rat spinal motoneurons. J Neurophysiol 80:3047-3061.

Gordon T, Pattullo MC (1993) Plasticity of muscle fiber and motor unit types. Exerc Sport Sci Rev 21:331-362.

Gould TW, Buss RR, Vinsant S, Prevette D, Sun W, Knudson CM, Milligan CE, Oppenheim RW (2006) Complete dissociation of motor neuron death from motor dysfunction by Bax deletion in a mouse model of ALS. J Neurosci 26:8774-8786.

Granit R, Kernell D, Shortess GK (1963) Quatitative aspects of repetitive firing of mammalian motoneurones, caused by injected currents. J Physiol 168:911-931.

Grumbles RM, Sesodia S, Wood PM, Thomas CK (2009) Neurotrophic factors improve motoneuron survival and function of muscle reinnervated by embryonic neurons. J Neuropathol Exp Neurol 68:736-746.

Grumbles RM, Liu Y, Thomas CM, Wood PM, Thomas CK (2013) Acute stimulation of transplanted neurons improves motoneuron survival, axon growth, and muscle reinnervation. J Neurotrauma 30:1062-1069.

Gurney ME (1994) Transgenic-mouse model of amyotrophic lateral sclerosis. N Engl J Med 331:1721-1722.

Haidet-Phillips AM, Hester ME, Miranda CJ, Meyer K, Braun L, Frakes A, Song S, Likhite S, Murtha MJ, Foust KD, Rao M, Eagle A, Kammesheidt A, Christensen A, Mendell JR, Burghes AH, Kaspar BK (2011) Astrocytes from familial and sporadic ALS patients are toxic to motor neurons. Nat Biotechnol 29:824-828.

Hamburger V (1948) The mitotic patterns in the spinal cord of the chick embryo and their relation to histogenetic processes. J Comp Neurol 88:221-283.

Hamilton G, Gillingwater TH (2013) Spinal muscular atrophy: going beyond the motor neuron. Trends Mol Med 19:40-50.

Hanson MG, Landmesser LT (2004) Normal patterns of spontaneous activity are required for correct motor axon guidance and the expression of specific guidance molecules. Neuron 43:687-701.

Harrison RG (1907) Experiments in transplanting limbs and their bearings on the problems of the development of nerves. J Exp Zool 4:239–281.

Harrison RG. (1910) The outgrowth of the nerve fiber as a mode of protoplasmic movement. J Exp Zool 9:787–846.

Hatzipetros T, Bogdanik LP, Tassinari VR, Kidd JD, Moreno AJ, Davis C, Osborne M, Austin A, Vieira FG, Lutz C, Perrin S (2014) C57BL/6J congenic Prp-TDP43A315T mice develop progressive neurodegeneration in the myenteric plexus of the colon without exhibiting key features of ALS. Brain Res 1584:59-72.

Helmbacher F, Schneider-Maunoury S, Topilko P, Tiret L, Charnay P (2000) Targeting of the EphA4 tyrosine kinase receptor affects dorsal/ventral pathfinding of limb motor axons. Development 127:3313-3324.

Hennig R, Lomo T (1985) Firing patterns of motor units in normal rats. Nature 314:164-166.

Hester ME, Murtha MJ, Song S, Rao M, Miranda CJ, Meyer K, Tian J, Boulting G, Schaffer DV, Zhu MX, Pfaff SL, Gage FH, Kaspar BK (2011) Rapid and efficient generation of functional motor neurons from human pluripotent stem cells using gene delivered transcription factor codes. Mol Ther 19:1905-1912.

Hollyday M, Hamburger V (1977) An autoradiographic study of the formation of the lateral motor column in the chick embryo. Brain Res 132:197-208.

Hu BY, Weick JP, Yu J, Ma LX, Zhang XQ, Thomson JA, Zhang SC (2010) Neural differentiation of human induced pluripotent stem cells follows developmental principles but with variable potency. Proc Natl Acad Sci U S A 107:4335-4340.

Hu BY, Zhang SC (2009) Differentiation of spinal motor neurons from pluripotent human stem cells. Nat Protoc 4:1295-1304.

Ichida JK, Blanchard J, Lam K, Son EY, Chung JE, Egli D, Loh KM, Carter AC, Di Giorgio FP, Koszka K, Huangfu D, Akutsu H, Liu DR, Rubin LL, Eggan K (2009) A small-molecule inhibitor of tgf-Beta signaling replaces sox2 in reprogramming by inducing nanog. Cell Stem Cell 5:491-503.

Ichida JK, T CWJ, Williams LA, Carter AC, Shi Y, Moura MT, Ziller M, Singh S, Amabile G, Bock C, Umezawa A, Rubin LL, Bradner JE, Akutsu H, Meissner A, Eggan K (2014) Notch inhibition allows oncogene-independent generation of iPS cells. Nat Chem Biol 10:632-639.

Ieda M, Fu JD, Delgado-Olguin P, Vedantham V, Hayashi Y, Bruneau BG, Srivastava D (2010) Direct reprogramming of fibroblasts into functional cardiomyocytes by defined factors. Cell 142:375-386.

James DW, Tresman RL (1968) De novo formation of neuro-muscular junctions in tissue culture. Nature 220:384-385.

Jessell TM (2000) Neuronal specification in the spinal cord: inductive signals and transcriptional codes. Nat Rev Genet 1:20-29.

Jiang ZG, Shen E, Dun NJ (1990) Excitatory and inhibitory transmission from dorsal root afferents to neonate rat motoneurons in vitro. Brain Res 535:110-118.

Juurlink BH, Munoz DG, Devon RM (1990) Calcitonin gene-related peptide identifies spinal motoneurons in vitro. J Neurosci Res 26:238-241.

Kania A, Jessell TM (2003) Topographic motor projections in the limb imposed by LIM homeodomain protein regulation of ephrin-A:EphA interactions. Neuron 38:581-596.

Kania A, Johnson RL, Jessell TM (2000) Coordinate roles for LIM homeobox genes in directing the dorsoventral trajectory of motor axons in the vertebrate limb. Cell 102:161-173.

Kanning KC, Kaplan A, Henderson CE (2010) Motor neuron diversity in development and disease. Annu Rev Neurosci 33:409-440.

Kaplan A, Spiller KJ, Towne C, Kanning KC, Choe GT, Geber A, Akay T, Aebischer P, Henderson CE (2014) Neuronal matrix metalloproteinase-9 is a determinant of selective neurodegeneration. Neuron 81:333-348.

Karumbayaram S, Novitch BG, Patterson M, Umbach JA, Richter L, Lindgren A, Conway AE, Clark AT, Goldman SA, Plath K, Wiedau-Pazos M, Kornblum HI, Lowry WE (2009) Directed differentiation of human-induced pluripotent stem cells generates active motor neurons. Stem Cells 27:806-811.

Kaye JA, Finkbeiner S (2013) Modeling Huntington's disease with induced pluripotent stem cells. Mol Cell Neurosci 56:50-64.

Kernell D, Monster AW (1982) Time course and properties of late adaptation in spinal motoneurones of the cat. Exp Brain Res 46:191-196.

Kernell D, Eerbeek O, Verhey BA, Donselaar Y (1987) Effects of physiological amounts of high- and low-rate chronic stimulation on fast-twitch muscle of the cat hindlimb. I. Speed- and force-related properties. J Neurophysiol 58:598-613.

Keshishian H (2004) Ross Harrison's "The outgrowth of the nerve fiber as a mode of protoplasmic movement". J Exp Zool A Comp Exp Biol 301:201-203.

Kim K et al. (2010) Epigenetic memory in induced pluripotent stem cells. Nature 467:285-290.

Ko HS, Uehara T, Tsuruma K, Nomura Y (2004) Ubiquilin interacts with ubiquitylated proteins and proteasome through its ubiquitin-associated and ubiquitin-like domains. FEBS Lett 566:110-114.

Kuo JJ, Schonewille M, Siddique T, Schults AN, Fu R, Bar PR, Anelli R, Heckman CJ, Kroese AB (2004) Hyperexcitability of cultured spinal motoneurons from presymptomatic ALS mice. J Neurophysiol 91:571-575.

Kuusisto E, Salminen A, Alafuzoff I (2001) Ubiquitin-binding protein p62 is present in neuronal and glial inclusions in human tauopathies and synucleinopathies. Neuroreport 12:2085-2090.

Kwiatkowski TJ, Jr. et al. (2009) Mutations in the FUS/TLS gene on chromosome 16 cause familial amyotrophic lateral sclerosis. Science 323:1205-1208.

Lacas-Gervais S, Guo J, Strenzke N, Scarfone E, Kolpe M, Jahkel M, De Camilli P, Moser T, Rasband MN, Solimena M. (2004) BetaIVSigma1 spectrin stabilizes the nodes of Ranvier and axon initial segments. J Cell Biol 166:983-990.

Landmesser L (1978) The development of motor projection patterns in the chick hind limb. J Physiol 284:391-414.

Lee H, Shamy GA, Elkabetz Y, Schofield CM, Harrsion NL, Panagiotakos G, Socci ND, Tabar V, Studer L (2007) Directed differentiation and transplantation of human embryonic stem cell-derived motoneurons. Stem Cells 25:1931-1939.

Lee SK, Pfaff SL (2001) Transcriptional networks regulating neuronal identity in the developing spinal cord. Nat Neurosci 4 Suppl:1183-1191.

Li XJ, Du ZW, Zarnowska ED, Pankratz M, Hansen LO, Pearce RA, Zhang SC (2005) Specification of motoneurons from human embryonic stem cells. Nat Biotechnol 23:215-221.

Liu Y, Grumbles RM, Thomas CK (2013) Electrical stimulation of embryonic neurons for 1 hour improves axon regeneration and the number of reinnervated muscles that function. J Neuropathol Exp Neurol 72:697-707.

Lomen-Hoerth C, Anderson T, Miller B (2002) The overlap of amyotrophic lateral sclerosis and frontotemporal dementia. Neurology 59:1077-1079.

Lopez-Gonzalez R, Velasco I (2012) Therapeutic potential of motor neurons differentiated from embryonic stem cells and induced pluripotent stem cells. Arch Med Res 43:1-10.

Lupa MT, Hall ZW (1989) Progressive restriction of synaptic vesicle protein to the nerve terminal during development of the neuromuscular junction. J Neurosci 9:3937-3945.

Ma H et al. (2014) Abnormalities in human pluripotent cells due to reprogramming mechanisms. Nature 511:177-183.

Marchetti D, McManaman JL (1990) Characterization of nerve growth factor binding to embryonic rat spinal cord neurons. J Neurosci Res 27:211-218.

Marchetto MC, Muotri AR, Mu Y, Smith AM, Cezar GG, Gage FH (2008) Non-cell-autonomous effect of human SOD1 G37R astrocytes on motor neurons derived from human embryonic stem cells. Cell Stem Cell 3:649-657.

Martinou JC, Martinou I, Kato AC (1992) Cholinergic differentiation factor (CDF/LIF) promotes survival of isolated rat embryonic motoneurons in vitro. Neuron 8:737-744.

Martinou JC, Le Van Thai A, Cassar G, Roubinet F, Weber MJ (1989) Characterization of two factors enhancing choline acetyltransferase activity in cultures of purified rat motoneurons. J Neurosci 9:3645-3656.

Masuko S, Kuromi H, Shimada Y (1979) Isolation and culture of motoneurons from embryonic chicken spinal cords. Proc Natl Acad Sci U S A 76:3537-3541.

Mazzoni EO, Mahony S (2013) Saltatory remodeling of Hox chromatin in response to rostrocaudal patterning signals. 16:1191-1198.

McHanwell S, Biscoe TJ (1981) The sizes of motoneurons supplying hindlimb muscles in the mouse. Proc R Soc Lond B Biol Sci 213:201-216.

McMahan UJ (1990) The agrin hypothesis. Cold Spring Harb Symp Quant Biol 55:407-418.

Miles GB, Yohn DC, Wichterle H, Jessell TM, Rafuse VF, Brownstone RM (2004) Functional properties of motoneurons derived from mouse embryonic stem cells. J Neurosci 24:7848-7858.

Mitne-Neto M, Machado-Costa M, Marchetto MC, Bengtson MH, Joazeiro CA, Tsuda H, Bellen HJ, Silva HC, Oliveira AS, Lazar M, Muotri AR, Zatz M (2011) Downregulation of VAPB expression in motor neurons derived from induced pluripotent stem cells of ALS8 patients. Hum Mol Genet 20:3642-3652.

Muhr J, Graziano E, Wilson S, Jessell TM, Edlund T (1999) Convergent inductive signals specify midbrain, hindbrain, and spinal cord identity in gastrula stage chick embryos. Neuron 23:689-702.

Murray LM, Comley LH, Thomson D, Parkinson N, Talbot K, Gillingwater TH (2008) Selective vulnerability of motor neurons and dissociation of pre- and post-synaptic pathology at the neuromuscular junction in mouse models of spinal muscular atrophy. Hum Mol Genet 17:949-962.

Nagai M, Re DB, Nagata T, Chalazonitis A, Jessell TM, Wichterle H, Przedborski S (2007) Astrocytes expressing ALS-linked mutated SOD1 release factors selectively toxic to motor neurons. Nat Neurosci 10:615-622.

Nakagawa M, Koyanagi M, Tanabe K, Takahashi K, Ichisaka T, Aoi T, Okita K, Mochiduki Y, Takizawa N, Yamanaka S (2008) Generation of induced pluripotent stem cells without Myc from mouse and human fibroblasts. Nat Biotechnol 26:101-106.

Nakanishi ST, Whelan PJ (2010) Diversification of intrinsic motoneuron electrical properties during normal development and botulinum toxin-induced muscle paralysis in early postnatal mice. J Neurophysiol 103:2833-2845.

Nedelec S, Peljto M, Shi P, Amoroso MW, Kam LC, Wichterle H (2012) Concentration-dependent requirement for local protein synthesis in motor neuron subtype-specific response to axon guidance cues. J Neurosci 32:1496-1506.

Neumann M, Sampathu DM, Kwong LK, Truax AC, Micsenyi MC, Chou TT, Bruce J, Schuck T, Grossman M, Clark CM, McCluskey LF, Miller BL, Masliah E, Mackenzie IR, Feldman H, Feiden W, Kretzschmar HA, Trojanowski JQ, Lee VM (2006) Ubiquitinated TDP-43 in frontotemporal lobar degeneration and amyotrophic lateral sclerosis. Science 314:130-133.

Ostendorff HP, Tursun B, Cornils K, Schluter A, Drung A, Gungor C, Bach I (2006) Dynamic expression of LIM cofactors in the developing mouse neural tube. Dev Dyn 235:786-791.

Palmesino E, Rousso DL, Kao TJ, Klar A, Laufer E, Uemura O, Okamoto H, Novitch BG, Kania A (2010) Foxp1 and lhx1 coordinate motor neuron migration with axon trajectory choice by gating Reelin signalling. PLoS Biol 8:e1000446.

Pang ZP, Yang N, Vierbuchen T, Ostermeier A, Fuentes DR, Yang TQ, Citri A, Sebastiano V, Marro S, Sudhof TC, Wernig M (2011) Induction of human neuronal cells by defined transcription factors. Nature 476:220-223.

Peljto M, Wichterle H (2011) Programming embryonic stem cells to neuronal subtypes. Curr Opin Neurobiol 21:43-51.

Peljto M, Dasen JS, Mazzoni EO, Jessell TM, Wichterle H (2010) Functional diversity of ESC-derived motor neuron subtypes revealed through intraspinal transplantation. Cell Stem Cell 7:355-366.

Peljto M et al. (2006) Recovery from paralysis in adult rats using embryonic stem cells. Nat Neurosci 60:32-44.

Peterson ER, Crain SM (1970) Innervation in cultures of fetal rodent skeletal muscle by organotypic explants of spinal cord from different animals. Z Zellforsch Mikrosk Anat.106(1):1-21.

Pfisterer U, Wood J, Nihlberg K, Hallgren O, Bjermer L, Westergren-Thorsson G, Lindvall O, Parmar M (2011) Efficient induction of functional neurons from adult human fibroblasts. Cell Cycle 10:3311-3316.

Phillips WD, Lai K, Bennett MR (1985) Spatial distribution and size of acetylcholine receptor clusters determined by motor nerves in developing chick muscles. J Neurocytol 14:309-325.

Pieri M, Albo F, Gaetti C, Spalloni A, Bengtson CP, Longone P, Cavalcanti S, Zona C (2003) Altered excitability of motor neurons in a transgenic mouse model of familial amyotrophic lateral sclerosis. Neurosci Lett 351:153-156.

Pillai A, Mansouri A, Behringer R, Westphal H, Goulding M (2007) Lhx1 and Lhx5 maintain the inhibitory-neurotransmitter status of interneurons in the dorsal spinal cord. Development 134:357-366.

Pinter MJ, Curtis RL, Hosko MJ (1983) Voltage threshold and excitability among variously sized cat hindlimb motoneurons. J Neurophysiol 50:644-657.

Placzek M, Yamada T, Tessier-Lavigne M, Jessell T, Dodd J (1991) Control of dorsoventral pattern in vertebrate neural development: induction and polarizing properties of the floor plate. Development Suppl 2:105-122.

Pun S, Santos AF, Saxena S, Xu L, Caroni P (2006) Selective vulnerability and pruning of phasic motoneuron axons in motoneuron disease alleviated by CNTF. Nat Neurosci 9:408-419.

Re DB, Le Verche V, Yu C, Amoroso MW, Politi KA, Phani S, Ikiz B, Hoffmann L, Koolen M, Nagata T, Papadimitriou D, Nagy P, Mitsumoto H, Kariya S, Wichterle H, Henderson CE, Przedborski S (2014) Necroptosis drives motor neuron death in models of both sporadic and familial ALS. Neuron 81:1001-1008.

Renton AE et al. (2011) A hexanucleotide repeat expansion in C9ORF72 is the cause of chromosome 9p21-linked ALS-FTD. Neuron 72:257-268.

Ribchester RR, Mao F, Betz WJ (1994) Optical measurements of activity-dependent membrane recycling in motor nerve terminals of mammalian skeletal muscle. Proc Biol Sci 255:61-66.

Ricard MJ, Gudas LJ (2013) Cytochrome p450 cyp26a1 alters spinal motor neuron subtype identity in differentiating embryonic stem cells. J Biol Chem 288:28801-28813.

Richard JP, Maragakis NJ (2015) Induced pluripotent stem cells from ALS patients for disease modeling. Brain Res 1607:15-25.

Rickwood D, Birnie GD (1975) Metrizamide, a new density-gradient medium. FEBS Lett 50:102-110.

Rickwood D, Ford T, Graham J (1982) Nycodenz: a new nonionic iodinated gradient medium. Anal Biochem 123:23-31.

Robbins N, Yonezawa T (1971a) Developing neuromuscular junctions: first signs of chemical transmission during formation in tissue culture. Science 172:395-398.

Robbins N, Yonezawa T (1971b) Physiological studies during formation and development of rat neuromuscular junctions in tissue culture. J Gen Physiol 58:467-481.

Rosen DR, Siddique T, Patterson D, Figlewicz DA, Sapp P, Hentati A, Donaldson D, Goto J, O'Regan JP, Deng HX, et al. (1993) Mutations in Cu/Zn superoxide dismutase gene are associated with familial amyotrophic lateral sclerosis. Nature 362:59-62.

Rossant J, Zirngibl R, Cado D, Shago M, Giguere V (1991) Expression of a retinoic acid response element-hsplacZ transgene defines specific domains of transcriptional activity during mouse embryogenesis. Genes Dev 5:1333-1344.

Rousso DL, Gaber ZB, Wellik D, Morrisey EE, Novitch BG (2008) Coordinated actions of the forkhead protein Foxp1 and Hox proteins in the columnar organization of spinal motor neurons. Neuron 59:226-240.

Roy RR, Pierotti DJ, Baldwin KM, Zhong H, Hodgson JA, Edgerton VR (1998) Cyclical passive stretch influences the mechanical properties of the inactive cat soleus. Exp Physiol 83:377-385.

Sandell LL, Sanderson BW, Moiseyev G, Johnson T, Mushegian A, Young K, Rey JP, Ma JX, Staehling-Hampton K, Trainor PA (2007) RDH10 is essential for synthesis of embryonic retinoic acid and is required for limb, craniofacial, and organ development. Genes Dev 21:1113-1124.

Sareen D, O'Rourke JG, Meera P, Muhammad AK, Grant S, Simpkinson M, Bell S, Carmona S, Ornelas L, Sahabian A, Gendron T, Petrucelli L, Baughn M, Ravits J, Harms MB, Rigo F, Bennett CF, Otis TS, Svendsen CN, Baloh RH (2013)

Targeting RNA foci in iPSC-derived motor neurons from ALS patients with a C9ORF72 repeat expansion. Sci Transl Med 5:208ra149.

Schaffner AE, St John PA, Barker JL (1987) Fluorescence-activated cell sorting of embryonic mouse and rat motoneurons and their long-term survival in vitro. J Neurosci 7:3088-3104.

Schnaar RI, Schaffner AE (1981) Separation of cell types from embryonic chicken and rat spinal cord: characterization of motoneuron-enriched fractions. J Neurosci 1:204-217.

Serio A, Bilican B, Barmada SJ, Ando DM, Zhao C, Siller R, Burr K, Haghi G, Story D, Nishimura AL, Carrasco MA, Phatnani HP, Shum C, Wilmut I, Maniatis T, Shaw CE, Finkbeiner S, Chandran S (2013) Astrocyte pathology and the absence of non-cell autonomy in an induced pluripotent stem cell model of TDP-43 proteinopathy. Proc Natl Acad Sci U S A 110:4697-4702.

Sharma K, Leonard AE, Lettieri K, Pfaff SL (2000) Genetic and epigenetic mechanisms contribute to motor neuron pathfinding. Nature 406:515-519.

Sharma K, Sheng HZ, Lettieri K, Li H, Karavanov A, Potter S, Westphal H, Pfaff SL (1998) LIM homeodomain factors Lhx3 and Lhx4 assign subtype identities for motor neurons. Cell 95:817-828.

Shimada Y, Fischman DA, Moscona AA (1969) Formation of neuromuscular junctions in embryonic cell cultures. Proc Natl Acad Sci U S A 62:715-721.

Shirasaki R, Lewcock JW, Lettieri K, Pfaff SL (2006) FGF as a target-derived chemoattractant for developing motor axons genetically programmed by the LIM code. Neuron 50:841-853.

Slater CR (1982) Postnatal maturation of nerve-muscle junctions in hindlimb muscles of the mouse. Dev Biol 94:11-22.

Smith BN et al. (2014) Exome-wide Rare Variant Analysis Identifies TUBA4A Mutations Associated with Familial ALS. Neuron 84:324-331.

Smith RG, Vaca K, McManaman J, Appel SH (1986) Selective effects of skeletal muscle extract fractions on motoneuron development in vitro. J Neurosci 6:439-447.

Sockanathan S, Jessell TM (1998) Motor neuron-derived retinoid signaling specifies the subtype identity of spinal motor neurons. Cell 94:503-514.

Son EY, Ichida JK, Wainger BJ, Toma JS, Rafuse VF, Woolf CJ, Eggan K (2011) Conversion of mouse and human fibroblasts into functional spinal motor neurons. Cell Stem Cell 9:205-218.

Soundararajan P, Fawcett JP, Rafuse VF (2010) Guidance of postural motoneurons requires MAPK/ERK signaling downstream of fibroblast growth factor receptor 1. J Neurosci 30:6595-6606.

Soundararajan P, Lindsey BW, Leopold C, Rafuse VF (2007) Easy and rapid differentiation of embryonic stem cells into functional motoneurons using sonic hedgehog-producing cells. Stem Cells 25:1697-1706.

Soundararajan P, Miles GB, Rubin LL, Brownstone RM, Rafuse VF (2006) Motoneurons derived from embryonic stem cells express transcription factors and develop phenotypes characteristic of medial motor column neurons. J Neurosci 26:3256-3268.

Studzinski GP (2001) Cell Differentiation *In Vitro*: Model Systems. John Wiley & Sons Ltd, Chichester.

Su H, Wang L, Cai J, Yuan Q, Yang X, Yao X, Wong WM, Huang W, Li Z, Wan JB, Wang Y, Pei D, So KF, Qin D, Wu W (2013) Transplanted motoneurons derived from human induced pluripotent stem cells form functional connections with target muscle. Stem Cell Res 11:529-539.

Suzuki N, Maroof AM, Merkle FT, Koszka K, Intoh A, Armstrong I, Moccia R, Davis-Dusenbery BN, Eggan K (2013) The mouse C9ORF72 ortholog is enriched in neurons known to degenerate in ALS and FTD. Nat Neurosci 16:1725-1727.

Suzuki T, Maruyama A, Sugiura T, Machida S, Miyata H (2009) Age-related changes in two- and three-dimensional morphology of type-identified endplates in the rat diaphragm. J Physiol Sci 59:57-62.

Szabo E, Rampalli S, Risueno RM, Schnerch A, Mitchell R, Fiebig-Comyn A, Levadoux-Martin M, Bhatia M (2010) Direct conversion of human fibroblasts to multilineage blood progenitors. Nature 468:521-526.

Takahashi K, Yamanaka S (2006) Induction of pluripotent stem cells from mouse embryonic and adult fibroblast cultures by defined factors. Cell 126:663-676.

Thaler J, Harrison K, Sharma K, Lettieri K, Kehrl J, Pfaff SL (1999) Active suppression of interneuron programs within developing motor neurons revealed by analysis of homeodomain factor HB9. Neuron 23:675-687.

Thomas CK, Erb DE, Grumbles RM, Bunge RP (2000) Embryonic cord transplants in peripheral nerve restore skeletal muscle function. J Neurophysiol 84:591-595.

Thomson SR, Nahon JE, Mutsaers CA, Thomson D, Hamilton G, Parson SH, Gillingwater TH (2012) Morphological characteristics of motor neurons do not

determine their relative susceptibility to degeneration in a mouse model of severe spinal muscular atrophy. PLoS One 7:e52605.

Tosney KW, Landmesser LT (1985) Development of the major pathways for neurite outgrowth in the chick hindlimb. Dev Biol 109:193-214.

Tsuchida T, Ensini M, Morton SB, Baldassare M, Edlund T, Jessell TM, Pfaff SL. (1994) Topographic organization of embryonic motor neurons defined by expression of LIMhomeobox genes. Cell 79:957-970.

Ulfhake B, Cullheim S (1988) Postnatal development of cat hind limb motoneurons. III: Changes in size of motoneurons supplying the triceps surae muscle. J Comp Neurol 278:103-120.

van Es MA et al. (2008) Genetic variation in DPP6 is associated with susceptibility to amyotrophic lateral sclerosis. Nat Genet 40:29-31.

van Zundert B, Peuscher MH, Hynynen M, Chen A, Neve RL, Brown RH, Jr., Constantine-Paton M, Bellingham MC (2008) Neonatal neuronal circuitry shows hyperexcitable disturbance in a mouse model of the adult-onset neurodegenerative disease amyotrophic lateral sclerosis. J Neurosci 28:10864-10874.

Vance C et al. (2009) Mutations in FUS, an RNA processing protein, cause familial amyotrophic lateral sclerosis type 6. Science 323:1208-1211.

Vermot J, Schuhbaur B, Le Mouellic H, McCaffery P, Garnier JM, Hentsch D, Brulet P, Niederreither K, Chambon P, Dolle P, Le Roux I (2005) Retinaldehyde dehydrogenase 2 and Hoxc8 are required in the murine brachial spinal cord for the specification of Lim1+ motoneurons and the correct distribution of Islet1+ motoneurons. Development 132:1611-1621.

Veyrat-Durebex C, Corcia P, Dangoumau A, Laumonnier F, Piver E, Gordon PH, Andres CR, Vourc'h P, Blasco H (2014) Advances in cellular models to explore the pathophysiology of amyotrophic lateral sclerosis. Mol Neurobiol 49:966-983.

Vierbuchen T, Ostermeier A, Pang ZP, Kokubu Y, Sudhof TC, Wernig M (2010) Direct conversion of fibroblasts to functional neurons by defined factors. Nature 463:1035-1041.

Wainger BJ, Kiskinis E, Mellin C, Wiskow O, Han SS, Sandoe J, Perez NP, Williams LA, Lee S, Boulting G, Berry JD, Brown RH, Jr., Cudkowicz ME, Bean BP, Eggan K, Woolf CJ (2014) Intrinsic membrane hyperexcitability of amyotrophic lateral sclerosis patient-derived motor neurons. Cell Rep 7:1-11.

Wegorzewska I, Baloh RH (2011) TDP-43-based animal models of neurodegeneration: new insights into ALS pathology and pathophysiology. Neurodegener Dis 8:262-274.

Wichterle H, Lieberam I, Porter JA, Jessell TM (2002) Directed differentiation of embryonic stem cells into motor neurons. Cell 110:385-397.

Wong PC, Pardo CA, Borchelt DR, Lee MK, Copeland NG, Jenkins NA, Sisodia SS, Cleveland DW, Price DL (1995) An adverse property of a familial ALS-linked SOD1 mutation causes motor neuron disease characterized by vacuolar degeneration of mitochondria. Neuron 14:1105-1116.

Xie H, Ziskind-Conhaim L (1995) Blocking Ca(2+)-dependent synaptic release delays motoneuron differentiation in the rat spinal cord. J Neurosci 15:5900-5911.

Yamada T, Placzek M, Tanaka H, Dodd J, Jessell TM (1991) Control of cell pattern in the developing nervous system: polarizing activity of the floor plate and notochord. Cell 64:635-647.

Yamamoto Y, Livet J, Pollock RA, Garces A, Arce V, deLapeyriere O, Henderson CE (1997) Hepatocyte growth factor (HGF/SF) is a muscle-derived survival factor for a subpopulation of embryonic motoneurons. Development 124:2903-2913.

Yang YM, Gupta SK, Kim KJ, Powers BE, Cerqueira A, Wainger BJ, Ngo HD, Rosowski KA, Schein PA, Ackeifi CA, Arvanites AC, Davidow LS, Woolf CJ, Rubin LL (2013) A small molecule screen in stem-cell-derived motor neurons identifies a kinase inhibitor as a candidate therapeutic for ALS. Cell Stem Cell 12:713-726.

Yao XL, Ye CH, Liu Q, Wan JB, Zhen J, Xiang AP, Li WQ, Wang Y, Su H, Lu XL (2013) Motoneuron differentiation of induced pluripotent stem cells from SOD1G93A mice. PLoS One 8:e64720.

Yohn DC, Miles GB, Rafuse VF, Brownstone RM (2008) Transplanted mouse embryonic stem-cell-derived motoneurons form functional motor units and reduce muscle atrophy. J Neurosci 28:12409-12418.

Yu J, Hu K, Smuga-Otto K, Tian S, Stewart R, Slukvin, II, Thomson JA (2009) Human induced pluripotent stem cells free of vector and transgene sequences. Science 324:797-801.

Yu J, Vodyanik MA, Smuga-Otto K, Antosiewicz-Bourget J, Frane JL, Tian S, Nie J, Jonsdottir GA, Ruotti V, Stewart R, Slukvin, II, Thomson JA (2007) Induced pluripotent stem cell lines derived from human somatic cells. Science 318:1917-1920.

Zhou Q, Choi G, Anderson DJ (2001) The bHLH transcription factor Olig2 promotes oligodendrocyte differentiation in collaboration with Nkx2.2. Neuron 31:791-807.

APPENDIX A: COPYRIGHT PERMISSION LETTERS

ELSEVIER LICENSE
TERMS AND CONDITIONS

Sep 22, 2014

This is a License Agreement between Jeremy Toma ("You") and Elsevier ("Elsevier") provided by Copyright Clearance Center ("CCC"). The license consists of your order details, the terms and conditions provided by Elsevier, and the payment terms and conditions.

All payments must be made in full to CCC. For payment instructions, please see information listed at the bottom of this form.

Supplier

Elsevier Limited
The Boulevard,Langford Lane
Kidlington,Oxford,OX5 1GB,UK

Registered Company Number

1982084

Customer name

Jeremy Toma

Customer address

6-6057 Coburg Rd.

Halifax, NS B3H1Z1

License number

3474400053353

License date

Sep 22, 2014

Licensed content publisher

Elsevier

Licensed content publication

Cell Stem Cell

Licensed content title

Conversion of Mouse and Human Fibroblasts into Functional Spinal Motor Neurons

Licensed content author

Esther Y. Son,Justin K. Ichida,Brian J. Wainger,Jeremy S. Toma,Victor F. Rafuse,Clifford J. Woolf,Kevin Eggan

Licensed content date

2 September 2011

Licensed content volume number

9

Licensed content issue number

3

Number of pages

14

Start Page

205

End Page

218

Type of Use

reuse in a thesis/dissertation

Portion

full article

Format

both print and electronic

Are you the author of this Elsevier article?

Yes

Will you be translating?

No

Title of your thesis/dissertation

In vitro Model Systems for Investigation of Motoneuron Development and Disease

Expected completion date

Dec 2014

Estimated size (number of pages)

200

Elsevier VAT number

GB 494 6272 12

Permissions price

0.00 USD

VAT/Local Sales Tax

0.00 USD / 0.00 GBP

Total

0.00 USD

INTRODUCTION

1. The publisher for this copyrighted material is Elsevier. By clicking "accept" in connection with completing this licensing transaction, you agree that the following terms and conditions apply to this transaction (along with the Billing and Payment terms and conditions established by Copyright Clearance Center, Inc. ("CCC"), at the time that you opened your Rightslink account and that are available at any time at http://myaccount.copyright.com).

GENERAL TERMS

2. Elsevier hereby grants you permission to reproduce the aforementioned material subject to the terms and conditions indicated.

3. Acknowledgement: If any part of the material to be used (for example, figures) has appeared in our publication with credit or acknowledgement to another source, permission must also be sought from that source. If such permission is not obtained then that material may not be included in your publication/copies. Suitable acknowledgement to the source must be made, either as a footnote or in a reference list at the end of your publication, as follows:

"Reprinted from Publication title, Vol /edition number, Author(s), Title of article / title of chapter, Pages No., Copyright (Year), with permission from Elsevier [OR APPLICABLE SOCIETY COPYRIGHT OWNER]." Also Lancet special credit - "Reprinted from The Lancet, Vol. number, Author(s), Title of article, Pages No., Copyright (Year), with permission from Elsevier."

4. Reproduction of this material is confined to the purpose and/or media for which permission is hereby given.

5. Altering/Modifying Material: Not Permitted. However figures and illustrations may be altered/adapted minimally to serve your work. Any other abbreviations, additions, deletions and/or any other alterations shall be made only with prior written authorization of Elsevier Ltd. (Please contact Elsevier at permissions@elsevier.com)

6. If the permission fee for the requested use of our material is waived in this instance, please be advised that your future requests for Elsevier materials may attract a fee.

7. Reservation of Rights: Publisher reserves all rights not specifically granted in the combination of (i) the license details provided by you and accepted in the course of this licensing transaction, (ii) these terms and conditions and (iii) CCC's Billing and Payment terms and conditions.

8. License Contingent Upon Payment: While you may exercise the rights licensed immediately upon issuance of the license at the end of the licensing process for the transaction, provided that you have disclosed complete and accurate details of your proposed use, no license is finally effective unless and until full payment is received from you (either by publisher or by CCC) as provided in CCC's Billing and Payment terms and conditions. If full payment is not received on a timely basis, then any license preliminarily granted shall be deemed automatically revoked and shall be void as if never granted. Further, in the event that you breach any of these terms and conditions or any of CCC's Billing and Payment terms and conditions, the license is automatically revoked and shall be void as if never granted. Use of materials as described in a revoked license, as well as any use of the materials beyond the scope of an unrevoked license, may constitute copyright infringement and publisher reserves the right to take any and all action to protect its copyright in the materials.

198

9. Warranties: Publisher makes no representations or warranties with respect to the licensed material.

10. Indemnity: You hereby indemnify and agree to hold harmless publisher and CCC, and their respective officers, directors, employees and agents, from and against any and all claims arising out of your use of the licensed material other than as specifically authorized pursuant to this license.

11. No Transfer of License: This license is personal to you and may not be sublicensed, assigned, or transferred by you to any other person without publisher's written permission.

12. No Amendment Except in Writing: This license may not be amended except in a writing signed by both parties (or, in the case of publisher, by CCC on publisher's behalf).

13. Objection to Contrary Terms: Publisher hereby objects to any terms contained in any purchase order, acknowledgment, check endorsement or other writing prepared by you, which terms are inconsistent with these terms and conditions or CCC's Billing and Payment terms and conditions. These terms and conditions, together with CCC's Billing and Payment terms and conditions (which are incorporated herein), comprise the entire agreement between you and publisher (and CCC) concerning this licensing transaction. In the event of any conflict between your obligations established by these terms and conditions and those established by CCC's Billing and Payment terms and conditions, these terms and conditions shall control.

14. Revocation: Elsevier or Copyright Clearance Center may deny the permissions described in this License at their sole discretion, for any reason or no reason, with a full refund payable to you. Notice of such denial will be made using the contact information provided by you. Failure to receive such notice will not alter or invalidate the denial. In no event will Elsevier or Copyright Clearance Center be responsible or liable for any costs, expenses or damage incurred by you as a result of a denial of your permission request, other than a refund of the amount(s) paid by you to Elsevier and/or Copyright Clearance Center for denied permissions.

LIMITED LICENSE

The following terms and conditions apply only to specific license types:

15. **Translation**: This permission is granted for non-exclusive world **English** rights only unless your license was granted for translation rights. If you licensed translation rights you may only translate this content into the languages you requested. A professional translator must perform all translations and reproduce the content word for word preserving the integrity of the article. If this license is to re-use 1 or 2 figures then permission is granted for non-exclusive world rights in all languages.

16. **Posting licensed content on any Website**: The following terms and conditions apply as follows: Licensing material from an Elsevier journal: All content posted to the web site must maintain the copyright information line on the bottom of each image; A hyper-text must be included to the Homepage of the journal from which you are licensing at http://www.sciencedirect.com/science/journal/xxxxx or the Elsevier homepage for books at http://www.elsevier.com; Central Storage: This license does not include permission for a scanned version of the material to be stored in a central repository such as that provided by Heron/XanEdu.

Licensing material from an Elsevier book: A hyper-text link must be included to the Elsevier homepage at http://www.elsevier.com . All content posted to the web site must maintain the copyright information line on the bottom of each image.

Posting licensed content on Electronic reserve: In addition to the above the following clauses are applicable: The web site must be password-protected and made available only to bona fide students registered on a relevant course. This permission is granted for 1 year only. You may obtain a new license for future website posting.

For journal authors: the following clauses are applicable in addition to the above: Permission granted is limited to the author accepted manuscript version* of your paper.

*Accepted Author Manuscript (AAM) Definition: An accepted author manuscript (AAM) is the author's version of the manuscript of an article that has been accepted for publication and which may include any author-incorporated changes suggested through the processes of submission processing, peer review, and editor-author communications. AAMs do not include other publisher value-added contributions such as copy-editing, formatting, technical enhancements and (if relevant) pagination.

You are not allowed to download and post the published journal article (whether PDF or HTML, proof or final version), nor may you scan the printed edition to create an electronic version. A hyper-text must be included to the Homepage of the journal from which you are licensing at http://www.sciencedirect.com/science/journal/xxxxx. As part of our normal production process, you will receive an e-mail notice when your article appears on Elsevier's online service ScienceDirect (www.sciencedirect.com). That e-mail will include the article's Digital Object Identifier (DOI). This number provides the electronic link to the published article and should be included in the posting of your personal version. We ask that you wait until you receive this e-mail and have the DOI to do any posting.

Posting to a repository: Authors may post their AAM immediately to their employer's institutional repository for internal use only and may make their manuscript publically available after the journal-specific embargo period has ended.

Please also refer to Elsevier's Article Posting Policy for further information.

18. For book authors the following clauses are applicable in addition to the above: Authors are permitted to place a brief summary of their work online only.. You are not allowed to download and post the published electronic version of your chapter, nor may you scan the printed edition to create an electronic version. **Posting to a repository:** Authors are permitted to post a summary of their chapter only in their institution's repository.

20. Thesis/Dissertation: If your license is for use in a thesis/dissertation your thesis may be submitted to your institution in either print or electronic form. Should your thesis be published commercially, please reapply for permission. These requirements include permission for the Library and Archives of Canada to supply single copies, on demand, of the complete thesis and include permission for UMI to supply single copies, on demand, of the complete thesis. Should your thesis be published commercially, please reapply for permission.

Elsevier Open Access Terms and Conditions

Elsevier publishes Open Access articles in both its Open Access journals and via its Open Access articles option in subscription journals.

Authors publishing in an Open Access journal or who choose to make their article Open Access in an Elsevier subscription journal select one of the following Creative Commons user licenses, which define how a reader may reuse their work: Creative Commons Attribution License (CC BY), Creative

Commons Attribution – Non Commercial -ShareAlike (CC BY NC SA) and Creative Commons Attribution – Non Commercial – No Derivatives (CC BY NC ND)

Terms & Conditions applicable to all Elsevier Open Access articles:

Any reuse of the article must not represent the author as endorsing the adaptation of the article nor should the article be modified in such a way as to damage the author's honour or reputation.

The author(s) must be appropriately credited.

If any part of the material to be used (for example, figures) has appeared in our publication with credit or acknowledgement to another source it is the responsibility of the user to ensure their reuse complies with the terms and conditions determined by the rights holder.

Additional Terms & Conditions applicable to each Creative Commons user license:

CC BY: You may distribute and copy the article, create extracts, abstracts, and other revised versions, adaptations or derivative works of or from an article (such as a translation), to include in a collective work (such as an anthology), to text or data mine the article, including for commercial purposes without permission from Elsevier

CC BY NC SA: For non-commercial purposes you may distribute and copy the article, create extracts, abstracts and other revised versions, adaptations or derivative works of or from an article (such as a translation), to include in a collective work (such as an anthology), to text and data mine the article and license new adaptations or creations under identical terms without permission from Elsevier

CC BY NC ND: For non-commercial purposes you may distribute and copy the article and include it in a collective work (such as an anthology), provided you do not alter or modify the article, without permission from Elsevier

Any commercial reuse of Open Access articles published with a CC BY NC SA or CC BY NC ND license requires permission from Elsevier and will be subject to a fee.

Commercial reuse includes:

- Promotional purposes (advertising or marketing)

- Commercial exploitation (e.g. a product for sale or loan)

- Systematic distribution (for a fee or free of charge)

Please refer to Elsevier's Open Access Policy for further information.

21. Other Conditions:

v1.6

Gratis licenses (referencing $0 in the Total field) are free. Please retain this printable license for your reference. No payment is required.

RE: Copyright permission

jn permissions <jnpermissions@sfn.org>

Fri 20/03/2015 18:02

Inbox

To:Jeremy Toma <jeremytoma@Dal.Ca>;

Dear Jeremy Toma,

Thank you for your email. Permission is granted to reproduce the requested material listed below with NO fee in print and electronic format for use in your doctoral thesis/dissertation. Please contact me if you have any questions or if you need another form of permission.

Regards,
SfN Central Office

Motoneurons Derived from Induced Pluripotent Stem Cells Develop Mature Phenotypes Typical of Endogenous Spinal Motoneurons

Jeremy S. Toma, Basavaraj C. Shettar, Peter H. Chipman, Devanand M. Pinto, Joanna P. Borowska, Justin K. Ichida, James P. Fawcett, Ying Zhang, Kevin Eggan, and Victor F. Rafuse

The Journal of Neuroscience, 21 January 2015, 35(3):1291-1306, doi:10.1523/JNEUROSCI.2126-14.2015

From: Jeremy Toma [jeremytoma@Dal.Ca]
Sent: Thursday, February 26, 2015 10:01 AM
To: jn permissions
Subject: Re: Copyright permission

Dear Michael,

The article will be modified from its original form (for thesis formatting purposes) and supporting data not in the original publication but pertaining to the experiments described in the article will be added. The article is titled "Motoneurons derived from induced pluripotent stem cells develop mature phenotypes typical of endogenous spinal motoneurons" J Neurosci. 2015 Jan 21;35(3):1291-306. doi: 10.1523/JNEUROSCI.2126-14.2015.

Thank you,
Jeremy Toma

From: jn permissions <jnpermissions@sfn.org>
Sent: 25 February 2015 17:51
To: Jeremy Toma
Subject: RE: Copyright permission

Dear Dr. Toma,

Could you provide more information on how you will be reprinting the material as well as the title or citation information for your article?

Regards,
Michael
Sfn Central Office

From: Jeremy Toma [jeremytoma@Dal.Ca]
Sent: Tuesday, January 06, 2015 11:55 AM
To: jn permissions
Subject: Copyright permission

Hello,

I have recently had a manuscript accepted for publication and would like to use this material for my PhD thesis. I understand I do not need to contact the journal for the right to reprint this material in my thesis, however, the journal has exclusive publication rights for the first 6 months following publication, and I will need to be able to reprint this material within this 6 month timeframe for my PhD thesis. Do I require special permission from the journal for this purpose?

Thank you,

Jeremy Toma